



MONASH University
Medicine, Nursing and Health Sciences

**Interplay Between Macrophages and Endometrial Stem/Stromal Cells on Mesh
Performance in Animal Models**

Saeedeh Darzi

BSc (Medical Laboratory Science), MSc (Immunology)

The Ritchie Centre, Hudson Institute of Medical Research
Department of Obstetrics and Gynaecology
Faculty of Medicine, Nursing, and Health Sciences
Monash University, Melbourne, Australia

Submitted to fulfil the requirements for the degree of
Doctor of Philosophy
August 2017

Supervisors Prof. Caroline Gargett

The Ritchie Centre, Hudson Institute of Medical Research and
Monash University Department of Obstetrics and Gynaecology,
Melbourne, VIC, Australia

Prof. Jerome Werkmeister,

CSIRO Manufacturing, Clayton, VIC, Australia

Dr. James Deane

The Ritchie Centre, Hudson Institute of Medical Research and Monash University

Department of Obstetrics and Gynaecology, Melbourne, VIC, Australia

Notice 1

Under the Copyright Act 1968, this thesis must be used only under the normal conditions of scholarly fair dealing. In particular, no results or conclusions should be extracted from it, nor should it be copied or closely paraphrased in whole or in part without the written consent of the author. Proper written acknowledgement should be made for any assistance obtained from this thesis.

Notice 2

I certify that I have made all reasonable efforts to secure copyright permissions for third-party content included in this thesis and have not knowingly added copyright content to my work without the owner's permission.

Table of Contents

Acknowledgments	vii
List of Abbreviations	ix
Summary	xi
General Declaration	xv
Publications and Abstracts	xvii
CHAPTER 1	19
1.1 Pelvic Organ Prolapse	20
1.1.1. Anatomy of the pelvis	21
1.1.2. Symptoms, etiology and incidence of POP	22
1.1.3. POP diagnosis	24
1.2. Treatment options for Pelvic Organ Prolapse	25
1.2.1. Surgery for POP repair	26
1.2.2. Surgical treatment options with synthetic and biological meshes	27
1.2.3. Mesh classification	29
1.2.4. Anterior vaginal wall repair with mesh	29
1.2.5. Posterior vaginal wall repair with mesh	31
1.2.6. Apical compartment repair with mesh	32
1.3. Problems associated with synthetic mesh	33
1.3.1. Mesh exposure and erosion	34
1.3.2. Mesh contracture	34
1.4. Problems associated with biological meshes	35
1.5. New meshes for vaginal POP surgery	36
1.5.1. Mesh products with collagen coating	37
1.6. Mesenchymal Stem Cells	38
1.6.1. Properties and phenotype of Mesenchymal Stem Cells	38
1.6.2. MSC niche	40
1.6.3. Sources of MSC	41
1.6.4. MSC as modulator of the immune system	42
1.6.5. MSC and innate immune system	42
1.6.6. MSC and adaptive immune system	43
1.6.7. MSC- Graft-Versus-Host-Disease (GVHD)	44
1.6.8. MSC role in tissue regeneration and wound repair	44
1.7. Endometrial Mesenchymal Stem Cells	45
1.7.1. Markers identifying eMSC	46

1.7.2.	eMSC niche-----	47
1.7.3.	Endometrial regenerative cells in menstrual blood (ERC)-----	49
1.7.4.	Immunomodulatory properties of eMSC-----	49
1.8.	Tissue engineering-----	50
1.8.1.	MSC in tissue engineering-----	51
1.8.2.	Tissue engineering approach for POP treatment – use of eMSC-----	51
1.9.	Animal models for investigating POP-----	52
1.9.1.	Rodent models-----	53
1.9.2.	Ovine model-----	54
1.10.	Host response to tissue engineering construct-----	55
1.10.1.	Role of macrophage polarization following biomaterial implantation-----	56
1.10.2.	MSC – Macrophage Interaction-----	58
1.10.3.	MSC fate after transplantation-----	59
1.11.	Rationale for the Thesis-----	60
1.12.	Hypothesis and Aims-----	62
CHAPTER 2-----		64
2.1. Introductory statement-----		65
CHAPTER 3-----		80
3.1. Introductory statement-----		81
3.2.	Abstract-----	85
3.3.	Introduction-----	86
3.4.	Results-----	89
3.4.1.	eMSC transduction and survival in vivo on PA+G mesh-----	89
3.4.2.	eMSC induce macrophage polarization-----	90
3.4.3.	eMSC modulate inflammatory cytokine mRNA expression-----	91
3.4.4.	eMSC modulate inflammatory cytokine secretion-----	92
3.4.5.	eMSC induce the expression of M2 macrophage markers-----	93
3.5.	Discussion-----	94
3.6.	Material and Methods-----	98
3.6.1.	Endometrial Tissues-----	98
3.6.2.	Isolation of SUSD2 ⁺ eMSC and Culture-----	99
3.6.3.	mCherry Lentivirus Transduction of eMSC-----	100
3.6.4.	mCherry ⁺ / SUSD2 ⁺ eMSC Sorting-----	100
3.6.5.	Fabrication of PA+G mesh and seeding with human eMSC-----	101
3.6.6.	Implantation of eMSC-seeded PA+G Tissue Engineering Constructs-----	102
3.6.7.	Immunofluorescence-----	103
3.6.8.	Image analysis-----	103
3.6.9.	Lysate preparation and protein assay-----	104
3.6.10.	ELISAs-----	104

3.6.11.	qRT-PCR	105
3.6.12.	Statistics	105
CHAPTER 4		134
4.1.	Introductory statement	135
4.2.	Abstract	137
4.3.	Introduction	139
4.4.	Material and Methods	140
4.4.1.	Human samples	140
4.4.2.	eMSC isolation, culture and transduction	140
4.4.3.	PA+G mesh fabrication	141
4.4.4.	Macrophage depletion	141
4.4.5.	Animal surgery and tissue collection	142
4.4.6.	Flow cytometry	143
4.4.7.	Immunostaining	144
4.4.8.	Image analysis	146
4.5.	Results	146
4.5.1.	Labelling eMSC for cell tracking in vivo	146
4.5.2.	Clodronate depletes macrophage from the spleen	146
4.5.3.	eMSC survival in implanted mesh in the absence of macrophages	149
4.5.4.	Macrophage presence around mesh filament in clodronate and PBS injected mice	150
4.5.5.	Absence of immature monocytes in tissue around mesh	154
4.5.6.	Lack of local macrophage proliferation in implanted mesh of clodronate treated mice	154
4.6.	Discussion	157
CHAPTER 5		160
REFERENCES		168
APPENDIX		201

List of Tables

Table 1. Prolapse Classification.....	25
--	----

List of Figures

Figure 1. Different types of Pelvic Organ prolapse	20
Figure 2. Schematic of the three levels of pelvic organ support.....	21
Figure 3. Points and landmarks for POP-Q system examination	24
Figure 4. Anterior colporrhaphy	30
Figure 5. Posterior colporrhaphy	32
Figure 6. Abdominal sacrocolpopexy.....	33
Figure 7. Optical micrograph of fabricated meshes.....	37
Figure 8. Cellular hierarchy showing self-renewal ability of adult stem cells.....	40
Figure 9. Location of eMSC in human endometrium.....	48

Acknowledgments

The first and greatest thank should go to my senior supervisor, Associate Professor Caroline Gargett. I have known her since working in the area of endometrial cells as a part of my Masters' program. Her interesting work in this area was so inspiring which assist me in developing my research thesis and further motivated me to pursue my education under her supervision at a PhD level. I immensely appreciate her time, patience, continuous support, encouragements and great ideas that made my PhD experience productive and enjoyable. The grave enthusiasm she has for the research in women health has been contagious to me keeping me motivated during entire period of my PhD journey. My sincere thanks also go to my co-supervisors, Prof Jerome Werkmeister for his exceptional support and knowledge sharing across different stages of my PhD; Dr James Deane for his fantastic scientific inputs including valuable assistance in mice surgeries and injections.

I acknowledge the contribution of lovely students and staff members of Gargett's group who genuinely offered their time to me to have a quality time at the Hudson Institute of Medical Research. The group has been always a source of friendships and encouragement as well as good advice and collaboration.

To my kind friend and colleague, Dr Shanti Gurung, who was always available whenever I needed her. Thank you for all the happy and sad moments we passed through together. I thank Kersin Tan who helped me to learn lab techniques and patiently answered all my questions.

I would like also to thank our two wonderful research fellows, Dr. Fiona Cousins and Dr. Shayanti Mukherjee for their scientific advice and technical consultation. I would like to thank Nikeh Shariatian and Mina Khalaji, for their great friendship and interesting chats we had during lunch time; they made my PhD life joyful. My special thank also goes to my colleagues Luke, Lisa, Raffaella and Xiao Qing for being part of my PhD journey.

I would like to acknowledge the CSIRO members who provided technical advice and support during my PhD especially Jacinta White for Siruis Red staining and birefringence analysis, Dr. Kai Su for biochemical studies, Aditya Vashi and Dr Sharon Edwards for the PA+G mesh preparation for my experiments. I also acknowledge the Ritchie Centre and the Hudson Institute of Medical Research for providing the facilities and financial support for attending national and international conferences.

To my dearest family and the best mother and sister ever, Adileh Hashemi and Soheila Darzi. Thank you for all your support throughout my life, for believing in me and to provide me all the opportunities to pursue my dreams. This thesis dedicated to the memory of my dad (Amir) who always believed in my ability to be successful in the academic area. You are gone but your belief in me has made this journey possible.

List of Abbreviations

ASC	Adipose derived stem cell
AT I	Angiotensin one
AT II	Angiotensin two
bmMSC	Bone marrow mesenchymal stem cell
CFU	Colony forming unit
CO	Carbon monoxide
DC	Dendritic cell
eMSC	Endometrial mesenchymal stem cell
ERC	Endometrial regenerative cell
FBGC	Foreign body giant cell
GAG	Glycosaminoglycan
GAL-1	Galectin one
GAL-2	Galectin two
GRC	Graft related complication
GVHD	Graft versus host disease
IDO	Indoleamine 2,3-dioxygenase
IL1 β	Interleukin one-beta
LIF	Leukemia inhibitory factor
NKP30	Natural cytotoxicity receptor 30
NKP44	Natural cytotoxicity receptor 44
NO	Nitric oxide
PA	Poly amide
PA+G	Polyamide + gelatin
PGE2	Prostaglandin E2
POP	Pelvic organ prolapse
SIS	Small Intestine Submucosa

TE	Tissue engineering
TGF β	Transforming growth factor beta
TNF- α	Tumor necrosis factor-alpha
VEGF	Vascular endothelial growth factor

Summary

Tissue engineering, is a prominent alternative solution that aims to restore, maintain and improve the tissue function. Huge advances in tissue engineering have occurred over the past two decades and the rapid development of new biomaterials has great potential in Women's urogynaecological health. Tissue engineering could revolutionize the treatment of Stress Urinary Incontinence (SUI) and Pelvic Organ Prolapse (POP), common pelvic floor disorders affecting large numbers of women worldwide.

Pelvic organ prolapse is the downward descent of one or more of the pelvic organs (uterus, bladder, and bowel) into the vagina. Women with prolapse commonly have a variety of pelvic floor symptoms. Generalised symptoms include pelvic heaviness, bulge, lump or protrusion coming down from the vagina. Symptoms of bladder, bowel or sexual dysfunction are frequently present. The aetiology of POP is complex and multifactorial. Possible risk factors include pregnancy, vaginal delivery, congenital or acquired connective tissue abnormalities, denervation or weakness of the pelvic floor muscles, ageing, hysterectomy, menopause and factors associated with chronically raised intra-abdominal pressure. Reconstructive surgery is the main treatment option for women with symptomatic POP. However, due to relatively high failure rate of POP native tissue surgery, synthetic meshes were introduced about 15 years ago. The aim was to provide additional support not provided by existing and damaged pelvic floor musculature, ligaments and endopelvic fascia to augment surgical reconstruction. Although mesh surgery was, until very recently, the most common type of treatment for POP, a wide range of complications have arisen from the use of transvaginal mesh in POP surgery for ~10% of cases.

Designing new mesh with improved characteristics and investigating the use of a tissue engineered construct are important advances needed to progress the field. In the first part of this thesis, I assessed whether the format of collagen coating a mesh affects the ovine vaginal wall response to the mesh. Meshes containing collagen, either as a coated sheet or in soluble form around individual filaments, did not reduce leukocyte accumulation around the mesh filaments and the majority of inflammatory leukocytes around the filaments were macrophages. Secondly, increased micro-vessel density and therefore vascularization was found around the collagen coated mesh filaments at 60 days, which had resolved by 6 months. Thirdly, there were significant differences at the micro-molecular level at the mesh-tissue interface, using birefringence of Sirius Red stained tissues and quantitative morphometric image analysis to track the maturation of newly laid down collagen fibres during the healing phase following mesh implantation. Both mesh containing collagen lead to physiological tissue formation approaching that of normal tissue.

One of the main issues resulting from biomaterial implantation, which should be taken into account, is the host response to implanted mesh. During this host response, two main types of macrophages play a key role. M1 inflammatory macrophages which are responsible for classic signs of inflammation and M2 regulatory macrophages which promote tissue healing. The balance between the M1 and M2 macrophage response determines the success or failure of implanted biomaterials. Since non-degradable biomaterials aim to provide long term mechanical support, it is important that the host response promotes biomaterial integration into the tissue with minimal M1 macrophage response. To prevent prolonged detrimental effects of M1 macrophages, a timely switch

from a M1 to M2 macrophage phenotype is required. Since Mesenchymal Stem Cells (MSC) facilitate the switch from M1 to M2 phenotype, co transplantation of MSC with biomaterial has been suggested.

Although bone marrow mesenchymal stem cells (bmMSC) showed promising results as cell-based therapies in preclinical models, their isolation from bone marrow is invasive and requires anaesthesia. In general, the isolation methods used (plastic adherence) fail to purify the undifferentiated MSC from the predominant population of fibroblasts and these cell preparations are heterogeneous. Human Endometrial Mesenchymal Stem/Stromal Cells (eMSC) are a newly identified MSC type that is easily accessible by minimally invasive office based procedure not requiring anaesthesia. In the second chapter of this thesis, the effects of mCherry labelled eMSC on macrophage response to implanted mesh was assessed in two mouse models; immunocompetent (C57BL6) and immunocompromised (NSG). Meshes seeded with mCherry eMSC (for tracking purposes) resulted in a reduced inflammatory response and greater numbers of M2 macrophages in the early days post implantation in C57BL6 and at later time points in NSG mice. eMSC showed inhibitory effects in both immune intact and immune compromised systems suggesting that immune intact mice are suitable for tissue engineering studies using stem/progenitor cells, although the implanted cells do not persist.

In the third part of my thesis, the source of macrophages responding to implanted mesh was studied. Following systemic depletion of monocytes with IV injection of clodronate. I found that the accumulated macrophage population around the mesh filaments were not blood recruited monocytes. The assessment of resident macrophage behaviour revealed

that macrophages accumulated around the mesh filaments were not proliferating. The next step would be assessment of the migration of tissue macrophages to the site of implantation. However, this was not feasible within the time frame of this thesis.

In conclusion, a tissue engineering construct using MSC could be an appropriate alternative treatment for POP and eMSC are a promising source of mesenchymal stem cells for use in tissue engineering studies. Further assessment of responding macrophages to implanted biomaterials is needed for the future design of materials which evoke immune responses that improve the integration of biomaterial rather than rejection and fibrosis.

General Declaration

In accordance with Monash University Doctorate Regulation 17 Doctor of Philosophy (PhD) regulations, the following declarations are made:

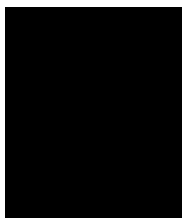
I declare that this thesis contains no material which has been accepted for the award of any other degree or diploma at any university or equivalent institution and that, to the best of my knowledge and belief, this thesis contains no material previously published or written by another person, except where due reference is made in the text of the thesis.

This thesis includes one original paper published in peer reviewed journal (Chapter 2) and one submitted manuscripts which is under review (Chapter 3) and one review manuscript published in peer reviewed journal (included in the appendix). The core theme of the thesis is tissue engineering and human mesenchymal stem cells. The ideas, development and writing up of all the papers in the thesis were the principal responsibility of myself, the candidate, working within the Ritchie Centre, Hudson Institute of Medical Research under the supervision of Professor Caroline Gargett, Professor Jerome Werkmeister and Doctor James Deane.

The inclusion of co-authors reflects the fact that the work came from active collaboration between researchers and acknowledges input into team-based research.

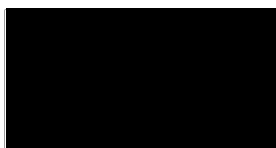
Thesis Chapter	Publication Title	Publication Status	Nature and extent of candidate's contribution
1	Identification and Characterization of Human Endometrial Mesenchymal Stem/Stromal Cells and Their Potential for Cellular Therapy	Published (Appended)	75%
2	Tissue response to collagen containing polypropylene meshes in an ovine vaginal repair model	Published	80%
3	Endometrial Mesenchymal Stem/Stromal Cells Modulate the Macrophage Response to Implanted Polyamide/Gelatin Composite Mesh in Immunocompromised and Immunocompetent Mice	Submitted	85%

Student signature:



Date: 12.08.2017

Main supervisor signature:



Date: 12.08.2017

Publications and Abstracts

Published Journal Articles

Darzi S, Urbankova I, Su K, White J, Lo C, Alexander D, Werkmeister JA, Gargett CE, Deprest J. Tissue response to collagen containing polypropylene meshes in an ovine vaginal repair model. 2016 Jul 15; 39:114-23. doi: 10.1016/j.actbio.2016.05.010

Darzi S, Werkmeister JA, Deane JA, Gargett CE. Identification and Characterization of Human Endometrial Mesenchymal Stem/Stromal Cells and Their Potential for Cellular Therapy. 2016 Sep;5(9):1127-32. doi: 10.5966/sctm.2015-0190.

Submitted Journal Articles

Darzi S, Nold C, Deane JA, Edwards S, Daniel Gough, Mukherjee S, Gurung S, Tan KS, Adi Vashi, Gurung S, Werkmeister JA, Gargett CE. Endometrial Mesenchymal Stromal/Stem Cells Modulate the Macrophage Response to Implanted Polyamide/gelatin Composite Mesh in a Mouse Model

Presentations

Saeedeh Darzi, James Deane, Claudia Nold, Sharon Edwards, Daniel Gough, Shayanti Mukherjee, Shanti Gurung, Kersin Tan, Aditya Vashi, Jerome Werkmeister, Caroline Gargett. “Endometrial Mesenchymal Stromal/Stem Cells Modulate the Macrophage Response to Implanted Polyamide/Gelatin Composite Mesh in Immunocompromised and Immunocompetent Mice”. Society for Reproductive Science, Perth, Australia, 27-30th August 2017.

Saeedeh Darzi, James Deane, Sharon Edwards, Daniel Gough, Jerome Werkmeister, Caroline E Gargett. “Interplay Between Macrophages and Human Endometrial

Stem/Stromal Cells on Mesh Implants in a Mouse Model”. International Congress of Immunology, Melbourne, Australia. 21-26th August 2016.

Saeedeh Darzi’ James Deane, Sharon Edwards, Daniel Gough, Jerome Werkmeister, Caroline E Gargett. “Interplay Between Macrophages and Human Endometrial Stem/Stromal Cells on Mesh Implants in a Mouse Model”. International Society for Stem Cell Research, San Francisco, California, USA. 22-25th June 2016.

Saeedeh Darzi’ James Deane, Sharon Edwards’ Daniel Gough, Jerome Werkmeister, Caroline E Gargett. “Interplay Between Macrophages and Human Endometrial Stem/Stromal Cells on Mesh Implants in a Mouse Model”. 4th World International Congress on Tissue Engineering and Regenerative Medicine International Society Boston, USA, 8-11th September 2015.

Chapter 1

Introduction

1.1. Pelvic Organ Prolapse

Pelvic organ prolapse is the downward descent of one or more of the pelvic organs (uterus, bladder, and bowel) into the vagina (Fig.1) It is a disorder exclusive to women and can affect the anterior vaginal wall, where the bladder herniates to form a cystocele, and/or, posterior vaginal wall where the prolapsed bowel causes a rectocele. Apical prolapse involving the small intestine forms a enterocele, and uterine or apex (in hysterectomised women) causes uterine descent or vault collapse of the vagina, often in combination.

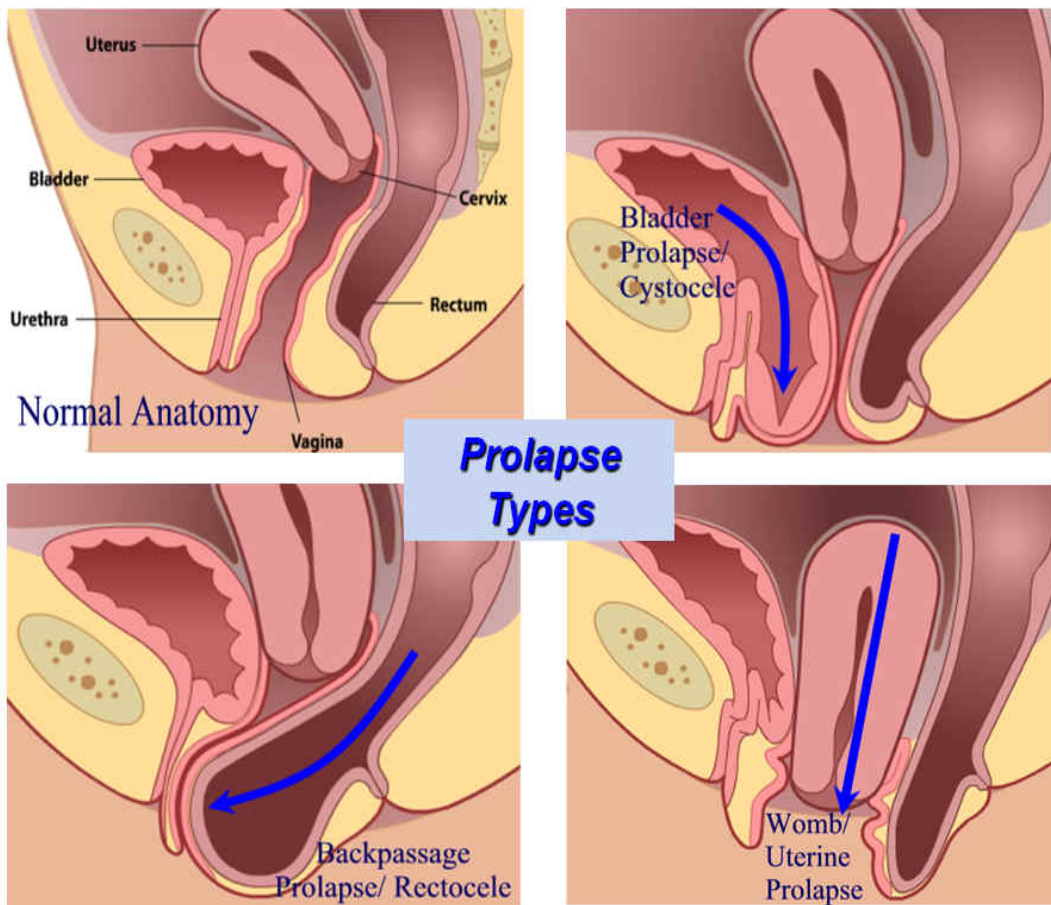


Figure 1. Different types of Pelvic Organ prolapse

Anterior vaginal wall (Cystocele), Posterior vaginal wall (Rectocele) and Uterine prolapse.
Image is adapted from www.vanea.com.au

1.1.1. Anatomy of the pelvis

The anatomic structure of female pelvic floor comprise several muscles of pelvic floor, the surrounding dense fibromuscular connective tissue of the vagina known as the endopelvic fascia and the suspensory ligaments. These structures provide three levels of pelvic organ support (Fig.2) (Ashton-Miller and DeLancey, 2007).

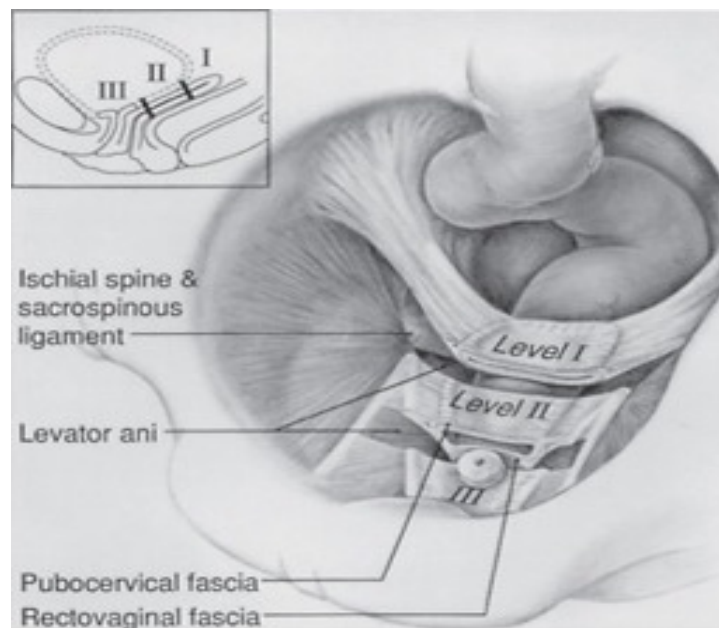


Figure 2. Schematic of the three levels of pelvic organ support

The schematic shows the ligaments at level I, endopelvic fascia at level II and muscles at level III– Reproduced with permission from Delancey, AJOG 1992.

Endopelvic fascia (level II) is a fibrous connective tissue layer surrounding the vaginal walls. The levator ani is a broad muscular sheet of variable thickness attached to the

internal surface of the true pelvis. It has the ability to contract quickly with a sudden increase in abdominal pressure, e.g. during a cough, sneeze or physical activity, thereby minimizing the maximum stretch the muscle experiences (Schwertner-Tiepelmann et al., 2012). The interaction between the pelvic floor muscles and the supportive ligaments is critical for pelvic organ support. Any form of prolapse can occur due to weakened or damaged muscles and/or any other failure in this supporting complex of the pelvic floor components e.g. pelvic fascia, ligaments and pelvic floor muscles (Ashton-Miller and DeLancey, 2007).

1.1.2. Symptoms, etiology and incidence of POP

Women with prolapse commonly have a variety of pelvic floor symptoms. Generalised symptoms include pelvic heaviness, bulge, lump or protrusion coming down from the vagina; a dragging sensation in the vagina or backache. Symptoms of bladder, bowel or sexual dysfunction are frequently present (Jelovsek et al., 2007).

The aetiology of POP is complex and multifactorial. Possible risk factors include pregnancy, vaginal delivery, congenital or acquired connective tissue abnormalities, denervation or weakness of the pelvic floor, ageing, hysterectomy, menopause and factors associated with chronically raised intra-abdominal pressure (Jelovsek et al., 2007). During **vaginal delivery**, pelvic floor muscles, nerves and connective tissues are stretched and compressed. Neurophysiologic studies revealed that vaginal deliveries cause partial denervation of the pelvic floor muscles in most women (Snooks et al., 1984, Sultan et al., 1994) and overstretching of ligaments and endopelvic fascia. In 10-20% of women delivering their first child, forceps delivery, prolonged second stage labour, large

infant birth weight, anal sphincter laceration and episiotomy exacerbate pelvic floor injury leading to POP (Ashton-Miller and Delancey, 2009). Women having vaginal delivery have higher risk of developing POP comparing to those undergoing caesarean (Lukacz et al., 2006), however 9 caesarean sections are needed to prevent one incidence of POP requiring surgery (Deprest and Feola, 2013).

Obesity is associated with chronically increased abdominal pressure. An increased body mass index puts continual extra force on the pelvic support structures that may have a role in the development of POP. Women who are overweight (body-mass index 25-30kg/m²) and obese, are at high risk of developing POP (Moalli et al., 2003).

Collagen concentration could be another important factor in POP pathogenesis. The endopelvic connective tissue in younger women with POP contains less collagen compared to controls without POP (Soderberg et al., 2004). However, in a contradictory study, in women with POP the total collagen, predominantly collagen III, was higher in vaginal apex, compared to women without POP, which suggested that the tissue is actively remodelling (Moalli et al., 2005b). Disorders of collagen metabolism are also a causative factor in some women (Jelovsek et al., 2007). There may be some changes in collagen metabolism including decreased collagen I and increased collagen III in people with POP (Jelovsek et al., 2007).

Elastin is one of the most stable protein in extracellular matrix (Mecham et al., 1997). However, in female reproductive system, the amount of elastin significantly increases during pregnancy (Woessner and Brewer, 1963). Studies showed that elastin plays an important role in providing support for female pelvic (Liu et al., 2006) floor and women with elastin deficiency have higher risk of developing POP (Paladini et al., 2007).

Aging is considered as a risk factor for POP (Rortveit et al., 2010). However, it is not clear whether accompanying risks associated with ageing eg diabetes are also contributing factors. In a study involving 971 interviews of women between 17-90 years with 31% complaining of prolapse symptoms, the correlation between ageing and POP development was not significant (Dietz, 2008). The incidence of POP in developing countries is 19.7% (Walker and Gunasekera, 2011) and 25% of all women in U.S have one or more symptoms of pelvic floor disorders which includes 2.9% with POP (Nygaard et al., 2008). In a review by Barber and Maher based on the English-language scientific literature in PubMed (up to January 2012) POP has a prevalence of 3-6% when defined by symptoms and 50% when based on vaginal diagnosis (Barber and Maher, 2013). Wu et al. have predicted that by 2050 the number of women suffering from symptomatic POP in the United States will increase by a minimum of 46% up to 200% (Wu et al., 2009).

1.1.3. POP diagnosis

Diagnosis is based on a clinical score. Pelvic organ prolapse quantification (POP-Q) is the only acceptable grading system which is highly reproducible and reliable (Bump et al., 1996). In this system, the hymen is the fixed point of reference and six defined points are measured in centimetres above or below the hymen (Fig.3). POP is categorised into 4 stages based on the POP-Q. (Table 1) (Persu et al., 2011).

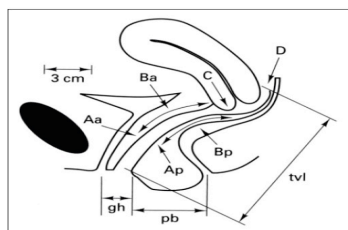


Figure 3. Points and landmarks for POP-Q system examination

Aa, point A anterior, **Ap**, point A posterior,
Ba, point B anterior; **Bp**, point B posterior; **C**, cervix or vaginal cuff;
D, posterior fornix (if cervix is present); **gh**, genital hiatus; **pb**,
perineal body; **tvl**, total vaginal length. Adapted from Persu C et al.,
Journal of Med Life, 2011, with permission.

Stage	Clinical symptoms
0	Prolapse is not demonstrated
I	The most distal portion of the prolapse is more than 1 cm above the level of the hymen
II	The most distal portion of the prolapse is 1 cm or less proximal or distal to the hymenal plane
III	The most distal portion of the prolapse protrudes more than 1 cm below the hymen but no farther than 2 cm less than the total vaginal length (for example, not all of the vagina has prolapsed).
IV	vaginal eversion is essentially complete

Table 1. Prolapse Classification

Reproduced with permission from Persu C et al., Journal of Med Life Vol. 4, No.1, P75-81, 2011

1.2. Treatment options for Pelvic Organ Prolapse

Treatment of prolapse depends on the severity of the prolapse, the symptoms, the woman's general health, and surgeon preference and capabilities. Options available for treatment are conservative (non-surgical), or surgical interventions. Pelvic floor muscle training and pessary use are both non-surgical treatments. Pelvic floor exercise may limit the progression of mild prolapse and lessen mild symptoms (Braekken et al., 2010). Pessaries are inserted into the vagina to provide support to the related pelvic structures, and to reduce pressure on the bladder and bowel (Jelovsek et al., 2007).

1.2.1. Surgery for POP repair

Reconstructive surgery is a treatment option for women with symptomatic POP. In 1997, Olsen et al. estimated the incidence of surgically managed POP and urinary incontinence (UI) in a cohort of women in a general population. They showed 11.1% lifetime risk of a single operation for POP and UI and a large proportion (29.2%) of women requiring reoperation (Olsen et al., 1997). In 44,728 incident cases obtained from Western Australia Data Linkage System of women aged 18 years or older between 1981 – 2005, Smith et al found that by age 85, 20.5% required POP surgery between 1981–1985, 21.1% between 1991–1995 and 19.0% for the period 2001–2005 (Smith et al., 2010b). The annual incidence of POP surgery ranges between 1.5 and 1.8 cases per 1,000 women-years, and the incidence peak is in women between 60 and 69 years. In USA, POP is the leading cause of more than 300,000 surgical procedures per year in women (22.7 per 10,000 women) with 25% undergoing reoperations at a total annual cost of more than 1 billion dollars per annum (Barber and Maher, 2013). Reoperation after POP surgery for recurrence is an important measure of procedure efficacy related to unsuccessful surgical outcomes or surgical failures. A 5-year prospective follow-up study of community-based women who underwent POP surgery between 1998 and 2001 found that vaginal prolapse surgery was associated with a high anatomical recurrence rate with the anterior compartment most prone (Miedel et al., 2008). A prospective cohort analysis of 374 women who were > 20 years old and underwent surgery for POP and UI in 1995 reported a 17% reoperation rate (Denman et al., 2008).

Surgical treatment for POP can be categorised into reconstructive and obliterative techniques. Reconstructive surgery for prolapse aims to correct the prolapsed vagina and

maintain or improve vaginal sexual function along with relieving any associated pelvic symptoms. There are two routes; abdominal or vaginal surgery. Epidemiological studies revealed that vaginal surgery is the preferred route with approximately 80–90% of operations done this way (Olsen et al., 1997). Experts and the majority of published literature suggest that the anterior wall is the most challenging surgery for POP (Jelovsek et al., 2007).

1.2.2. Surgical treatment options with synthetic and biological meshes

Due to relatively high failure rate of POP surgery, synthetic meshes were introduced about two decades ago (Kohli, 2012). The aim was to provide additional support not provided by existing and damaged pelvic floor musculature, ligaments and endopelvic fascia following native tissue surgical reconstruction (Hiltunen et al., 2007). Meshes used in urogynaecology were initially designed for abdominal hernia repair and the first synthetic polymeric mesh was made from nylon (polyamide), and introduced in the 1960's (Choe, 2003, Winters et al., 2006). Later, polypropylene (PP) which was used in hernia repair, was adopted for gynaecological applications. PP is the most widely used material to produce cheap, inert, and easily tailorable implants with appropriate mesh characteristics (monofilament and large pore size). PP is non-degradable and maintains its chemical and mechanical integrity for years (Deprest et al., 2006). PP implants work by inducing an inflammatory foreign body reaction, resulting in fibrosis and scarring that supposedly provides strength to the weakened support structure (Deprest et al., 2006, Choe, 2003).

The PP meshes used in this study were heavy weight PP meshes in clinical use at the time of commencing this thesis. Lighter weight PP meshes (eg Restorelle) have since been introduced but not studied herein.

Biological meshes are three dimensional acellular, degradable, extracellular matrices comprising mainly collagen type I, elastin fibres and other molecules such as proteoglycans and growth factors (e.g. VEGF) (Peppas et al., 2010). They were introduced in the 1990s and may be derived from human donor (allograft), self-donor (auto-graft) or animal (xenograft: porcine or bovine) tissues which have been de-cellularised. They allow neovascularization and regeneration due to infiltration of endogenous fibroblasts and provide the extracellular scaffold necessary to the support reconstruction of healthy tissue (Smart et al., 2012). In one study, a total of 47 women with Stage III or IV POP underwent surgical treatment with porcine skin collagen implantation using anterior transobturator and posterior bilateral sacrospinous fixations. In this study, no rejection of the porcine grafts occurred and the subjective cure rate was 93.6%) (David-Montefiore et al., 2005). However, a systematic review by Schimpf et al comparing transvaginal prolapse repair including native tissue repair or use of different grafts or mesh with anatomic and symptomatic outcomes with minimum 12 months follow up revealed that mesh surgery for anterior wall prolapse improved anatomic and symptomatic outcomes compared with native tissue repair. Biological graft did not improve the outcomes but mesh erosion occurred in about 36% of patients (Schimpf et al., 2016). Both synthetic and biologic mesh are associated with complications (section 1.3) .There are two routes for mesh insertion; abdominal in which the surgical mesh is attached to the vaginal vault through an abdominal incision and secured to the sacral

promontory and vaginal in which the mesh is placed through an incision made into the vagina (Jelovsek et al., 2007).

1.2.3. Mesh classification

Synthetic meshes are classified to 4 types with respect to pore size, composition (polymer type), filament type (monofilament or multifilament), knitted mesh design and surface properties (coated versus non-coated). Monofilament mesh induces less inflammation compared to multifilament because immune cells get trapped between the filaments (Klinge et al., 2002) and larger pore sizes induce better tissue integration and less inflammation (Pascual et al., 2008). Microporous mesh (10um pores) induces a greater host response because immune cells are unable to go into the mesh. Overall, monofilament mesh with large pore size is preferable (Huebner et al., 2006).

1.2.4. Anterior vaginal wall repair with mesh

The anatomic cure rate for anterior colporrhaphy using degradable or non-degradable materials ranges from 92 to 97% after 12 months follow up (Hinoul et al., 2008, Milani et al., 2011, Stanford et al., 2011) (Fig.4).



Figure 4. Anterior colporrhaphy

Schematic shows placement of synthetic or biological graft material used to repair the prolapse in the Ba region – reproduced with permission from BARD Medical.

There was 94% success rate in non-absorbable polypropylene mesh-reinforced anterior colporrhaphy in a group of 63 women (mean age 63 years) who were followed for 17months. In this study, dyspareunia increased by 20%, 6.5% of women had vaginal erosion of the mesh, and one required mesh removal for pelvic abscess (Milani et al., 2005).

Comparing the efficacy and safety of anterior colporrhaphy and transvaginal monofilament PP mesh surgery in a controlled trial study which was carried out on 43 women with prolapse stage II or higher, showed greater improvement in symptoms and quality of life in mesh treatment group after 2 years, although mesh exposure rate was 13.5% (Dias et al., 2016). In another study by Nieminen K et al, 202 women underwent colporrhaphy alone or PP vaginal mesh surgery and were followed up for a maximum 36

months after surgery. Although the anatomic recurrences in mesh treated group was less than surgery alone, the symptomatic recurrence rate was not significantly different and mesh erosion rate was high (19%) (Nieminen et al., 2010).

1.2.5. Posterior vaginal wall repair with mesh

It was reported that the cure rate for posterior vaginal wall repair with mesh is between 75-92% (de Tayrac et al., 2006b) (Fig.5); however, the mesh complication rate is also high (up to 25%) (Stanford et al., 2011).

Initial experience of surgical rectocele repair used a biological material in the form of a rectangular dermal allograft in 43 women with advanced posterior vaginal wall prolapse. At an average follow-up period of 12.9 months, surgical cure was 93% (Kohli and Miklos, 2003). The functional and anatomic outcomes after transvaginal rectocele repair using Pelvicol (CR Bard), a non-crosslinked porcine collagen mesh, was evaluated in 32 patients. At the 6 and 12-month follow-up visits, five and seven patients were found to have at least stage II prolapse of the posterior segment, respectively. The authors concluded that there may be a substantial risk for rectocele recurrence 1 year after surgery with degradable biological mesh (Altman et al., 2005). Three randomized controlled trials comparing native tissue repair to synthetic mesh in posterior vaginal wall prolapse failed to show a significant difference between groups (Carey et al., 2009, Sokol et al., 2012, Withagen et al., 2011).

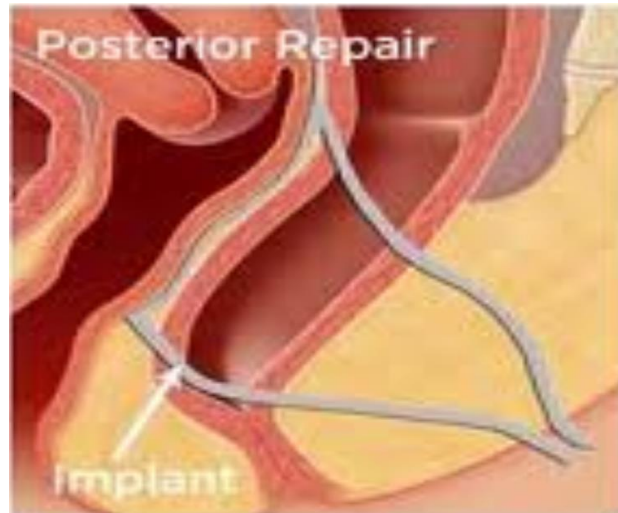


Figure 5. Posterior colporrhaphy

Schematic shows a graft material placed in the Bp region of the posterior vaginal wall. The schematic is reproduced with a permission from the BARD Medical.

1.2.6. Apical compartment repair with mesh

Abdominal sacrocolpopexy has remained the best treatment for apical vaginal prolapse (Fig.6). Success rates to preserve the apical support for this procedure ranged from 78 to 100% over a follow-up period of 6 months to 3 years (Nygaard et al., 2004). Mesh or erosion rates were between 3-12% of patients after 6-36 month follow up (Drutz and Alarab, 2006). Prolapse recurrence at the level of the anterior and apical compartment occurs significantly more often when using a bio-graft, in comparison to polypropylene (21 vs 3%, $p < 0.01$ and 36 vs 19 %, $p < 0.05$ respectively) (Deprest et al., 2009) indicating that biological materials fail due to resorption.



Figure 6. Abdominal sacrocolpopexy

Adopted with permission from American Urological Association Update Series, Vol 31, lesson 11, Dr. Burgess and Dr. Elliot.

1.3. Problems associated with synthetic mesh

Although transvaginal mesh surgery is simpler and less invasive than traditional surgical treatment for POP, it may cause complications in approximately 10% of women (de Tayrac R, 2006). According to the recent ACOG committee's opinion (American College of Obstetricians and Gynaecologists), synthetic mesh erosion or exposure is the most common complication (Ellington and Richter, 2013a). Other reported problems are infections, pain, nerve damage, urinary problems and recurrence of prolapse. On Oct. 20, 2008, the FDA issued a public health notification and additional patient Information on serious complications associated with surgical mesh placed through the vagina (transvaginal) for POP treatment. From 2008 to 2010, the most frequently reported complications from vaginal mesh surgery included vaginal mesh erosion (exposure,

extrusion), pain, infection, bleeding and urinary problems (FDA, 2011). Based on an updated analysis of adverse events reported to the FDA since 2008 and complications described in the scientific literature, the FDA identified surgical mesh for transvaginal repair of POP as an area of continuing serious concern. On Jul 2011 the FDA issued an update to inform health care providers and patients that serious complications associated with the use of surgical mesh for transvaginal repair of POP are not rare (FDA, 2008, FDA, 2011). This led to class action litigation and some companies withdrawing vaginal surgical mesh from the market.

1.3.1. Mesh exposure and erosion

An erosion is defined as vaginal mesh visualized through adjacent organs (bladder and bowel), whereas a mesh exposure is the gradual passage of mesh through vaginal epithelium (Haylen et al., 2011). Two studies which evaluating the use of polypropylene mesh to enhance the surgical correction of anterior vaginal prolapse reported an erosion rate of 8.3–11% (Milani et al., 2005, de Tayrac et al., 2006a). In an update to their original 2008 systematic review, The Society of Gynaecologic Surgeons (SGS) analysed 110 studies reporting adverse events associated with vaginal mesh applications in POP surgery and revealed an overall erosion rate of 10.3% (Abed et al., 2011).

1.3.2. Mesh contracture

Another complication of vaginally-placed mesh is contraction, shrinkage, or reduction in the size of the vaginal mesh implant that may lead to vaginal shortening and pain. The etiology is still unclear and several possibilities have been suggested. One is inadequate tissue ingrowth into the mesh. A comparison of tissue ingrowth between large pieces of polyester (PE) and heavyweight PP and mesh contraction revealed a significant

correlation between tissue ingrowth force and mesh size. In this study PE resulted in less contraction than PP, indicating that strong integration of mesh into tissue prevents contracture. They have also reported the importance of suturing as the meshes which detached from their anchor point underwent the greatest contraction (Gonzalez et al., 2005) Another theory is that contracture results from the consequences of inflammatory response to the mesh. In a study by Garcias, the contraction of PP mesh was assessed after implantation in an abdominal muscle defect. They found a significant degree of PP contraction occurred during the scaring and remodeling process. They considered this contraction as a consequence of mesh incorporation to scar tissue which shrinks as it matures (Garcia-Urena et al., 2007).

A recent case series reported that all seventeen women undergoing surgical intervention for mesh contraction presented with severe vaginal pain and focal tenderness over the contracted portions of the shortened mesh. Furthermore, seven had vaginal tightness, and five vaginal shortening (Milani et al., 2005, Ellington and Richter, 2013b).

1.4. Problems associated with biological meshes

Biological meshes can be an alternative for synthetic meshes to avoid local complications but due to their similarity with native tissue, they also are associated with problems that should be taken into account. These include autologous grafts which have surgical morbidity and their unpredictable durability of the repair, because after absorption, the replacement host connective tissue is inherently weak (Deprest et al., 2006). Allografts can overcome the problem of surgical morbidity, but do not address the unpredictable resorption and integration process (de Tayrac R, 2006).

The recurrence rate of cystocele repair with porcine dermis in 119 patients was 36% compared with to 4% in PP mesh surgery and 6% in anterior colporrhaphy (Handel et al., 2007). There was a high anatomical and functional failure rate of 25% in a follow up study of sacrocolpopexy for apical vaginal prolapse using xenogeneic porcine graft in 22 patients with symptomatic apical prolapse and increased risk of Graft Related Complication (GRC) (Claerhout et al., 2010). In an animal study, rats were implanted with Small Intestine Submucosa (SIS) developed seromas with fluid accumulation between tissue layers in first 14 days, and even some low-grade local infections (Konstantinovic et al., 2005).

In summary, the ideal mesh for vaginal POP surgery has not yet been reported and given the complications associated with synthetic and biological mesh, there is an urgent need for alternative and newly designed mesh for treatment of women suffering from POP.

1.5. New meshes for vaginal POP surgery

The ideal mesh for POP surgery is inert, sterile, resistant, not carcinogenic, and causes less inflammatory response (Depreest et al., 2006). In addition, it is inexpensive, readily available and easy to use. However, none of the currently available graft materials fulfil the 'ideal'. Recently, our laboratory has shown that meshes knitted from alternative materials (polyether-ether-ketone and polyamide (PA) with similar physical characteristics to the commercially available PP meshes have improved biomechanical properties with reduced stiffness and a lower bending rigidity (Edwards et al., 2013) (Fig.7). Biocompatibility assessment of these meshes in a rat abdominal hernia model showed that PA and particularly PA+Gelatin (PA+G) composite meshes capable of delivering cells, resulted in better tissue integration and new collagen deposition as well

as greater neovascularization compared with PP meshes. In addition, PA and PA+G meshes induced a milder inflammatory response (Ulrich et al., 2012)

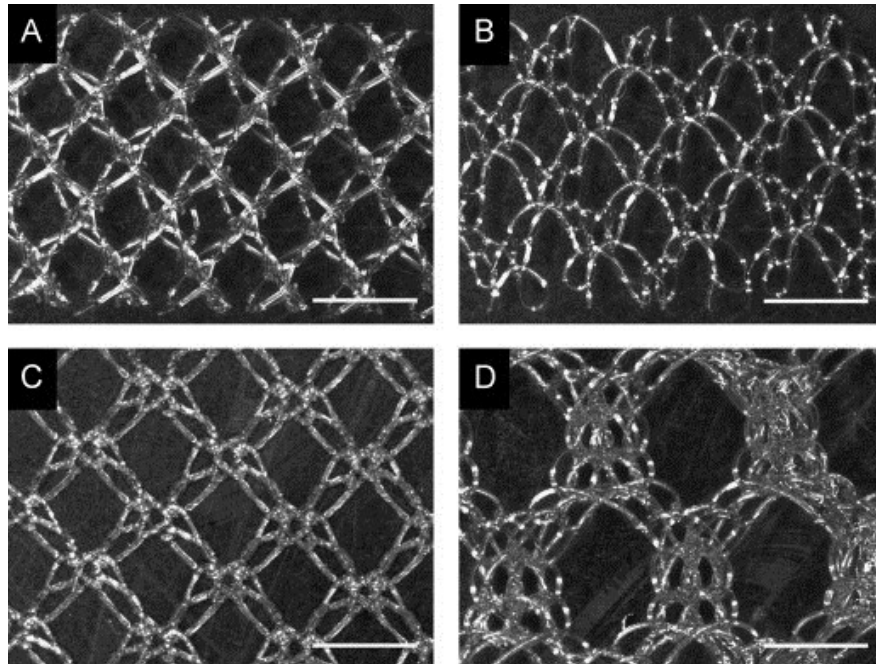


Figure 7. Optical micrograph of fabricated meshes

A. polyamide, B. poly-ether-ether-ketone (PEEK1), C. Polyform (PP) clinical mesh D. poly-ether-ether-ketone (PEEK2). PEEK2 possessed pores approximately twice the size of the PEEK1 mesh. Reproduced with permission from Edwards et al., 2013. J Mech Behav Biomed Mater.

1.5.1. Mesh products with collagen coating

Several human studies have reported on the use of composite meshes that include collagen layers (Meschia et al., 2007, Rudnicki et al., 2016, Lo et al., 2016). In these studies, less erosion, lower reoccurrence rate and increased neovascularization was

reported in groups treated with collagen-coated mesh. Compared to non-coated mesh, Soft Prolene, and Ugytex collagen-coated meshes resulted in fewer erosions (16.7% vs. 33.3%) following anterior and posterior implantation in a sheep model (de Tayrac et al., 2007). The authors hypothesized that this reduction could have been due to lesser adhesion of the collagen-coated mesh to the wound. However, some studies failed to show the modulatory effect of collagen coating of PP on the host response compared with non-coated PP (Feola et al., 2015). Assessing the host response to two synthetic PP mesh (collagen-coated and non-coated) in rabbit vagina showed that both meshes induced mild inflammatory responses without evidence of erosion (Huffaker et al., 2008). More studies are needed to assess the effect of collagen coated PP mesh in the host response and biocompatibility of the mesh.

1.6. Mesenchymal Stem Cells

In addition to hematopoietic stem cells and endothelial progenitor cells, bone-marrow contains a subset of non-hematopoietic stem/stromal cells possessing multi-lineage mesodermal differentiation potential, commonly called marrow stromal stem cells or mesenchymal stem cells or multipotent mesenchymal cells (MSC) (Malgieri et al., 2010, Bianco et al., 2013, Caplan, 2010).

1.6.1. Properties and phenotype of Mesenchymal Stem Cells

Bone-marrow mesenchymal stromal/stem cells were the first MSC to be isolated and extensively characterized. Friedenstein et al. were the first to demonstrate that within the stromal fraction of bone marrow, there existed a clonogenic population with the ability to create heterotopic bone and bone marrow microenvironment upon *in vivo* transplantation in mice (Friedenstein et al., 1968). Based on International Society for Cellular Therapy

(ISCT) guidelines, MSC must fulfil three criteria including: plastic adherence, multi-lineage differentiation into osteoblasts, adipocytes, chondrocytes and express the surface markers such as CD29, CD44, CD73, CD105 and CD146 but not the hematopoietic cell markers including CD34, CD45, CD14, CD11b, CD79a, CD19 and HLA-DR (Dominici et al., 2006, Caplan, 2007). However, MSC from different tissues may have unique markers which can be used for their isolation and the ISCT criteria may not be useful to characterise MSC from every tissue type. For example, the ISCT surface markers are not unique and are found on many other cells including fibroblasts (Darzi et al., 2016b).

MSC have colony-forming unit (CFU) activity which is defined as the ability of a single cell to form a clone of cells when seeded at extremely low density (Deans and Moseley, 2000). Bone-marrow CFU-F also exhibit self-renewal ability (Bianco et al., 2001). Through asymmetric divisions, stem cells produce the right number of more differentiated transit amplifying (TA) cells, as well as daughter stem cells with properties identical to those from which they arose. TA cells have properties intermediate between stem cells and differentiated cells. They have limited proliferative potential and inability to self-renew, however, they undergo several rounds of cell division and acquire differentiation markers as part of the cellular amplification process. (Morrison et al., 1997) (Fig.8).

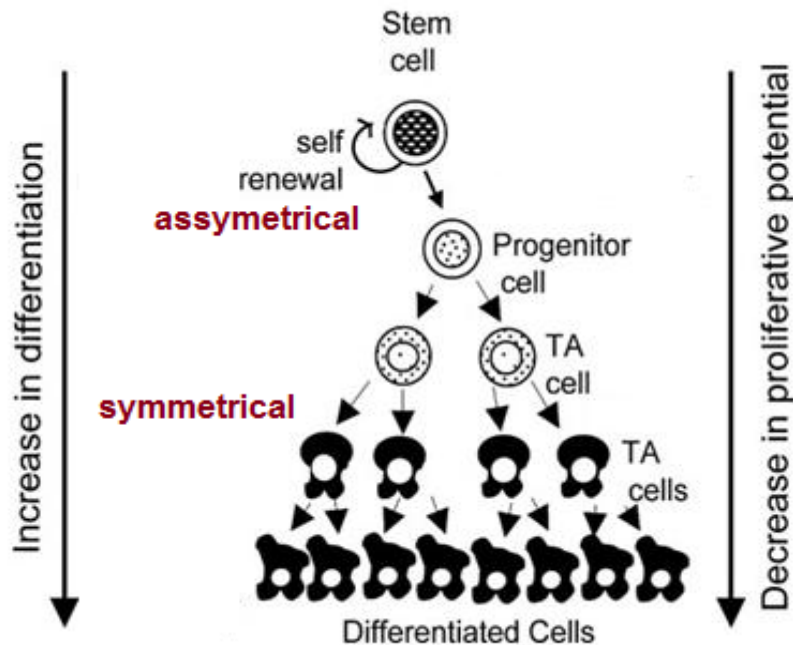


Figure 8. Cellular hierarchy showing self-renewal ability of adult stem cells

Stem cells undergo asymmetric/symmetric cell divisions, which enable them to self-renew and replace themselves and differentiate to give rise to committed progenitors, then more differentiated Transit Amplifying cells and finally fully differentiated functional cells of the tissue. Reproduced with permission from Chan et al Biology of Reproduction 2004.

1.6.2. MSC niche

The identification of CD146 as a marker of pericytes, shows that MSC with self-renewing and skeletogenic capacities occupy a perivascular niche in the bone marrow (Sacchetti et al., 2007). Moreover, non-endothelial, non-hematopoietic cells expressing CD146 from different tissues overlapped with pericytes in situ and these cells also expressed MSC markers and had MSC properties *in-vitro*. Indeed, most of the large and small blood vessels in the body have a perivascular MSC on the abluminal surface of the endothelial

cells. When these vascular-associated cells are isolated and assayed in culture, they have MSC-like characteristics (Caplan, 2007). The observations clearly show that a subpopulation of cells with MSC markers also express pericyte markers and it is speculated that all MSC are pericytes (Caplan, 2008). This relationship is further emphasized by cell sorting for pericytes (CD146⁺, CD34⁻, CD45⁻, CD56⁻) and their subsequent *in vitro* expansion. The sorted cells form clones which are multipotent differentiation into osteogenic, chondrogenic, adipogenic lineages *in vitro*, hallmarks of MSC identity (Caplan, 2007, Caplan, 2008).

Some of the MSC properties including differentiation to mesodermal lineages, mesenchymal marker expression and proliferation are common with fibroblasts, however fibroblasts are not clonogenic and they are not perivascularly located (Gargett et al., 2016).

1.6.3. Sources of MSC

MSC have been isolated from almost every type of tissue including bone marrow, adipose tissue, dental pulp, umbilical cord, corneal stroma, cord blood, skeletal muscle, placenta and endometrium (Gronthos et al., 2000, Gronthos et al., 2001, De Bari et al., 2003, Schwab and Gargett, 2007, Crisan et al., 2008, Brooke et al., 2009, Branch et al., 2012). MSC can differentiate to ectodermal and endodermal lineages as well as mesodermal germ layers which make them an attractive source for cell based therapies (Pittenger et al., 1999). It is now recognised that MSC home to damaged tissue where they act in paracrine manner to promote tissue repair by secreting growth factors and bioactive molecules including Vascular Endothelial Growth Factor (VEGF), Angiotensin (AT I and II), indoleamine 2,3-dioxygenase (IDO) and Transforming Growth Factor beta (TGFβ).

These secreted molecules induce angiogenesis, inhibit inflammation and apoptosis and promote the proliferation of tissue specific progenitor cells (Caplan, 2009, Murphy et al., 2013).

1.6.4. MSC as modulator of the immune system

MSC have received renewed interest clinically, particularly for their use in transplantation medicine as modulators of the immune system. MSC have the ability to influence almost all cells of the innate and adaptive immune systems, through secretion of bioactive molecules which modulate cellular proliferation, differentiation, maturation, and function by exerting anti-inflammatory effects (De Miguel et al., 2012).

1.6.5. MSC and innate immune system

MSC modulate the innate and adaptive immune systems. Co-culture of monocytes with human or mouse bone marrow MSC (bmMSC) promotes their conversion to M2 macrophages, which produce high levels of IL-10, increase their phagocytic activity, reduce their production of Tumor Necrosis Factor alpha (TNF- α) and Interferon gamma (IFN- γ) production, and lowers MHC class II expression (Le Blanc and Davies, 2015). These effects on monocyte differentiation results from a combination of cell-contact-dependent and soluble-factor-dependent mechanisms. These include increasing MSC-derived IDO activity and the binding of MSC-derived PGE2 to macrophage PGE2 receptors (Maggini et al., 2010). Human MSC also modulate NK cell activity by inhibiting IL-2 and IL-15 driven proliferation but do not affect their cytotoxicity (Sotiropoulou et al., 2006). By contrast, MSC co-cultured with IL-2 or IL-15 activated NK cells interfere with cytotoxic activity, cytokine production, granzyme B release and the expression of activating killer receptors (e.g. NKp30, NKp44 and NKG2D) by these cells (Spaggiari et

al., 2006). MSC can modulate Dendritic Cell (DC) responses. DC bridge the innate and adaptive immune system by producing cytokines and act as antigen presenting cells. MSC inhibit endocytosis in DC and suppress MHCII expression on these cells as well as inhibition of co-stimulatory molecules (Wang et al., 2014). Taken together, MSC modulate the key cells with specific roles in inflammation, and the innate immune system.

1.6.6. MSC and adaptive immune system

T lymphocytes (T cells) and B lymphocytes (B cells) are the two major executor cells of the adaptive immune response, and MSC modulate the function of both cell types. MSC affect the proliferation, differentiation and maturation of B cells in a dose dependent manner (Augello et al., 2005, Corcione et al., 2006, Comoli et al., 2008). MSC can inhibit the T cell response to mitogens, antibodies and allogeneic cells (Bartholomew et al., 2002, Di Nicola et al., 2002).

MSC release a vast array of molecules e.g. IL-10, TGF β , Galectin 1, (GAL-1) Galectin 3 (GAL-3) and Leukemia Inhibitory Factor (LIF) and bioactive metabolites e.g. Nitric Oxide (NO), Carbon Monoxide (CO) and Prostaglandin E2 (PGE2) that have immunomodulating properties (Le Blanc and Mougiakakos, 2012). They do not express MHC class II or most of the classical co-stimulatory molecules, CD80, CD86, or CD40, involved in immunological processes. However, MSC can express class II molecules on their surface under specific conditions, after induction with IFN- γ (Le Blanc et al., 2003). This is a relevant finding because in many inflammatory milieus, IFN- γ is up regulated, which in turn may result in an increase in the expression of MHC class II or MSC in the vicinity. (Le Blanc et al., 2003). MSC modulate cellular and humoral immunity by affecting T and B lymphocyte proliferation, maturation and activation.

1.6.7. MSC- Graft-Versus-Host-Disease (GVHD)

GVHD is a common problem following allogeneic tissue transplantation and is associated with high rates of mortality. Recipients of allogeneic transplants often experience acute GVHD due to alloreactive T cells present in the allograft (Zeng et al., 2004, Elfenbein and Sackstein, 2004). MSC can effectively suppress the GVHD process. Patients with steroid-resistant, severe, acute GVHD were treated with MSC obtained from HLA-identical sibling donors, haplo-identical donors and HLA-mismatched donors. No patient showed side effects during or after MSC injection. Seventy percent of recipients responded to MSC treatment and survival was significantly higher in this group compared to those with partial or no response (Barrett and Le Blanc, 2008). The ability of MSC to interact with HLA-unrelated immune cells and modulate their response has important implications in transplantation biology.

1.6.8. MSC role in tissue regeneration and wound repair

MSC respond to stress or injury in a similar manner as the adaptive and innate immune system cells respond to pathogens (Dimarino et al., 2013). MSC home to sites of injury and inflammation, sensing the requirement of the environment and producing factors and bioactive molecules which promote angiogenesis, cellular recruitment and tissue remodeling. Since MSC are pericytes, injury effects on blood vessels may stimulate their differentiation into MSC which modulate the microenvironment through trophic factor secretion (Caplan, 2008, Crisan et al., 2008). The ability of MSC response to different tissue microenvironments operates through receptor recognition and signal transduction followed by the release of factors and molecules which in turn contribute to the milieu to

control inflammation and promote repair (Dimarino et al., 2013). MSC are involved in the wound healing process mainly through their immune inhibitory effects. They inhibit TNF- α production in a co-culture system while simultaneously increasing the secretion of the anti-inflammatory cytokine IL10 (Aggarwal and Pittenger, 2005). It has also been recognized that MSC have anti-microbial activity which is mediated by two mechanisms; secretion of anti-microbial factors such as IL37, and secretion of immune -suppressive factors (Mei et al., 2010, Nold et al., 2010).

1.7. Endometrial Mesenchymal Stem Cells

Human endometrium is a highly regenerative tissue which undergoes more than 400 cycles of regeneration, differentiation and shedding during a woman's reproductive life (Jabbour et al., 2006, Gargett, 2007a). Human endometrium is structurally and functionally divided into two regions; 1. The functionalis which comprises the upper layer of endometrium and is shed every month during menses and the lower layer which contains dense stroma, gland bases and vessels and is responsible for generating a new functionalis layer each month (Spencer et al., 2005, Gargett, 2007b). Each month, the endometrial thickness increases between 4-10mm during the proliferative stage of the menstrual cycle. This level of new tissue growth is similar to cellular turn over in highly regenerative haematopoietic tissue of the bone marrow (Gargett, 2007a)

Human endometrial mesenchymal stem cells (eMSC) were first identified in cell cloning studies, which showed that a small proportion of clonogenic human endometrial stromal cells can generate colonies containing small, densely packed cells, likely originated from stromal stem cells or Colony Forming Unit (CFU-F) (Chan et al., 2004). These CFU-F initiating cells are highly proliferative and are able to undergo more than 30 population

doublings before reaching senescence. They are able to grow at very low densities (5-10 cell/cm²) in serial cloning assays indicating self-renewal *in-vitro* (Gargett et al., 2009). Stromal CFU-F differentiate into classical mesodermal lineages including smooth muscle and express the typical MSC surface markers including CD29, CD44, CD73, CD90 and are negative for hematopoietic markers such as CD31, CD34 and CD45 (Gargett et al., 2009). Stromal CFU were also detected in non-cycling endometrium from women on oral contraceptives and also from post-menopausal endometrium (Schwab et al., 2005, Ulrich et al., 2014c) suggesting that under oestrogen influence, the CFU-F may play a role in regeneration of atrophic endometrial stroma (Gargett and Masuda, 2010). Indeed, in post-menopausal women treated with oral estradiol valerate for 8 weeks, CFU-F with all the classic MSC properties were identified in their regenerated endometrium (Ulrich et al., 2014d).

1.7.1. Markers identifying eMSC

Clonogenic eMSC express the perivascular markers, CD140b and CD146, with almost all the endometrial CFU-F found in CD140b⁺CD146⁺ sorted population (7.7% versus 0.7% in the CD140b⁻CD146⁻ population) (Schwab and Gargett, 2007). In 2012, our group reported SUSD2 as a novel single perivascular marker enabling the prospective isolation of multipotent, self-renewing eMSC that generated endometrial stroma *in vivo* (Fig.9) (Masuda et al., 2012). In this study, magnetic bead selected SUSD2⁺ eMSC self-renewed *in vitro* and differentiated into adipogenic, osteogenic, chondrogenic, endothelial and myogenic cell lineages. The CFU-F capacity of sorted SUSD2⁺ eMSC showed a 3-fold increase over unsorted stromal cells and 14.7-fold increases over SUSD2⁻ cells. Almost all the clonogenic stromal cells sorted into the SUSD2⁺ population. SUSD2⁺ eMSC

expressed typical MSC markers, underwent multilineage mesodermal differentiation and were found in a perivascular region of both basalis and functionalise layers of human endometrium (Masuda et al., 2012) and in postmenopausal endometrium (Ulrich et al., 2014d)

1.7.2. eMSC niche

The putative eMSC niche was first identified in a Label Retaining Cell (LRC) study in mice. In this study, mouse endometrial cells were labelled with a DNA synthesis label (BrdU) and the label was chased over a long period of 8 weeks (Chan and Gargett 2006). With each cell division, the BrdU is diluted 50% until it reaches undetectable levels by immunofluorescence after 3–4 cell divisions, revealing the location of slow dividing cells, and their stem cell niche. Six percent of mouse endometrial stromal cells were identified as LRC, with approximately one third located near blood vessels close to the endometrial–myometrial junction and expressing α SMA (Alpha Smooth Muscle Actin) , suggesting that some LRC are perivascular cells (Chan and Gargett, 2006) similar to human endometrial $CD146^+PDGFR\beta^+$ co-expressing cells or $SUSD2^+$ pericyte and perivascular cells (Fig.9). (Gargett et al., 2016) The role of endometrial stromal cells in initiating the estrogen-stimulated endometrial growth was investigated with a single injection of 17β -estradiol (E2) in BRDU labeled and chased, ovariectomized mice. Eight hours after E2 injection, 12% of stromal LRC initiated a proliferative response. Stromal LRC lack the estrogen receptor (ESR1). This finding suggested that the ability of these cells to act as stem cells receiving proliferative signals from $ESR1^+$ niche cells to initiate new endometrial stromal growth (Chan et al., 2012)

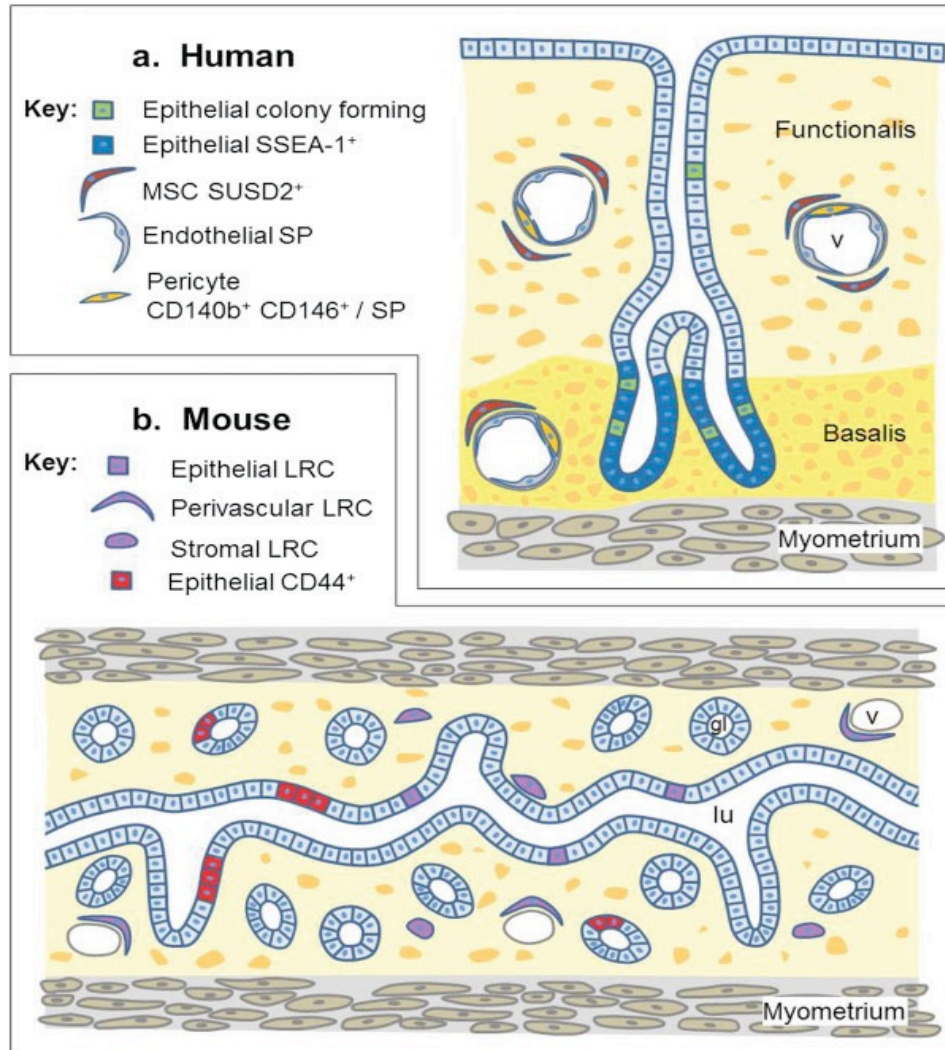


Figure 9. Location of eMSC in human endometrium.

a. In human endometrium eMSC are pericytes and perivascular cells of blood vessels in both the basalis and functionalis. b. in mouse endometrium stromal LRC are located in perivascular region and endometrial stroma. reproduced with permission from Gargett et al, Human Reproduction Update 2012, Oxford University Press.

1.7.3. Endometrial regenerative cells in menstrual blood (ERC)

Since eMSC have been identified in the functionalis and basalis, it is expected that they would be shed in menstrual blood (Gargett and Masuda, 2010). Indeed, several studies have cultured stromal cells from menstrual blood in a manner similar to bone marrow-derived MSC (Meng et al., 2007, Patel et al., 2008, Darzi et al., 2012). In these studies, menstrual blood was cultured directly onto plastic flasks resulting in adherent heterogeneous cultures of stromal fibroblasts and MSC. The adherent cells rapidly expand, doubling every 18–36 h, and undergoing 25-30 population doublings (Hida et al., 2008). Cultured menstrual blood MSC (mbMSC) (also called endometrial regenerative cells and menstrual blood stromal stem cells) have a fibroblastic morphology and express similar phenotypic surface markers as clonogenic and CD146⁺PDGF-R β ⁺ eMSC, and similarly lacked haematopoietic, endothelial and other stem cell and MSC (Stro-1) markers (Cui Ch, 2007, Hida et al., 2008). They fulfilled the ISCT criteria for MSC.

1.7.4. Immunomodulatory properties of eMSC

Given that the MSC properties of endometrial stem/stromal cells are similar to bone marrow MSC, their immune regulatory properties are also likely similar. However, few studies on eMSC-immune system interactions exist. A study by Peron et al revealed that mice receiving intraperitoneal injection of human endometrial derived MSC (hedMSC) from endometrial biopsies collected during the proliferative phase, significantly reduced a clinical score in an experimental autoimmune encephalomyelitis mouse model (Peron et al., 2012). Fewer infiltrating immune cells were observed in the central nervous system of hedMSC-treated animals compared to the control group. The hedMSC treated animals also displayed a lower percentage and absolute numbers of both inflammatory Th1-

(CD4⁺ IFN- γ) and Th17 (CD4⁺IL17⁺) cells. Moreover, the expression of the tryptophan-depleting enzyme, IDO, was also up-regulated in the hedMSc-treated group, which was associated with increased Foxp3 cells, indicating a higher percentage of regulatory T cells (Peron et al., 2012). Addition of endometrial regenerative cells (ERC) to an ongoing mixed lymphocyte reaction resulted in suppression of T cell proliferation, inhibition of IFN- γ production, stimulation of IL-4 secretion, and inhibition of TNF- α after LPS stimulation (Murphy et al., 2008). These few studies indicate that plastic adherent eMSC/fibroblasts have immunoregulatory effects. However, it is not known if purified populations of eMSC have immunomodulatory effects.

1.8. Tissue engineering

Tissue engineering (TE) is a combination of cells and materials implanted into the body to improve repair of injured tissues. It is a major area of research in regenerative medicine that aims to restore, maintain and improve tissue function (Langer and Vacanti, 1993, Vacanti and Langer, 1999, Shafiee and Atala, 2016). Tissue engineering strategies are classified into two categories: the use of acellular scaffolds or scaffolds seeded with cells (Boennelycke et al., 2013, Langer and Vacanti, 2016). A wide range of synthetic non-degradable and degradable polymers as well as biological materials have been used in tissue engineering applications. Different cell types can be used in TE including autologous (from same person or animal), allogeneic (from different person or animal strain) or xenogeneic (different species) (Fisher and Mauck, 2013). Autologous cells are preferred as they do not evoke an immune response and rejection is unlikely to occur. MSC can be used for allogeneic transplantation considering their modulatory effects on immune cells.

1.8.1. MSC in tissue engineering

The differentiation ability of MSC has been exploited to restore and regenerate tissues, by embedding them in scaffolds and implanting them into injured tissues. Different techniques have been employed to use MSC in tissue regeneration. MSC can be loaded into the scaffolds *in vitro* and implanted to the tissue site after short term culture (eg several days) (Solchaga et al., 2000). Alternatively, MSC-loaded scaffolds are cultured in differentiation medium to pre-differentiate MSC to the required specific lineage, before implantation (Ohgushi et al., 2005). These methods have resulted in better integration of the cells and newly formed tissues.

1.8.2. Tissue engineering approach for POP treatment – use of eMSC

Stem cell therapy for POP treatment is challenging as the herniated tissue requires support for the herniated pelvic organs. In tissue engineering approaches, degradable and non-degradable scaffolds provide a three-dimensional base in which the stem cells can be delivered, grow and form new tissue. The loaded scaffolds provide the mechanical support of prolapsed organs either directly by generating new tissue from transplanted cells or indirectly by paracrine stimulation of resident-tissue stem cells (Ulrich et al., 2013b). A number of tissue engineering approaches using bmMSC have been explored in abdominal wall hernia repair (Drewa et al., 2005, Falco et al., 2008, Ayele et al., 2010). To develop a tissue engineered material for SUI and POP, human adipose-derived stem cells (ASC) and oral fibroblasts were compared for extracellular matrix (ECM) production and attachment on a biodegradable scaffold of thermo-annealed poly-L-lactic acid (PLA) for two weeks. Both cells showed good attachment and proliferation and hAMSC seeded

scaffolds produced more total collagen and a denser ECM in both conditions than scaffold alone (Roman et al., 2014).

Recently, our group assessed the biological and biomechanical behavior of a polyamide/gelatin mesh seeded with eMSC in a subcutaneous rat model of wound repair as a preclinical model for POP repair surgery (Ulrich et al., 2014).

Our results revealed that eMSC significantly improved the biocompatibility of these novel mesh designs. The eMSC promoted significantly greater early neovascularization, a stronger initial M1 inflammatory response which changed to a pro-wound healing M2 ($P < 0.05$) response over time, reducing the chronic inflammatory response around mesh filaments in the long term (90 days). Meshes seeded with eMSC were less stiff than those without cells (Ulrich et al., 2014). The amount of deposited rat collagen was similar for eMSC/mesh and mesh alone but the quality of collagen organization was enhanced in PA+G mesh seeded with eMSC (Edwards et al., 2015). Collagen fibers became oriented in mesh seeded with eMSC, showing physiological crimping rather than bands of scar tissue observed for mesh alone resulting in reduced stiffness than PA+G mesh without cells (Edwards et al., 2015).

1.9. Animal models for investigating POP

To study the natural progression of POP and assess novel treatments *in vivo*, an appropriate animal model is necessary. However, developing a functional animal model for POP is challenging as humans have a unique pelvic floor orientation and a difficult childbirth delivery process (Couri et al., 2012). Several animal models including small rodent models can be used to model abdominal hernia while the ovine model

spontaneously develop POP(Young et al., 2017). Several of these models have been used for assessing the biocompatibility of our eMSC/mesh tissue engineering constructs for our POP investigation.

1.9.1. Rodent models

Currently, rodents are the most widely used animal model for prolapse and incontinence research. Both rats and mice are small, inexpensive and easy to work with in large numbers (Abramowitch et al., 2009, Couri et al., 2012). An additional advantage of working with mice is the use of genetically modified animals to enable mechanism of action to be determined (Drewes et al., 2007). Rats have 4 day oestrus cycles and undergo gestation for 19–23 days before delivering litter sizes ranging from 4 to 16 fetuses (Chow and Agustin, 1965). Mice have a similar oestrous cycle between 4 and 5 days in length depending on environmental factors (Champlin et al., 1973). The similarity between the structure and function of the vaginal connective tissues in rodents and humans makes the rodent a preferred model for evaluating connective tissue support (Couri et al., 2012). The rat has been used as a model for evaluating the structural properties of the vagina and its supportive tissues, showing that rat vagina is supported by structures analogous to those in humans (Moalli et al., 2005a). In the first tissue engineering report for vaginal repair in a rodent model, mouse muscle-derived stem cells (MDSC) cultured on SIS generated smooth muscle cells upon implantation in a rat vaginal defect model (Ho et al 2009). The results revealed the stimulatory effects of MDSC/SIS on the regeneration of vaginal tissue 4 weeks after surgery (Ho et al., 2009). An abdominal hernia model has also been used to assess new mesh designs for potent POP treatment (Ulrich et al., 2012). Although, rodent models are useful, unlike human, the

pelvic floor is horizontally oriented and they have a smaller fetal head relative to the pelvic outlet than do humans (Couri et al., 2012)

1.9.2. Ovine model

The ewe has been evolving as a large animal model for evaluating POP and POP treatment. The sheep oestrus cycle is 17 days and average gestation is 147 days (Abramowitch et al., 2009). Advantages of the ovine model are that ewes have prolonged labors with relatively large fetuses and spontaneously develop POP postpartum, with an incidence highest in mature, multiparous sheep (Couri et al., 2012, Young et al., 2016). The pelvic connective tissue anatomy of the ewe is similar to that of macaque and human with the same three primary levels of support of the pelvic organs. Their similar vaginal dimensions to women make them amenable to prolapse repairs (abdominal and vaginal) with or without mesh implantation (Abramowitch et al., 2009, Urbankova et al., 2017). However, ewes lack the obturator pelvic floor muscle (Urbankova et al., 2017), which is frequently damaged in women following childbirth (Dietz et al., 2012). One issue that potentially limits the utility of the ewe as a pre-clinical model is that they are quadrupedal as opposed to humans who are bipedal and have upright posture. The ewe does not therefore experience the same increases in intra-abdominal pressures experienced by women which is a significant factor in the development of POP (Couri et al., 2012). This is partially offset when pregnant ewes ruminate facing uphill and where a perineal bulge can sometimes be observed (Couri et al., 2012). Our laboratory compared ovine and human posterior vaginal tissue for histological and biochemical tissue composition. Quantifying total collagen (collagen type I and III), GAG (Glycose-Amino-Glycans) and elastin-associated proteins biochemically showed that both sheep and human vaginal

tissue have comparable tissue composition (Ulrich et al., 2014c). Higher total collagen and GAG were observed nearest the cervix, but no significant differences were found along the length of the human vagina for extracellular matrix proteins. Biomechanically, the proximal region near the cervix was the stiffest and most distensible compared to the distal region (Ulrich et al., 2014c).

Given the similarities between human and ewe reproductive anatomy including the size of vagina, the pelvic structure and the biomechanics of vaginal tissue, the ewe may be a good animal model for POP studies.

Non-human primates could also be a suitable model for POP as they have a similar anatomy to human, have a more upright posture and spontaneously develop POP (Otto et al., 2002). However, they are expensive and ethical restrictions are another limiting factor (Knight et al., 2016).

1.10. Host response to tissue engineering construct

The host response to foreign implanted material occurs immediately after biomaterial implantation. Blood-material interaction results in protein adsorption to biomaterial surface which forms a matrix of plasma proteins around the material (Anderson et al., 2008) This matrix is rich in chemokines, cytokines and growth factors which are important factors for innate immune cell recruitment and activation in the early wound healing response (Anderson et al., 2008). Following matrix formation an acute inflammatory response ensues where the neutrophils along with mast cells are the first cells to arrive at the implanted wound site. These cells secrete histamine, cytokines and chemokines which then attract monocytes and macrophages to the implantation site (Tang et al., 1998). After the acute response, resolution or chronic inflammation ensues, depending

on the degradability of the implant. Chronic inflammation is identified by presence of mononuclear cells including, monocytes, lymphocytes, macrophages and foreign body giant cells (Anderson et al., 2008). Following resolution of the chronic response, granulation tissue is observed, comprising macrophages, fibroblast infiltration and neovascularization (Pascual et al., 2008).

During the host response to biomaterials, two main types of macrophages can be identified. These have been classified as “M1” and “M2” macrophages. Pro-inflammatory M1 macrophages are characterized by their role in pathogen killing and are associated with classic signs of inflammation. In the acute phase of this response, M1 macrophages promote the invasion of additional inflammatory cells by secreting the proinflammatory chemokines IL-8, Macrophage Chemotactic Protein (MCP-1), and Macrophage Inflammatory Protein 1 beta (MIP-1 β). Immuno-regulation, tissue repair and constructive tissue regeneration are promoted by the anti-inflammatory M2 macrophage phenotype which emerge during the chronic phase of the immune response. These macrophages inhibit pro-inflammatory cytokine secretion, promote anti-inflammatory cytokine secretion, and up regulate macrophage mannose receptors which are necessary for Foreign Body Giant Cell (FBGC) formation and play a role in matrix remodeling (Brown et al., 2009, Franz et al., 2011, Klopffleisch, 2016).

1.10.1. Role of macrophage polarization following biomaterial implantation

The macrophage response to biomaterial is very similar to their function in normal wound healing. Following the acute phase of the wound healing response, fibroblast proliferation and eventual remodeling of the wound occurs. However, in response to implanted biomaterials, macrophages attempt to phagocytose the foreign body by secreting

enzymes (Sridharan et al., 2015b). When macrophages cannot degrade non-degradable synthetic biomaterials, they fuse to form multinucleated FBGC to surround the material and prevent host tissue contact. FBGCs and recruited fibroblasts deposit collagen layers around the biomaterial and finally form a granulated tissue which over the time become a dense collagen capsule around the mesh which may also infiltrate the material if the pores are of sufficient size (Klopfleisch, 2016).

Synthetic, non-degradable or slowly degradable materials are normally encapsulated within 2-4 weeks and as the resident and recruited macrophages cannot ingest the material and may remain in contact the surface of material for years after implantation. The porosity and the surface topography of the biomaterial affects the macrophage response (Madden et al., 2010, Underwood et al., 2011). Material with a 40um pore size can be maintained for 28 days in C57BL6 mice with minimal fibrosis and extensive vascularization. The pores were infiltrated by macrophages but not the FBGC due to the restricted pore size (Fukano et al., 2010). Evaluation of host response to prototypical polypropylene mesh and Gynemesh PS (Ethicon) implanted by sacrocolpopexy showed that M1 macrophages are the predominant cell type 12 weeks post-surgery, however implantation of lighter mesh with higher porosity attenuates this response (Brown et al., 2015). Small pore size is also a risk factor for infections, particularly for urogynaecological applications, where a much larger pore size of around 1000 um is commonly used to avoid this complication, but these meshes will still elicit a foreign body response (Ridgeway et al., 2008).

Collagen has been suggested as a useful material to promote the efficient healing by preventing severe mesh adhesion to the wound. The initial inflammatory response is less

intense to collagen coated PP mesh compared with uncoated PP and there was a reduced risk of erosion (de Tayrac et al., 2007). However, the M1, M2 macrophage was not investigated in this study.

1.10.2. MSC – Macrophage Interaction

Several lines of evidence demonstrate crosstalk between macrophages and MSC. Assessing the anti-inflammatory effects of MSC in an experimental acute myocardial infarction model revealed that the M1 macrophage level was reduced in presence of bmMSC, while the proportion of M2 macrophages significantly increased (Dayan et al., 2011). Macrophages co-cultured with bmMSC expressed higher levels of CD206, the Mannose receptor, IL-10 and IL-6 and a low level of TNF- α (Kim and Hematti, 2009). In a co-culture system, MSC suppressed inflammatory cytokine production in LPS-stimulated peritoneal macrophages and increased the expression of anti-inflammatory cytokines (Maggini et al., 2010). MSC constitutively produce PGE2 which inhibited the production of TNF- α (Maggini et al., 2010). The relevance of MSC in reprogramming macrophages *in vivo* was demonstrated in a sepsis model. In this model, the infusion of mouse bmMSC decreased lethality, and the protective effect of the MSC was eliminated by macrophage depletion or by the administration of IL-10-specific neutralizing antibodies (Nemeth et al., 2009). The IL-10 produced by M2 macrophages blocked excessive neutrophil infiltration into the injured tissue and prevented further damage. Similar observations were made in an endotoxin-induced lung injury model, in which intrapulmonary delivery of mouse bmMSC decreased the production of TNF- α and CXCL2 and increased the production of IL-10 by alveolar macrophages (Nemeth et al.,

2009). In summary, MSC exert anti-inflammatory and immunomodulatory effects which appear to be mediated by their effect on macrophage phenotype and function.

1.10.3. MSC fate after transplantation

Although cell therapy and in particular MSC therapy is currently being translated into the clinic, there is no clear understanding of the fate of the transplanted MSC both in terms of the cells and over time. In a study by Agrawal et al, Dil labelled human adipose derived stem cell (ASC) were injected into immunocompromised and immunocompetent mice, as a single cell suspension or as self-assembled spheroids but 95% of the human cells were undetectable after 10 days (Agrawal et al., 2014). This clearance of implanted cells was faster in immunocompetent than immunocompromised mice. Unexpectedly, a significant signal was detected in macrophages and the authors suggested that hAMSC implantation stimulates a robust macrophage infiltration which correlates with loss of stem cell number (Agrawal et al., 2014). Tracing fluorescent dye (DIO) labeled eMSC implanted on PA+G mesh into immunocompromised nude rats showed that the number of labeled eMSC decreased between days 7 to 14 and had disappeared by day 30 (Ulrich et al., 2014a). The cells had not migrated to other organs including spleen, liver, brain, lung and heart, indicating loss at the local delivery site. In another study, labelled bmMSC, were phagocytosed by lung macrophages 1 day after IV injection, resulting in induction of suppressive M2 macrophage phenotype (Braza et al., 2016).

Together these studies show that both autologous and allogenic MSC are quickly cleared by cells of innate immune system. Macrophages play a key role in the interaction between innate immunity and MSC. It appears that MSC exert their inhibitory effect via macrophages even after they have been cleared by them.

1.11. Rationale for the Thesis

Despite the initial broad acceptance of mesh used in POP surgical repair there are an increasing number of published reports describing local wound disturbance, erosion, or other complications. This inflammatory reaction and its associated physiological wound contraction can cause the mesh to shrink and fold. The FDA posted several warnings on the use of transvaginal mesh insertion for vaginal repair surgery, several major companies have subsequently withdrawn mesh for POP surgery and they have been or still are the subject of class action litigations. An alternative POP therapy is urgently needed as native tissue surgical reconstruction has a high failure rate. New mesh for POP surgery that better integrates into tissue with a lesser inflammatory response may reduce the chronic inflammatory response to synthetic mesh and improve clinical outcomes. Collagen coating added as a surface layer on top of the PP mesh or monofibres of PP mesh coated with a solubilised layer of collagen may further reduce this chronic inflammatory response.

MSC have high proliferative capacity, and are attractive for tissue engineering applications, although invasive methods and anaesthesia are required for their procurement from bone marrow and adipose tissues (Darzi et al., 2016b). MSC secrete a variety of factors that promote tissue repair, stimulate proliferation and differentiation of endogenous tissue progenitors, and decrease inflammatory and immune reactions. These paracrine non-stem cell factors appear to best explain their healing activity. MSC can also induce macrophage infiltration to the wound site and convert them into an anti-inflammatory wound healing M2 phenotype. This immune cell recruitment may be

responsible for rapidly decreasing MSC cell numbers following implantation, however MSC can execute their inhibitory roles even after phagocytosis.

eMSC have been identified as a promising new source of MSC which are easily accessible from tissue obtained in an office based procedure without the need for anaesthetic (Darzi et al., 2016b, Ulrich et al., 2013b). eMSC have high proliferative capacity and regenerative properties (Masuda et al., 2012). However, the immunoregulatory properties of eMSC are poorly understood. Our laboratory has found that seeding polyamide/gelatin composite meshes with eMSC resulted in anti-inflammatory effects with promotion of wound repair, new tissue growth with minimal scarring fibrosis and improved biomechanical properties in a xenogeneic rat model. These eMSC may act in a paracrine manner to improve the biocompatibility of our new mesh design for POP surgical repair. The interaction between eMSC seeded on a tissue engineering construct and innate immune cells, in particular macrophages, has not been reported. Investigation of the host response to cell-seeded mesh is important as most mesh complications arise from the host inflammatory response which develop into chronic fibrosis causing unacceptable symptoms.

1.12. Hypothesis and Aims

Hypothesis 1

The method of collagen coating polypropylene mesh will alter the host response to this mesh implanted in the vaginal wall environment.

Aim 1

To compare the long-term host response to synthetic meshes incorporating collagen as a bilayer or soluble collagen coating of individual mesh filaments using an ovine vaginal surgery model.

The meshes which are used in this study are commercial meshes (BARD) coated with porcine collagen.

Hypothesis 2

Human endometrial mesenchymal stem/stromal cells (eMSC) delivered on PA+G mesh differentially modulates the macrophage response to the implanted mesh in xenogeneic heterologous models of immune intact and immunocompromised mice.

Aim 2

To determine whether human eMSC delivered on PA+G meshes differentially effect the macrophage M1/M2 phenotype in NSG (immunocompromised) and C57BL (immunocompetent) mice using a xenogenic subcutaneous wound repair model.

To determine the survival and paracrine effects of xenogeneic (human into mice) and heterologous (eMSC to fascial defect) eMSC in mice with normal and depleted immune systems.

Hypothesis 3

Circulating blood monocytes are recruited to the site of mesh implantation and determine the fate of locally delivered eMSC. Systemic depletion of monocytes results in longer survival of eMSC.

Aim 3

To determine whether blood monocytes or resident macrophages are the source of inflammatory cells at the mesh-tissue interface.

Chapter 2

Collagen Coated mesh for POP Treatment

2.1. Introductory statement

Despite the broad acceptance of mesh-augmented surgery for treating POP, there are some associated complications. The most common problem is mesh erosion through the vaginal epithelium which results in inflammation and pain. Studies have revealed that all PP mesh induces long lasting chronic inflammation.

It has been reported that collagen-coated mesh delayed the inflammatory response to PP mesh and reduced the risk of erosion by decreasing adhesion of the mesh to the wound (Meschia et al., 2007, Lo et al., 2016). In this chapter, I hypothesized that the format of collagen coating of PP mesh affects the host response and improves tissue healing in long term. This study was a collaboration with Professor Jan Deprest and his group in the Katholieke University Leuven, Leuven, Belgium. Animal surgery was performed by Dr Iva Urbankova in Leuven. I designed Immunohistochemistry experiments to determine the leukocyte and macrophage response to collagen-coated mesh implants. In collaboration with CSIRO, I assessed the biochemical properties of the harvested mesh/tissue complexes. I also determined total collagen content using Sirius Red staining and collagen fibril structure and organisation assessed by Birefringence analysis.

As there are few available antibodies or kits for sheep model and due to high expense of this animal model, we studied the host response to implanted mesh in mouse models which will be discussed in chapter 3 of this thesis.

I acknowledge Dr Kai for assisting with biochemical analysis and Ms Jacinta White for helping with Sirius Red staining and birefringence analysis. I also thank Dr Camden Lo for helping with Metamorph software image analysis.

Declaration

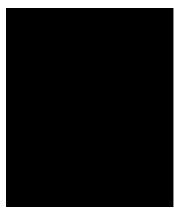
Monash University

Declaration for Thesis Chapter 2

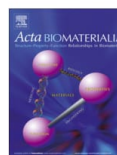
In the case of Chapter 2 my contribution to the work involved the following:

Name	Nature of Contribution	Extent of contribution (%) for student co-authors only
Saeedeh Darzi	Study design, perform experiments, data collection and analysis, writing paper	80%
Iva Urbankova	Animal surgery and tissue collection	N
Kai Sue	Perform experiments	N
Jacinta White	Perform experiments	N
Camden Lo	Imaging	N
David Alexander	Statistical advice, data analysis	N
Jerome Werkmeister	Study design, editing the manuscript	N
Caroline Gargett	Study design, revising the manuscript	N
Jan Deprest	Study design	N

Student signature:



Date: 12.08.2017



Full length article

Tissue response to collagen containing polypropylene meshes in an ovine vaginal repair model



Saeedeh Darzi^{a,b}, Iva Urbankova^c, Kai Su^d, Jacinta White^d, Camden Lo^a, David Alexander^d, Jerome A. Werkmeister^{b,d,1}, Caroline E. Gargett^{a,b,*}, Jan Deprest^{c,1}

^a Hudson Institute of Medical Research, 27–31 Wright Street, Clayton, Victoria 3168, Australia

^b Department of Obstetrics and Gynaecology, Monash University, Clayton, Victoria 3168, Australia

^c Centre for Surgical Technologies and Department of Development and Regeneration, KU Leuven, Leuven, Belgium

^d CSIRO Manufacturing, Bayview Avenue, Clayton, Victoria 3169, Australia

ARTICLE INFO

Article history:

Received 24 November 2015

Received in revised form 27 April 2016

Accepted 3 May 2016

Available online 6 May 2016

Keywords:

Pelvic Organ prolapse

Ovine model

Macrophage response

Collagen tissue regeneration

Birefringence

ABSTRACT

Pelvic Organ Prolapse (POP) is the herniation of pelvic organs into the vagina. Despite broad acceptance of mesh use in POP surgical repair, the complication rate is unacceptable. We hypothesized that collagen-containing polypropylene (PP) mesh types could modulate mesh-tissue integration and reduce long-term inflammation, thereby reducing mesh-associated complications. This study compared the long-term tissue response to an unmodified PP mesh and two collagen containing meshes in an ovine model which has similar pelvic anatomy and vaginal size to human. Three commercially available macroporous PP meshes, uncoated PP mesh (Avaluta Solo) (PP), the same textile PP mesh layered with a sheet of cross-linked porcine acellular matrix (Avaluta Plus) (PP-ACM) and a different yet also macroporous PP (Sofradim) mesh coated with solubilized atelocollagen (Ugytex) (PP-sCOL) were implanted in the ovine vagina and tissue explanted after 60 and 180 days. The macrophage phenotype and response to implanted meshes, and vascularity were quantified by immunostaining and morphometry. We quantified changes in extracellular matrix composition biochemically and collagen organisation and percentage area around the interface of the mesh implants by Sirius Red birefringence and morphometry. PP-ACM induced a more sustained inflammatory response, indicated by similar CD45⁺ leukocytes but reduced CD163⁺ M2 macrophages at 60 days ($P < 0.05$). PP-sCOL increased Von Willebrand Factor (vWF)-immunoreactive vessel profiles after 60 days. At the micro-molecular level, collagen birefringence quantification revealed significantly fewer mature collagen fibrils (red, thick fibrils) at the mesh-tissue interface than control tissue for all mesh types ($P < 0.001$) but still significantly greater than the proportion of immature (green thin fibrils) at 60 days ($P < 0.05$). The proportion of mature collagen fibrils increased with time around the mesh filaments, particularly those containing collagen. The total collagen percent area at the mesh interface was greatest around the PP-ACM mesh at 60 days ($P < 0.05$). By 180 days the total mature and immature collagen fibres at the interface of the mesh filaments resembled that of native tissue. In particular, these results suggest that both meshes containing collagen evoke different types of tissue responses at different times during the healing response yet both ultimately lead to physiological tissue formation approaching that of normal tissue.

Statement of Significance

Pelvic organ prolapse (POP) is the descent of the pelvic organs to the vagina. POP affects more than 25% of all women and the lifetime risk of undergoing POP surgery is 19%. Although synthetic polypropylene (PP) meshes have improved the outcome of the surgical treatment for POP, there was an unacceptable rate of adverse events including mesh exposure and contracture. It is hypothesized that coating the PP meshes with collagen would provide a protective effect by preventing severe mesh adhesions to the wound, resulting in a better controlled initial inflammatory response, and diminished risk of exposure. In this study we assessed the effect of two collagen-containing PP meshes on the long-term vaginal tissue response using new techniques to quantify these tissue responses.

© 2016 Acta Materialia Inc. Published by Elsevier Ltd. All rights reserved.

* Corresponding author at: The Ritchie Centre, Hudson Institute of Medical Research, 27–31 Wright Street, Clayton, Victoria 3168, Australia.

E-mail address: caroline.gargett@hudson.org.au (C.E. Gargett).

¹ Equal senior authors.

1. Introduction

Pelvic organ prolapse (POP) is defined as the downward descent or herniation of pelvic organs into the vagina [1]. Common symptoms of POP are pressure or bulge in the pelvic area, urinary incontinence and sexual dysfunction [2]. POP affects more than 25% of all women and it is estimated that the lifetime risk of undergoing surgery for POP is 19% [3,4]. Reconstructive surgery is the main treatment for POP and augmentation using synthetic polypropylene (PP) biomaterial meshes has improved the outcome of the surgical treatment for POP [5], although this is considered controversial. Lightweight, macro porous monofilament PP meshes were the most common non-degradable synthetic material used in transvaginal POP surgery as these showed lower foreign body tissue responses and reduced material stiffness [6]. While these mesh implants resulted in greater cure rates than native tissue surgery, there was an unacceptable rate of adverse events [7–9] including mesh exposure and contracture. The Food and Drug Administration (FDA), and later in Europe the Scientific Committee on Emerging and Newly Identified Health Risks (SCENIHR) issued warnings on the transvaginal placement of synthetic implants [10], resulting in companies withdrawing some mesh products from the market. New guidelines from the FDA and the International Urogynecological Association (IUGA) recommend testing new meshes in preclinical models to improve outcomes for any new mesh products being developed before translation to the clinic [11].

In addition, although mesh implantation induces a pro-inflammatory response, which is followed by fibrosis with a concomitant increase in the strength of surgical repair, this fibrotic response can cause pain and discomfort. In order to minimize fibrosis and pain, many investigations have examined the modification of mesh designs including, pore size (large versus small pore size), weight (lightweight or heavyweight) and collagen coating [12]. One approach to improve the biocompatibility of mesh was to coat the mesh with extracellular matrix (ECM) proteins. ECM coated meshes are degradable and can allow tissue remodelling and formation of appropriate soft tissue rather than fibrosis by inducing angiogenesis and promoting the accumulation of progenitor cells at the site of implantation [13]. It has been reported that coating the PP mesh with acellular porcine collagen resulted in less erosion and inflammation. It was hypothesized that the collagen would provide a protective effect by preventing severe mesh adhesions to the wound thereby decreasing direct mesh-tissue contact with the polymer, resulting in a better controlled initial inflammatory response, and diminished risk of exposure [14,15].

The host response to surgically implanted biomaterials is a critical determinant of its success or failure [16]. The early tissue response to a synthetic mesh is acute inflammation, characterised by an influx of neutrophils followed by pro-inflammatory (referred to as M1) macrophages. After the acute response following departure of the neutrophils, chronic inflammation develops that can vary in time and extent, particularly the rate at which M1 macrophages differentiate into an anti-inflammatory M2 macrophage phenotype, which will ultimately influence the wound healing response and the quality of new tissue formation [16].

An appropriate animal model is necessary to test new meshes to fulfil the IUGA requirement for preclinical studies. Although rodents are widely used because of their low cost and ease to work with, the small size of their vagina has prompted the recent shift to larger animal models [14,17]. The ovine model is attractive because the pelvis has similar anatomy and size as the human pelvis and has similar pelvic support structures as in women [18,19]. Ewes also have prolonged labours with relatively large foetuses and may also spontaneously develop postpartum POP [20,21]. The limitation of the ovine model is their quadrupedal posture,

which reduces intra-abdominal pressure experienced by the pelvis. However, it has been suggested that their ruminant physiology and tendency to ruminate facing uphill increases the pressure on the pelvic structures including the vaginal wall [19]. Moreover, their large size and hence vaginal capacity allows the examination of mesh with dimensions more representative of those implanted into women. In addition, several meshes can be implanted into the same animal [14].

The objective of this study was to evaluate whether the format of collagen coating on the PP mesh affects the chronic inflammatory host response and healing process in the long term to the implanted mesh. Sixty days was chosen to examine the tissue response to the effect of differential degradation of the collagen coating between the two modified PP meshes that used two different collagen formats and 180 days was chosen as a longer term steady state end point to examine if any differences were still apparent. We assessed the effect of two collagen-containing PP meshes on the long-term vaginal tissue response, evaluating the chronic inflammatory macrophage response, vascular response, the total collagen and glycosaminoglycans (GAG) content, and the organisation and density of collagen at the mesh-tissue interface in explanted vaginal tissues. We used standard techniques to measure these parameters and a new technique to quantify the collagen response at the mesh tissue interface by quantifying red (mature) and green (immature) collagen fibril deposition by assessing birefringence in 100 and 200 μm increments in an ovine model.

2. Methods

2.1. Mesh

Three commercially available so called Amid-I macroporous PP meshes were used where the PP component was the same in all; 1. Avaulta Solo (PP) (Bard Medical, Convington, GA, USA, 58 g/m^2), 2. Avaulta Plus (PP-ACM) (composed of the same fabric as PP with a hydrophilic slowly degrading cross-linked porcine acellular matrix (ACM) sheet comprising collagen, 0.5 mm thick and 1.8 mm pores, 100 g/m^2) and 3. PP-sCOL (PP-sCOL) (Sofradim International, Tre-voux, France, 38 g/m^2), comprising PP monofilaments coated with reconstituted enzyme-purified solubilized atelocollagen, polyethylene glycol and glycerol (Supplementary Fig. 1)

2.2. Animal implantation

Animal surgery and mesh implantation was undertaken at the KU Leuven in accordance with protocols approved by the local Animal Ethics Committee as previously reported [17]. Thirty-six multiparous Texel ewes underwent surgical implantation of mesh ($n = 12/\text{mesh type}$). Briefly, following general anaesthesia, antibiotic prophylaxis, and hydro-dissection of the rectovaginal space, a single vaginal incision was made and a 35×35 mm flat mesh was inserted and fixed to underlying tissue of the posterior wall with multiple interrupted 4/0 polypropylene sutures (Prolene; Ethicon, Zaventem, Belgium). We chose 35×35 mm mesh size to avoid graft related complications associated with implanting larger mesh sizes, including exposure and contraction [9]. The vaginal incision was closed with continuous 2/0 polyglactin 910 (Vicryl; Ethicon). Tissues were explanted after 60 and 180 days and processed as previously described to assess the effect of collagen after partial/complete resorption of collagen on the collagen-containing meshes and the chronic rather than acute inflammatory response [17]. Control tissues were collected from non-operated regions adjacent to the implants and at the same distance from the introitus as there are regional differences cranio-caudally and between

the anterior and posterior vaginal wall in sheep [22,23]. The 1.0 × 0.5 cm explants were fixed in formalin and embedded in paraffin or embedded in OCT and then frozen. Frozen and paraffin blocs were cut into 5 µm sections at the Hudson Institute. The gross anatomical outcomes and biomechanical evaluation of explants of these animals was already reported on before [24]. In cases of gross anatomic graft related complications (GRC) which was low (areas with exposure and local inflammation), outcome measurements described below were scored in areas away from GRC to ensure focus on the effects of collagen-coating were not complicated by a different type of inflammatory reaction to exposed mesh.

2.3. Immunohistochemical and histomorphometric analysis of explanted tissues

Frozen 5 µm sections were thawed and fixed with pre cooled acetone and then washed with PBS. Endogenous peroxidase was quenched with 0.3% v/v H₂O₂ followed by protein blocking (Protein Block serum free, Dako, USA) for 30 min at RT. After three washes in PBS, primary antibodies (CD45, CD163, CD206, vWF, αSMA) were incubated for 1 h at 37°C; isotype matched IgG antibodies were used as negative controls and applied at the same concentration (Table 1). HRP-labelled polymer (Dako, USA) conjugated anti-mouse secondary antibody was incubated for 30 min at RT. Haematoxylin was used for nuclear staining and the slides were coverslipped with mounting medium (Dako, USA). Images (2–6/section) were taken of immunostained sections for CD45, CD163, CD206, αSMA and vWF for each explant at both time-points using a Leica-DMR Microscope at 10x magnification and the images were analysed using Metamorph software (Molecular Devices, LLC) to measure positive staining around mesh filaments in 100 µm increments as described previously [25]. Briefly, individual filaments were outlined manually and the software counted the signal area around mesh filaments. The positive signal area (pixels) for every image in first 100 µm increment for CD45, CD163, and CD206, and the first 250 µm for αSMA and vWF was recorded and divided by the total tissue area examined and the average calculated per ovine sample and this was used for statistical analysis.

2.4. Biochemical analysis of total collagen and GAG content

Total collagen was determined from the supernatant of papain-digested tissue explants from implanted areas and control tissue areas, as previously described [26]. Briefly, frozen tissue explants were freeze dried for 6 h, weighed and digested in 1 mL papain digestion buffer (0.1 M Na₂HPO₄, 5 mM EDTA, 5 mM Cysteine-HCl, pH 7.4) containing 0.5 mg/mL papain for 12–16 h at 60°C. Following digestion, samples were centrifuged at 13,200 rpm for 10 min and 0.5 mL of supernatant hydrolysed in 6 N HCl at 115°C for 4 h. Hydroxyproline (Hyp) was measured spectrophotometrically at 560 nm after reaction with 0.05 mol/L chloramine-T (Sigma) and 10% (w/v in 2-methoxyethanol) P-dimethylaminobenzaldehyde (Sigma). A standard curve using L-hydroxyproline (0–10 mg/mL) (Sigma) was used to calculate the Hyp concentration. Total collagen was calculated using a hydroxyproline to collagen ratio of 0.143:1 [27].

Sulphated GAG was measured by reacting 40 µL of the papain-digest supernatant with 1 mL dimethylmethylene blue (DMMB) reagent solution (40 mM NaCl, 40 mM glycine, 0.1 M HCl, 46 mM DMMB (Sigma), pH 3.0) [28]. GAG content was measured by absorbance at 525 nm using a UV-vis spectrophotometer. A standard curve was created using 0.001 and 0.02 mg of whale cartilage chondroitin sulphate A (Sigma) dissolved in PBS and used to determine sulphated GAG concentration.

Table 1
Antibodies used for Immunostaining.

Primary antibodies	Concentration (µg/mL)	Isotype	Supplier
CD45	(0.5 µg/mL) 1/200	Mouse IgG1	AbD Serotec
CD163 (M2 macrophage marker)	(0.5 µg/mL) 1/200	Mouse IgG1	AbD Serotec
CD206 (M2 macrophage marker)	(0.5 µg/mL) 1/200	Mouse IgG1	Dendritics
A-Smooth Muscle Actin (αSMA)	1/400	Mouse IgG2a	Dako
Von Willebrand Factor (vWF)	1/50	Mouse IgG1	Dako

2.5. Collagen alignment by Sirius red birefringence image analysis

Paraffin sections of control tissue (distal tissue away from the mesh) and implant (mesh and tissue complex) were dewaxed and rehydrated in graded alcohols and stained with Sirius Red F3B (0.1 g/100 mL saturated picric acid solution) (Sigma-Aldrich, USA) for 1 h at room temperature (RT) to determine collagen alignment. For morphometric analysis, the stained slides were washed in running water (non-acidified) to remove the yellow picric acid counterstain. Sirius red stained sections were observed under a light microscope (Olympus BX61) (Fig. 1A). Using polarizing filters, the stained collagen fibres showed a mixed proportion of birefringent staining patterns ranging from green to yellow to orange/red, depicting immature to mature collagen fibril organisation, respectively (Fig. 1B). Threshold gating was set to segregate the polarized images into two distinct colours, red to capture the thicker mature fibrils and green to capture the thinner immature less organised fibril. The staining patterns were captured digitally and image segmentation of pixel area and intensity converted into areas of green and red as described below (Fig. 1C, E) and their relative proportion was measured by Metamorph software in 100 (Fig. 1D) and 200 (101–200) µm (Fig. 1F) increments around the mesh fibres.

2.6. Metamorph software

Image analysis was undertaken with MetaMorph v7.7.0.0. A user-defined region-of-interest (ROI) corresponding to the perimeter boundary of the mesh is used as the basis of the analysis. The perimeter of this ROI was processed using the Euclidean distance routine to establish a radial distance map of the tissue relative to the mesh. From this radial distance map, two band regions were established corresponding to a radial distance of 1–100 µm and 101–200 µm away from the perimeter of the ROI. Each band region was converted to binary masks and applied back to the original image to the corresponding isolate tissue areas, which was then thresholded for both green and red channels separately to measure both area and optical density. Thresholding criteria were selected as the upper 80% of the 8-bit linear signal range for each channel.

2.7. Statistical analysis

GraphPad Prism 6 was used for statistical analysis. Results are reported as mean ± SEM for each experimental group (n = 6 meshes/group/time point).

For birefringence analysis ANOVA was performed using R software. T tests for identifying differences between collagen levels in specific groups were calculated using estimates for each variance component derived from the ANOVA. The Pearson Chi-Square Normality Test and The D'Agostino Omnibus Test was used to assess the normal distribution of data and found not significant. We therefore used parametric analyses.

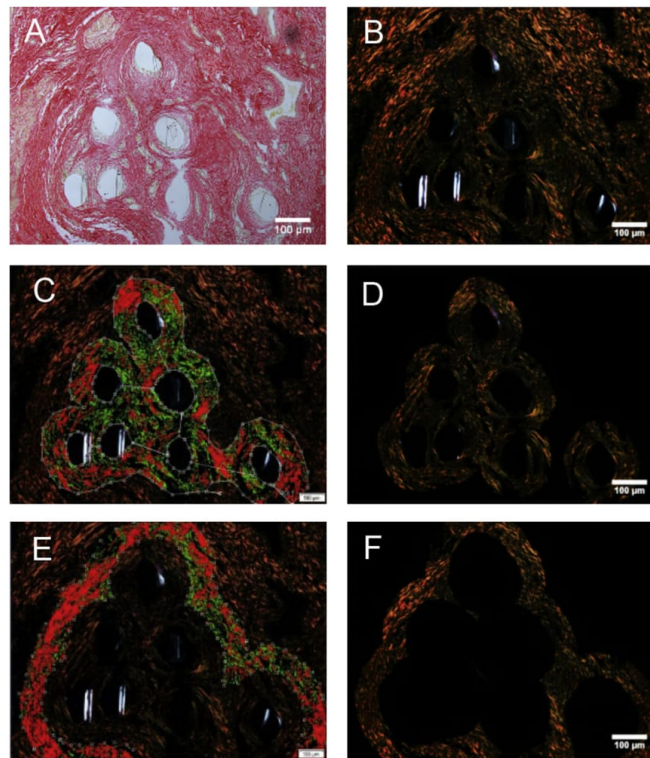


Fig. 1. Assessment of Sirius Red birefringence (A) Sirius red staining of tissue around a central filament bundle (B) image of the same slide under the polarizing microscope. Note that the majority of the fibres are red with a small number of green fibres. Black areas represent cells and extracellular matrix. Optical images from the polarizing microscope showing the (C, D) first 100 µm (0–100 µm) increment surrounding filament bundle (E, F) second 100 µm increment (100–200 µm) surrounding the same filament bundle. (For interpretation of the references to colour in this figure legend, the reader is referred to the web version of this article.)

3. Results

3.1. Inflammatory response to implanted collagen containing PP meshes

Immunohistochemistry was used to examine the chronic cellular response to the two implanted collagen containing polypropylene meshes and the unmodified PP mesh in the ovine vagina. The pan CD45 leukocyte marker showed that these inflammatory cells were concentrated around the individual PP mesh filaments and filament clusters in a similar pattern for all 3 meshes at both 60 and 180 days implantation (Fig. 2.1A–F). Image analysis quantification of the first 100 µm increments around individual mesh filaments showed no difference in CD45⁺ leukocyte density between mesh types after 60 days or 180 days (Fig. 2.1G). Since CD45 encompasses all inflammatory cell types associated with foreign mesh implants, we next investigated the proportion of tissue regenerative M2 macrophages that play a key role in the late inflammatory response to synthetic meshes [26]. Immunostaining was performed with two M2 phenotypic markers, CD163 and CD206 (Fig. 2.2A–F and 2.3 A–F, respectively). Again, the level of CD163⁺ and CD206⁺ cells was quantitated in the first 100 µm around the individual filaments. CD163 immunostained macrophages around PP-ACM filaments was significantly lower than around PP-sCOL at 60 days ($P < 0.05$) (Fig. 2.2G). No significant

differences were observed between meshes at 180 days. Neither was there a difference between 60 and 180 days for any of the three meshes (Fig. 2.2G). Unlike CD163, there were no differences in the percentage CD206⁺ cells between the three mesh types at 60 or 180 days (Fig. 2.3A–G), nor for individual meshes between 60 and 180 days.

3.2. Vascular response to collagen-containing PP meshes

The extent of vascularization into the mesh implanted tissues was assessed with endothelial (vWF) and vascular smooth muscle (α SMA) immunostaining in the first 250 µm around the PP filaments. A larger increment diameter around the filaments was examined because the vessels are more widely distributed around the mesh compared to macrophages. vWF (Fig. 3.1A–F) and α SMA (Fig. 3.2A–F) immunostaining showed that vessels are both between and around filament knots, and not as closely associated with filaments as the leukocytes. Monofilaments coated with collagen (PP-sCOL) showed greater numbers of small vWF⁺ vessel profiles within this 250 µm region around the filaments compared to non-collagen coated (PP) and the collagen layer coated PP mesh (PP-ACM) after 60 days (both $P < 0.05$) (Fig. 3.1G). By 180 days the level of vascularization had diminished around PP-sCOL filaments (Fig. 3.1D–F), and there were no significant differences between any of the 3 meshes (Fig. 3.1G). α SMA immunostained

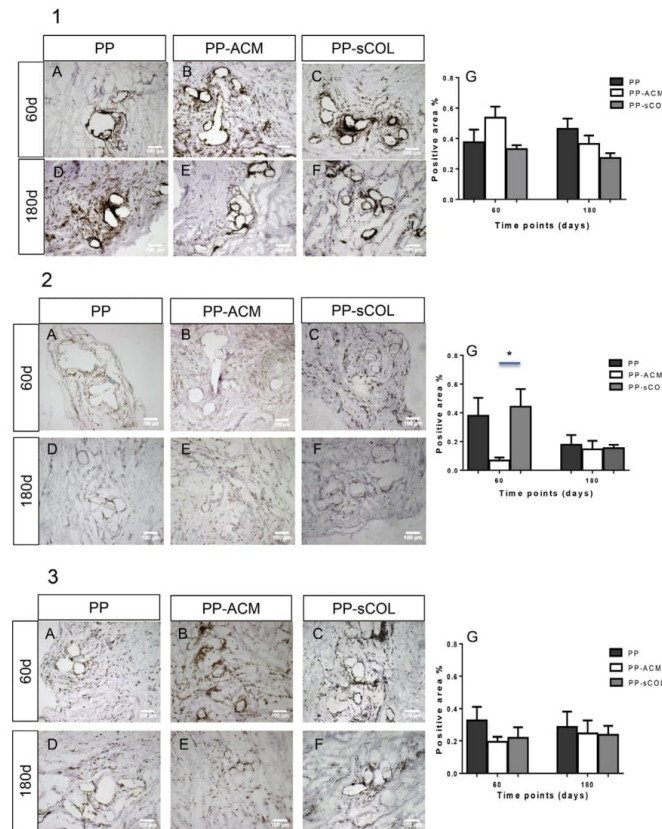


Fig. 2. 1. CD45 leukocyte 2. CD163 and 3. CD206 M2 macrophage accumulation around collagen containing PP mesh implants in ovine vagina. After 60 (A–C) and 180 (D–F) days. PP (control) (A, D), PP-ACM (B, E) PP-sCOL (C, F). (G) Percentage of positive immunostained area in the first 100 μm increment around mesh filaments. Data are Mean ± SEM of n = 6 animals/group. *P < 0.05.

vessel profiles appeared stronger than vWF staining and there were no significant difference between the mesh types at both time points nor for mesh types between the two time-points (Fig. 3.2A–F and G).

3.3. Total extracellular matrix synthesis in and round implanted collagen-coated PP meshes

Collagen and GAG are two major structural proteins and macromolecules in extracellular matrix. There was little difference in the total collagen deposition (Fig. 4A) and GAG content (Fig. 4B) between the mesh types, the control and explanted tissues or between 60 and 180 days implantation.

3.4. Collagen composition and organisation at the interface of implanted collagen-containing meshes

While the total ECM content, predominantly collagen, was substantially comparable between tissue from mesh implants and normal tissue, further analysis of the extent and organisation of new collagen deposition close to the mesh interface was undertaken to assess the quality of the collagen fibrils deposited as the tissue heals around the implanted mesh. Polarized light microscopy on

Picrosirius Red stained tissue (Fig. 1C) was used to quantify the level of mature (thicker fibrils with defined organised collagen packing) and immature (thinner fibrils with more likelihood of containing collagen type III) collagens [29]. As shown in Fig. 1C&E, collagen fibrils appear as a range of colours from red/orange, yellow and green when viewed under polarized light, representing thick, mature and thin, immature collagen, respectively. The background between these coloured fibrils comprised cells, and ECM, which appeared black thus allowing for quantitative morphometric analysis [29]. Fig. 5 shows the morphometric quantitation of mature and immature collagen fibrils. The mature red fibrils synthesis increased with the time in Mesh Tissue Complex (MTC) in both 100 and 200 μm increment zone but not in control (Fig. 5 and Supplementary Fig. 1A,B). However, the green, immature collagen fibrils did not change in either MTC or control after 60 and 180 days (Fig. 5 and Suppl Fig. 1C,D). As expected, there was always a greater proportion of mature red fibrils than immature green fibrils in all three groups in both MTC and control areas at both time points (Fig. 5A–H). In all groups, there were no significant differences in the proportion of green immature fibrils in both the MTC and control areas at both times points (Fig. 5E–H). Our results revealed significantly fewer mature red fibrils in the MTC than normal control tissue for all mesh types (overall all

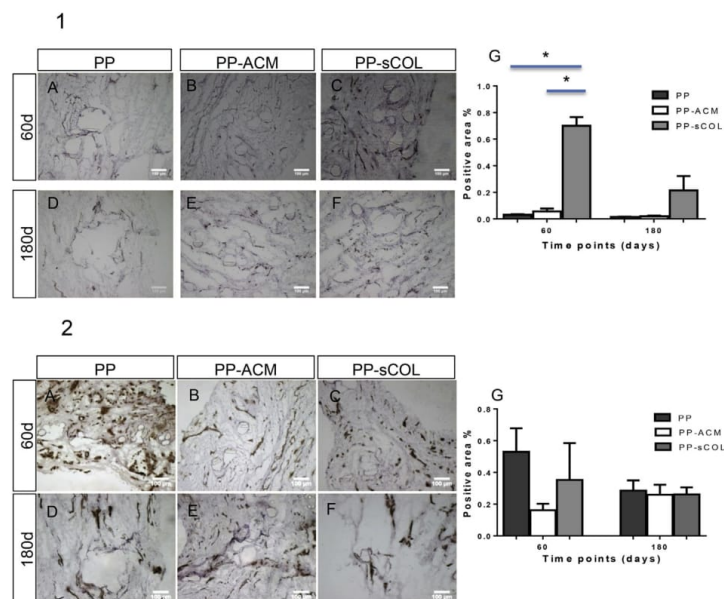


Fig. 3. Immunodetection of 1. endothelial marker vWF and 2. smooth muscle marker α SMA around collagen-containing PP meshes. After 60 (A–C) and 180 (D–F) days. PP (control) (A, D), PP-ACM (B, E), PP-sCOL (C, F). (G) Percentage of positive immunostained area in the first 250 μ m increments around mesh filaments. Data are mean \pm SEM of $n = 6$ animals/group. * $P < 0.05$.

$p < 0.001$). Mesh-tissue complexes also had significantly less total collagen density (red + green) than normal control tissue regions after 60 days for all three mesh types in both the inner 100 μ m interface adjacent to the PP filaments and the next 100 μ m increment zone (Fig. 5I–L; overall all $P < 0.001$). There were no significant differences in the proportion of red or green fibrils between any mesh types. However, the total collagen density was significantly greater around the PP-ACM meshes compared with PP ($P < 0.01$) but not PP-sCOL implant at 60 days; this may in part be due to the presence of remaining slowly degrading collagen tissue layer which was evident in some samples. In general, over the two time points, the proportion of green fibrils remained largely unchanged suggesting a constant rate of renewal of new collagen, but there were significant increases in both the red content ($P < 0.01$) and total collagen density ($P < 0.001$). There were no differences observed in control tissues over time. At 180 days, the total collagen content in both incremental zones of the MTC had increased and was comparable to control tissue ($P > 0.05$) in both collagen containing PP-ACM and PP-sCOL meshes. In contrast, there was still significantly less mature and immature collagen fibres deposited around the PP mesh at 180 days at both increments ($P < 0.005$) (Fig. 5J&L).

4. Discussion

The main findings of this study are firstly, that incorporation of collagen into the PP meshes, either as a coating of soluble protein (PP-sCOL) or as a layer of cross-linked collagen tissue (PP-ACM) did not reduce leukocyte accumulation around the mesh filaments compared to unmodified PP meshes at two and six months following vaginal implantation in an ovine model. The majority of inflammatory leukocytes around the filaments were macrophages, and CD163+ M2 macrophages were diminished around PP coated with

a sheet of acellular collagen matrix at 60 days but not at 180 days when the entire collagen sheet had been degraded. Secondly, increased microvessel density and therefore vascularization was found around the collagen coated mesh filaments at 60 days, which had resolved by 6 months. Thirdly, there were no differences in the total ECM composition around the implanted meshes using bulk biochemical analyses. However, there were significant differences at the micro-molecular level at the mesh-tissue interface, using birefringence of Sirius Red stained tissues and quantitative morphometric image analysis to track the maturation of newly laid down collagen fibres during the healing phase following mesh implantation. This detailed quantitative analysis demonstrated that mesh implantation reduced the amount of mature collagen around non-collagen containing implanted mesh (PP) for at least 6 months compared to the control regions in the same tissue. More importantly, collagen incorporation in the mesh apparently hastened the maturation of collagen fibres around the mesh filaments, whether it was delivered as a sheet over the mesh or as a soluble protein coating around individual PP filaments. Our analysis revealed that collagen layer-coated mesh delayed the differentiation of infiltrating macrophages to a certain but not all types of M2 wound healing phenotype; it is equally possible that these mesh types could have already begun to influence remodelling to a more mature collagen tissue. Certainly, collagen coated filaments promoted vascularisation between the mesh filaments that accelerated the maturation of newly laid down collagen to produce a connective tissue similar to the original tissue by 6 months.

Macrophages are a heterogeneous population of cells with a range of functional activities depending on their polarization status [30]. In general, they are classified as M1 pro-inflammatory or M2 anti-inflammatory types, both involved in tissue repair and remodelling. Upon activation, they release growth factors which

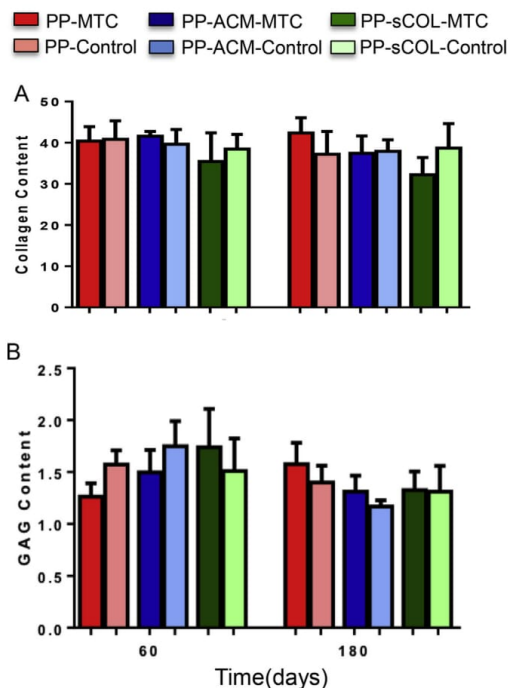


Fig. 4. Extracellular matrix content of collagen – containing mesh implanted tissue. (A) Total collagen and (B) GAG content (% per dry weight) determined by biochemical assay. Data are mean \pm SEM of $n = 6$ animals/group. MTC, Mesh/tissue complex, Control, distal tissue without mesh.

attract fibroblasts and smooth muscle cells to the wound site resulting in collagen production and neo-tissue formation [31]. A vigorous leukocyte response was observed around each of the mesh types, and given the similarity of the percent positive immunostained area, the majority of these leukocytes would appear to be M2 macrophages at the relatively late time points examined in this study. It was expected that the M1 macrophage response would have been seen during the initial wound healing response to these implants. It is also possible that M2 activation could have occurred earlier than 60 days for certain mesh types but was not possible to determine with this type of study design. In addition, several antibodies to M1 macrophages did not cross react with ovine epitopes and could not be assessed. Our finding is consistent with the higher median histology score of macrophage and Foreign Body Giant Cell (FBGC) accumulation observed around the collagen matrix sheet of the PP-ACM mesh in our previous study [17], although low grade infection was also present in this report that might have triggered an M1 type response, deduced from the difference between the CD45 and M2 percent positive areas. Both CD163 and CD206 markers largely showed a similar trend for the three mesh types at both time-points. However, it was difficult to explain the difference in the levels of the two M2 markers at 60 days. CD206 is the C-type mannose receptor 1 and is maintained in resident tissue macrophages independent of cytokine activation [32]. A decrease in CD206 expression is associated with upregulation of pro-inflammatory cytokine production and thus a delay in the ensuing wound healing process. CD163 is a haemoglobin-haptoglobin-scavenger receptor and its expression is not necessarily specific to M2

macrophages. Using double labelling, a sub-population of these CD163 macrophages are associated with the typical classical Thelper1/M1 response [30]. Macrophage polarisation is a dynamic process and it is not entirely clear in the present study what the significance of the transient reduction in CD163+ M2 macrophages means since CD206 M2 macrophages were equally frequent in all implants. Others have demonstrated varying degrees of acute and chronic inflammation following the implantation of collagen or non-collagen coated mesh using different *in vivo* models [15,33]. Similarly, in the ovine vaginal wall no differences in inflammatory response were reported between implantation of coated and non-coated PP mesh [14]. In these studies inflammation was assessed subjectively, based on scoring of macrophages and multinucleated giant cell numbers. In this study we used our new image analysis methods for quantifying positive signals to objectively assess cellular content and vascularization around mesh filaments. Implantation of collagen-coated PP mesh in the abdominal wall of rats induced less inflammatory response and granulation tissue at early 7 and 14 day time-points [33] but the M1/M2 status of the macrophages was not reported. For the first time we have used macrophage markers and a quantitative assay evaluating collagen maturation during the tissue response to vaginally implanted PP meshes in an ovine model. We assessed the gradient distribution of macrophages at the filament tissue interface at 100 μ m increments to more accurately assess the macrophage response as previously reported in a rat model [25].

Since angiogenesis is essential for wound healing we assessed the mesh/tissue complex for neo-vascularization. Our previous evaluation of Polyamide/Gelatin (collagen containing) meshes showed greater neovascularization in a rat abdominal hernia model [25]. In this study, implanted PP-sCOL showed a dramatically increased number of vWF⁺ vessel profiles after 60 days and together with the large accumulation of M2 macrophages suggests enhanced healing takes place around the collagen-coated filament mesh. Similarly a higher vascularization score was observed after 60 and 180 days in PP-sCOL-implanted ovine vagina [17]. In the PP-sCOL group, each mesh filament is coated with soluble non-cross-linked highly resorbing collagen, rather than a cross-linked layer of collagen tissue on top of the mesh, allowing the penetration of capillaries and therefore showing greater vascularization. Similar to the dampened M2 macrophage response, the slow degradation of the collagen sheet in PP-ACM may also have prevented vascularization at 60 days. During vascularization, new capillaries develop further to become arterioles and venules through recruitment of smooth muscle cells. In the PP-sCOL MTC, many small fragile capillaries without α SMA⁺(vWF) pericytes or mural cells persisted until 60 days but by 180 days these capillaries had acquired mural cells indicating vascular maturation with time. Vessels were assessed at 250 μ m increments to enable their quantification in neo-tissue as it develops.

Collagen and GAG are two of the main proteins in ECM that are synthesised and remodelled during tissue regeneration after injury and mesh implantation [34]. As the most abundant protein of the ECM, collagen provides strength, integrity and structure to the connective tissue. In the normal process of tissue regeneration and wound healing, fibroplasia and collagen deposition begins in the proliferation zone and continues as the tissue becomes less cellular and remodels to form a mature tissue or scar [35]. During the time of our study the ECM did not change in total collagen and GAG content in the bulk tissue explanted around the three mesh types, which were not different to normal vaginal tissue distant from the implant site. However, by using a quantitative morphometric analyses with Sirius Red birefringence of the newly synthesised collagen tissue, we were able to document the density and maturation of collagen formation at the micro-molecular interface of

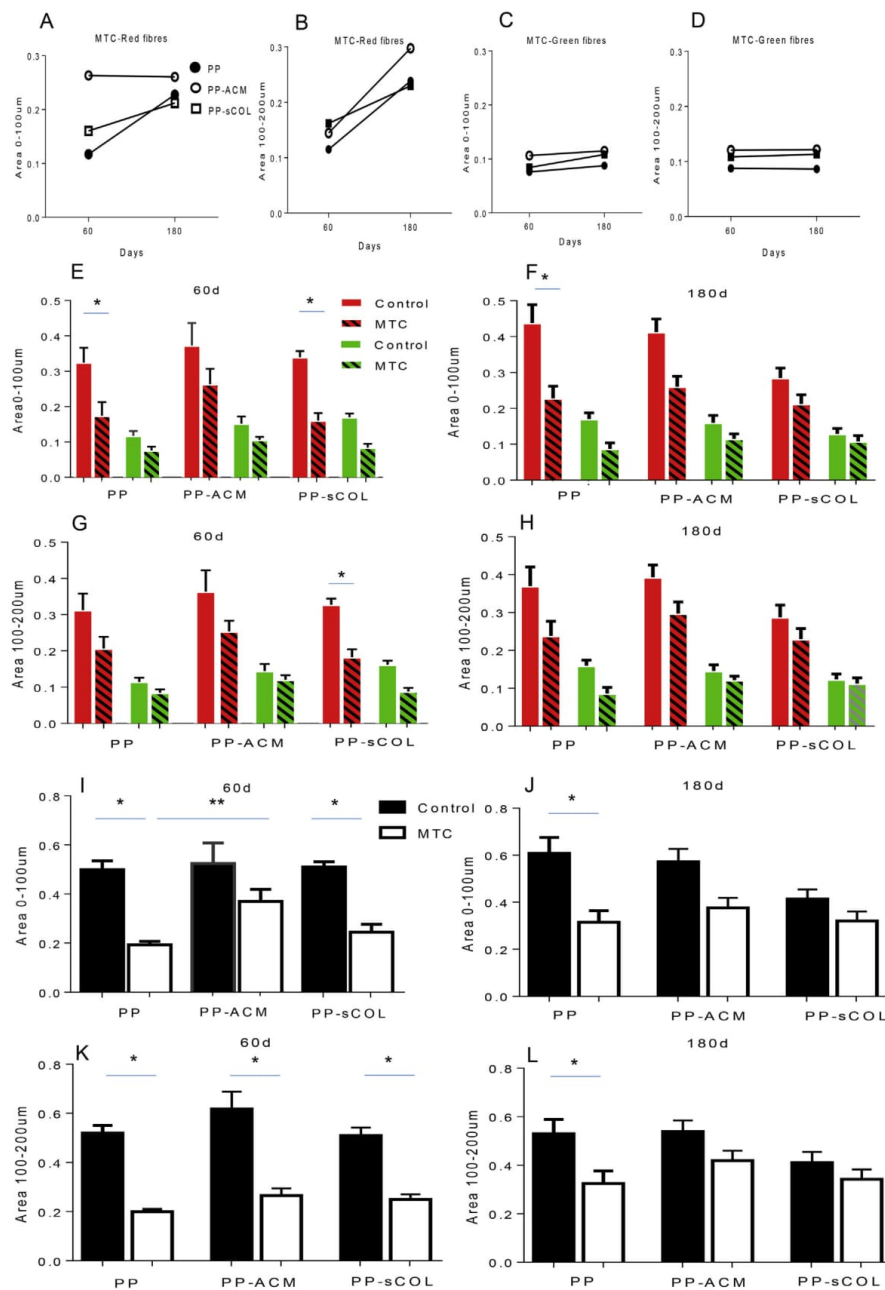


Fig. 5. Birefringence analysis of Sirius Red stained sections of collagen-containing PP meshes. (A–D) Area of red and green fibres in MTC (mesh/tissue complex) after 60 and 180 days in first (A&C) and second 100 µm (B&D). (E–H) Red and green fibres area in controls and MTC in first 100 µm after 60 days (E) and 180 (F) days. Red and Green fibre area in control and MTC in second 100 µm increment (100–200 µm) after 60 days (G) and 180 days (H). (I–L) Total collagen area (green + red) in first 100 µm in control (black) and MTC (white) in first 100 µm (I & J) and in the second 100 µm increment (K & L). Data expressed as mean \pm SEM (n = 6 animals/group). *P < 0.05, **P < 0.01. (For interpretation of the references to colour in this figure legend, the reader is referred to the web version of this article.)

the mesh implant. We have previously quantified the mature and immature collagen around mesh implants and validated it by Scanning Electron Microscopy (SEM) [36].

The maturity of collagen depends on fibril size. Mature collagen is thick heterodimers while immature ones are thin. Under the polarizing microscope, immature thin collagen fibrils appear green whereas the mature, thick fibrils are red, easily distinguished from black background areas lacking collagen fibre bundles or composed of cells or other ECM proteins. The amount of red mature and green immature collagen fibrils were quantitatively assessed in two larger radii around the mesh filament bundles to better understand the process of new collagen regeneration in relation to the interfacial distance from the mesh filaments. Our data showed consistent and higher levels of mature collagen in control vaginal tissues taken far from the implanted mesh site than around filaments of the three mesh types as expected for uninjured tissue representative of normal tissue with a more mature type of collagen. The Avaulta plus collagen layer is cross-linked with 1-ethyl-3-(3-dimethylaminopropyl) carbodiimide (EDAC) which slows collagen degradation (up to 6 months) allowing for longer-term and durable surgical repair. Based on our previous findings there were visible persisting remnants of the cross-linked collagen sheet in 50% and 17% of animals in PP-ACM groups after 60 and 180 days, respectively. Comparison of mesh types between the green, red and total birefringent collagen revealed that PP-ACM contained more collagen after 60 days, but this may have been due to the incomplete degradation of the ACM sheet, which could have contributed to the level of mature collagen in the mesh/tissue complex observed at 60 days. While both modified meshes contained collagen, the format of the coating was different. Unlike the PP-sCOL which contained a non cross-linked, non-immunogenic reconstituted soluble atelocollagen, PP-ACM mesh comprised a cross-linked decellularised natural tissue. As such, continuous slowly degrading collagen still present in this group after 60 days would delay the wound tissue response resulting in significantly fewer CD163 positive M2 macrophages (Fig. 3). At 180 days the collagen sheet had completely disappeared [17] and the levels of mature collagen and total collagen around the implants were similar for both types of collagen-containing meshes. Overall, there was a greater proportion of red rather than green birefringent fibrils with time indicating an advanced maturation process in the mesh implanted tissues approaching native vaginal wall tissue. After 180 days both total mature and immature collagen levels in the collagen coated meshes (PP-ACM and PP-sCOL) were closer to native tissue than PP mesh alone, supporting the beneficial effect the incorporation of collagen in the meshes has on the regenerative process.

The meshes used were the most common non-degradable synthetic meshes in use at the time of this study. All three meshes comprised the same polypropylene material, and two contained a collagen coating in two different formats; PP-sCOL in which individual filaments are coated with a non-cross-linked enzyme-purified solubilized atelocollagen, providing a fast resorbing layer between individual mesh filaments and the tissue, and PP-ACM, in which a natural decellularised and cross-linked slower degrading collagen tissue is layered on top of the whole mesh implanted. In this study our hypothesis was that PP meshes which are coated with collagen in different ways will induce different responses and that the biocompatibility of the mesh at the mesh tissue interface would be affected by this different format of collagen coating.

Our new more sophisticated quantitative analyses extend our previous study [17] which revealed a trend for increased vascularization in PP-sCOL mesh/tissue complexes using less sensitive histological scoring. With our image analysis method focussed at the interface of the mesh filaments and tissue, we found significantly greater vascularization compared to PP-ACM explants, indicating the increased sensitivity of our quantitative approach. Our

birefringent collagen analysis of Sirius red stained tissue explants also demonstrated significant differences between control tissue and mesh explants that were not detected by subjective scoring methods [17], particularly at 60 days where total collagen density was increased for the collagen covered PP mesh, likely due to inclusion of partially degraded collagen at the mesh-tissue interface. Our new quantitative methods applied for the first time to ovine vaginal tissues indicate their sensitivity in detecting differences in tissue response between PP-collagen composite mesh types in assessing chronic inflammation and collagen composition and organisation.

The ideal mesh for POP surgery should not erode into adjacent organs. Mild inflammation promotes neo-vascularization, new collagen deposition and better integration of the mesh. Macrophages play an important role in tissue remodelling and regeneration after mesh implantation and since collagen coating minimizes the contact area between the mesh and tissue, it can directly affect the early macrophage infiltration into the implanted area.

Based on our findings in this study, collagen coating can reduce chronic inflammation and promote the neovascularization and biocompatibility. However the biomechanical properties of the mesh, in particular mesh stiffness should be taken into account as one of the main reasons for complications associated with erosion and post-surgery complications. One major limitation of this study was the lack of earlier time points to assess these inflammatory responses and collagen changes and that we were unable to assess the effect of exogenous collagen alone on early tissue responses to implanted meshes. A second limitation was the limited number of antibodies available that cross-react with ovine cells in tissues, particularly to assess the inflammatory M1 macrophage role. A major advantage of this study is using the ovine vagina for implanting mesh due to similarities to human vaginal anatomy. Another strength is the use of non-biased, quantitative measurements of collagen maturity and the leukocyte response to implanted mesh in a field where subjective scoring methods are often used.

5. Conclusion

Using the ewe as an experimental model for vaginal prolapse surgery introduces a number of limitations for using advanced molecular techniques. Herein we describe the use of semi-quantitative methods for characterizing the host response. We used these for a medium term experiment evaluating the effect of collagen-containing PP meshes for POP surgery. Coating with solubilized atelocollagen showed improved biocompatibility and healing responses, by inducing sustained late neovascularisation and promoting neo-collagen maturation. Coverage of PP with an acellular collagen matrix delayed a partial M2 macrophage response which was likely due to the slow degradation of the exogenous collagen and may have contributed to the high level of mature collagen observed around the mesh 60 days after implantation. We speculate that the M2 macrophage response may result in the secretion of tissue growth factors such as PDGF and TGF β to recruit fibroblasts and smooth muscle cells for collagen production and stabilisation of neo-vessels. Further studies are needed to assess the macrophage response and collagen organisation at earlier time-points.

Appendix A. Supplementary data

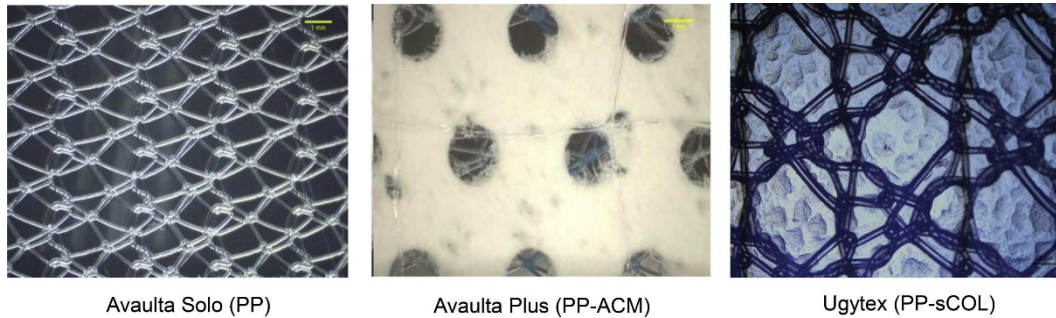
Supplementary data associated with this article can be found, in the online version, at <http://dx.doi.org/10.1016/j.actbio.2016.05.010>.

References

- [1] J.E. Jelovsek, C. Maher, M.D. Barber, Pelvic organ prolapse, *Lancet* 369 (2007) 1027–1038.
- [2] C. Maher, B. Feiner, K. Baessler, C. Schmid, Surgical management of pelvic organ prolapse in women, *Cochrane Database Syst. Rev.* 4 (2013). Cd004014.
- [3] A.L. Olsen, V. Smith, J. Bergstrom, J. Colling, A.L. Clark, Epidemiology of surgically managed pelvic organ prolapse and urinary incontinence, *Obstet. Gynecol.* 89 (1997) 501–506.
- [4] F.J. Smith, C.D.J. Holman, R.E. Moorin, N. Tsokos, Lifetime risk of undergoing surgery for pelvic organ prolapse, *Obstet. Gynecol.* 116 (2010) 1096–1100.
- [5] D. Altman, T. Vayrynen, M.E. Engh, S. Axelsen, C. Falconer, Anterior colporrhaphy versus transvaginal mesh for pelvic-organ prolapse, *N. Engl. J. Med.* 364 (2011) 1826–1836.
- [6] J. Deprest, F. Zheng, M. Konstantinovic, F. Spelzini, F. Claerhout, A. Steensma, Y. Ozog, D. De Ridder, The biology behind fascial defects and the use of implants in pelvic organ prolapse repair, *Int. Urogynecol. J. Pelvic Floor Dysfunct.* 17 (Suppl 1) (2006) S16–S25.
- [7] J. Deprest, A. Feola, The need for preclinical research on pelvic floor reconstruction, *BJOG* 120 (2013) 141–143.
- [8] R. Liang, S. Abramowitch, K. Knight, S. Palcsey, A. Nolfi, A. Feola, S. Stein, P.A. Moalli, Vaginal degeneration following implantation of synthetic mesh with increased stiffness, *BJOG* 120 (2013) 233–243.
- [9] S. Manodoro, M. Endo, P. Uvin, M. Albersen, J. Vlacil, A. Engels, B. Schmidt, D. De Ridder, A. Feola, J. Deprest, Graft-related complications and biaxial tensiometry following experimental vaginal implantation of flat mesh of variable dimensions, *BJOG* 120 (2013) 244–250.
- [10] FDA Update, Urogynecologic Surgical Mesh: Update on the Safety and Effectiveness of Transvaginal Placement for Pelvic Organ Prolapse (2011).
- [11] M. Slack, D. Ostergard, M. Cervigni, J. Deprest, A standardized description of graft-containing meshes and recommended steps before the introduction of medical devices for prolapse surgery. Consensus of the 2nd IUGA Grafts Roundtable: optimizing safety and appropriateness of graft use in transvaginal pelvic reconstructive surgery, *Int. Urogynecol. J.* 23 (Suppl. 1) (2012) S15–S26.
- [12] M.T. Wolf, C.A. Carruthers, C.L. Dearth, P.M. Crapo, A. Huber, O.A. Burnsed, R. Londono, S.A. Johnson, K.A. Daly, E.C. Stahl, J.M. Freund, C.J. Medberry, L.E. Carey, A. Nieponice, N.J. Amoroso, S.F. Badylak, Polypropylene surgical mesh coated with extracellular matrix mitigates the host foreign body response, *J. Biomed. Mater. Res. A* 102 (2014) 234–246.
- [13] J.E. Valentin, A.M. Stewart-Akers, T.W. Gilbert, S.F. Badylak, Macrophage participation in the degradation and remodeling of extracellular matrix scaffolds, *Tissue Eng. Part A* 15 (2009) 1687–1694.
- [14] R. de Tayrac, A. Alves, M. Therin, Collagen-coated vs noncoated low-weight polypropylene meshes in a sheep model for vaginal surgery. A pilot study, *Int. Urogynecol. J.* 18 (2007) 513–520.
- [15] R.K. Huffaker, T.W. Muir, A. Rao, S.S. Baumann, T.J. Kuehl, L.M. Pierce, Histologic response of porcine collagen-coated and uncoated polypropylene grafts in a rabbit vagina model, *Am. J. Obstet. Gynecol.* 198 (2008) 582.e581–582.e587.
- [16] J.M. Anderson, A. Rodriguez, D.T. Chang, Foreign body reaction to biomaterials, *Semin. Immunol.* 20 (2008) 86–100.
- [17] A. Feola, M. Endo, I. Urbankova, J. Vlacil, T. Deprest, S. Bettin, B. Klosterhalfen, J. Deprest, Host reaction to vaginally inserted collagen containing polypropylene implants in sheep, *Am. J. Obstet. Gynecol.* 212 (2015) 474.e471–474.e478.
- [18] S.D. Abramowitch, A. Feola, Z. Jallah, P.A. Moalli, Tissue mechanics, animal models, and pelvic organ prolapse: a review, *Eur. J. Obstet. Gynecol. Reprod. Biol.* 144 (Suppl. 1) (2009) S146–S158.
- [19] B.M. Couri, A.T. Lenis, A. Borazjani, M.F. Paraiso, M.S. Damaser, Animal models of female pelvic organ prolapse: lessons learned, *Exp. Rev. Obstet. Gynecol.* 7 (2012) 249–260.
- [20] F.G. Davies, The occurrence of vaginal eversion and allied disorders in fat ewes, *Res. Vet. Sci.* 11 (1970) 86–90.
- [21] S. Ennen, S. Kloss, G. Scheiner-Bobis, K. Failing, A. Wehrend, Histological, hormonal and biomolecular analysis of the pathogenesis of ovine Prolapsus vaginae ante partum, *Theriogenology* 75 (2011) 212–219.
- [22] L.C. Skoczylas, J.P. Shepherd, K.J. Smith, J.L. Lowder, Managing mesh exposure following vaginal prolapse repair: a decision analysis comparing conservative versus surgical treatment, *Int. Urogynecol. J.* 24 (2013) 119–125.
- [23] D. Ulrich, S.L. Edwards, V. Letouzey, K. Su, J.F. White, A. Rosamilia, C.E. Gargett, J.A. Werkmeister, Regional variation in tissue composition and biomechanical properties of postmenopausal ovine and human vagina, *PLoS ONE* 9 (2014) e104972.
- [24] M. Endo, I. Urbankova, J. Vlacil, S. Sengupta, T. Deprest, B. Klosterhalfen, A. Feola, J. Deprest, Cross-linked xenogenic collagen implantation in the sheep model for vaginal surgery, *Gynecol. Surg.* 12 (2015) 113–122.
- [25] D. Ulrich, S.L. Edwards, J.F. White, T. Supit, J.A. Ramshaw, C. Lo, A. Rosamilia, J.A. Werkmeister, C.E. Gargett, A preclinical evaluation of alternative synthetic biomaterials for fascial defect repair using a rat abdominal hernia model, *PLoS ONE* 7 (2012) e50044.
- [26] D. Ulrich, K. Su, K.-S. Tan, J.F. White, J.A.M. Ramshaw, C. Lo, A. Rosamilia, J.A. Werkmeister, C.E. Gargett, Human endometrial mesenchymal stem cells modulate the tissue response and mechanical behavior of polyamide mesh implants for pelvic organ prolapse repair, *Tissue Eng. Part A* 20 (2014) 785–798.
- [27] J.F. Woessner Jr., The determination of hydroxyproline in tissue and protein samples containing small proportions of this amino acid, *Arch. Biochem. Biophys.* 93 (1961) 440–447.
- [28] I. Barbosa, S. Garcia, V. Barbier-Chassefiere, J.P. Caruelle, I. Martelly, D. Papy-Garcia, Improved and simple micro assay for sulfated glycosaminoglycans quantification in biological extracts and its use in skin and muscle tissue studies, *Glycobiology* 13 (2003) 647–653.
- [29] R. Lattouf, R. Younes, D. Lutonski, N. Naaman, G. Godeau, K. Senni, S. Changotade, Picrosirius red staining: a useful tool to appraise collagen networks in normal and pathological tissues, *J. Histochem. Cytochem.* 62 (2014) 751–758.
- [30] M.H.M. Barros, F. Hauck, J.H. Dreyer, B. Kempkes, G. Niedobitek, Macrophage polarisation: an immunohistochemical approach for identifying M1 and M2 macrophages, *PLoS ONE* 8 (2013) e80908.
- [31] R.F. Diegelmann, M.C. Evans, Wound healing: an overview of acute, fibrotic and delayed healing, *Front. Biosci.* 9 (2004) 283–289.
- [32] T. Roszer, Understanding the mysterious M2 macrophage through activation markers and effector mechanisms, *Mediators Inflamm.* 2015 (2015) 816460.
- [33] R.T. Siniscalchi, M. Melo, P.C. Palma, I.M. Dal Fabbro, C. Vidal Bde, C.L. Ricetto, Highly purified collagen coating enhances tissue adherence and integration properties of monofilament polypropylene meshes, *Int. Urogynecol. J.* 24 (2013) 1747–1754.
- [34] L. Kati, P.C. Feldner, R. de Castro, E. Kobayashi, M. Sartori, H. Nader, M. Girao, Analysis of glycosaminoglycans in the parametrium and vaginal apex of women with and without uterine prolapse, *J. Womens Health* 19 (2010) 1341–1344.
- [35] K.S. Midwood, L.V. Williams, J.E. Schwarzbauer, Tissue repair and the dynamics of the extracellular matrix, *Int. J. Biochem. Cell Biol.* 36 (2004) 1031–1037.
- [36] S.L. Edwards, D. Ulrich, J.F. White, K. Su, A. Rosamilia, J.A. Ramshaw, C.E. Gargett, J.A. Werkmeister, Temporal changes in the biomechanical properties of endometrial mesenchymal stem cell seeded scaffolds in a rat model, *Acta Biomater.* 13 (2015) 286–294.

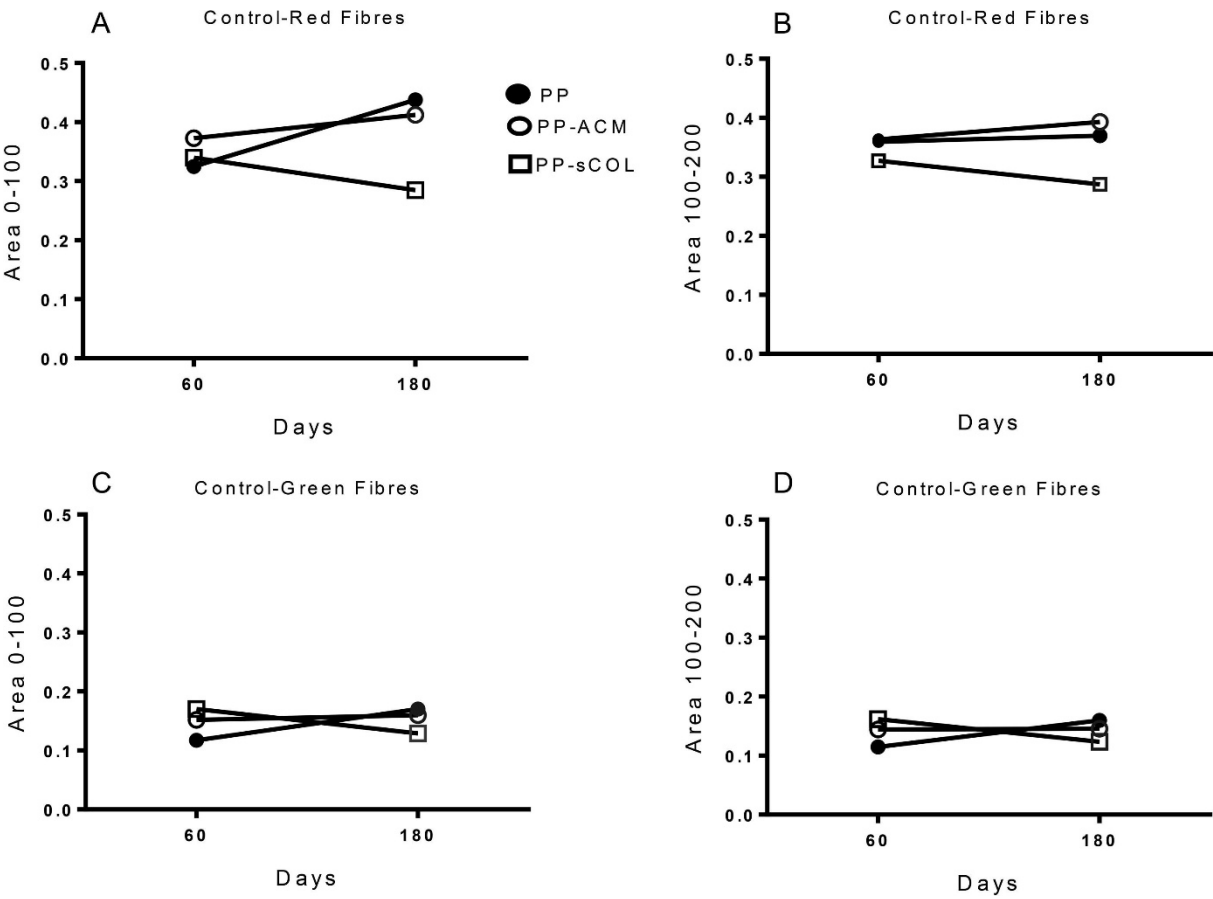
Supplementary Figure 1

Three Types of mesh implanted in Ovine vaginal wall



Supplementary Figure 2

Collagen quality analysis. The mature red fibrils synthesis increased with the time in Mesh Tissue Complex (MTC) in both 100 and 200 μm increment zone but not in control ([A,B](#)). However, the green, immature collagen fibrils did not change in either MTC or control after 60 and 180 days ([C,D](#)).



Chapter 3

Endometrial Mesenchymal Stem/ Stromal Cells Modulate the Macrophage Response to Implanted Polyamide/ Gelatin Composite Mesh in Immunocompromised and Immunocompetent Mice

3.1. Introductory statement

One of the main concern of biomaterial implantation is the host response to the implanted mesh. M1 inflammatory and M2 anti-inflammatory macrophages play key roles in this process. The balance between these two types of macrophages determines the failure or success of implanted mesh or biomaterial. The wound healing properties of M2 macrophages is increasingly exploited in biomaterial research to promote M2 macrophage dominance around the implanted biomaterial. Mesenchymal stem cells facilitate M1 macrophage differentiation towards an M2 phenotype. The isolation of MSC from bone marrow, as a main source of adult MSC, is invasive and needs anesthesia. Indeed, isolation methods used (plastic adherence) fail to purify the undifferentiated MSC from the predominant population of fibroblasts and these cell preparations are heterogeneous, mainly comprising fibroblasts.

Endometrial MSC (eMSC) are a newly identified source of MSC which are easily accessible without anaesthesia. They are clonogenic at very low densities (5-10 cell/cm²) in serial cloning assays indicating self-renewal in-vitro. Despite the unique properties of eMSC, including high proliferative potential, and mesodermal lineage differentiation, there are scant studies using eMSC for tissue engineering and cell-based therapies. Our group previously assessed the biological and biomechanical behavior of a novel gelatin/polyamide mesh (PA+G), seeded with eMSC in a subcutaneous rat model of wound repair as a preclinical model for POP repair surgery. Our results revealed that eMSC significantly improved the biocompatibility of these novel mesh designs. In this chapter, I investigated the effect of eMSC on the macrophage response to implanted

PA+G mesh. I determined that eMSC modulated the inflammatory response to implanted mesh and facilitated M2 macrophage differentiation.

Isolated human SUSD2⁺ eMSC were labelled with mCherry Lentivirus and seeded onto PA+G mesh, then implanted into a subcutaneous wound in mice and tissue collected at 3, 7, 14 and 30 days.

Collected tissues were assessed for

1. M1 and M2 macrophage markers
2. Inflammatory cytokine secretion
3. M2 macrophage marker mRNA expression

I thank Mrs Kersin Tan and Dr Shanti Gurung for assisting with mouse monitoring, Dr Shayanti Mukherjee for helping with immunostaining and Dr James Deane for assistance with animal surgery. I also thank Dr Kirstin Elgass for image analysis and confocal microscopy training and advice. I would also acknowledge Dr Sharon Edwards and Mr Aditya Vashi from CSIRO for PA+G mesh preparation.

Declaration

Monash University

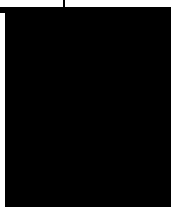
Declaration for Thesis Chapter 3

In the case of Chapter 3 my contribution to the work involved the following:

Chapter 3 - Endometrial Mesenchymal Stem/Stromal Cells Modulate the Macrophage Response

Name	Nature of Contribution	Extent of contribution (%) for student co-authors only
Saeedeh Darzi	Study design and performed the experiments, data collection and analysis, manuscript writing	85%
James Deane	Study conception and design, manuscript editing	N
Claudia Nold	experimental design	N
Sharon Edwards	Assistance with and provision of essential materials	N
Daniel Gough	Assistance with and provision of essential materials	N
Shayanti Mukherjee	Perform experiments	N
Shanti Gurung	Assistance with and provision of essential materials	5%
Kersin Tan	Perform experiments	N
Aditya Vashi	Assistance with and provision of essential materials	N
Jerome Werkmeister	Study conception and design, manuscript writing and editing	N
Caroline Gargett	Study conception and design, manuscript writing and editing	N

Student signature:



Date: 12.08.2017

Manuscript submitted to Scientific Reports

Running Title:

Endometrial Mesenchymal Stem/Stromal Cells Modulate the Macrophage Response to
Implanted Polyamide/Gelatin Composite Mesh in **Immunocompromised** and
Immunocompetent Mice

Darzi S^{a,b}, Deane JA^{a,b}, Nold CA^a, Edwards S^c, Gough DJ^a, Mukherjee S^a, Gurung S^{a,b}, Tan KS^a, Vashi AV^c, Werkmeister JA^{a,b,c}, Gargett CE^{a,b*}

- a. The Ritchie Centre, Hudson Institute of Medical Research, 27–31 Wright Street, Clayton, Victoria 3168, Australia
- b. Department of Obstetrics and Gynaecology, Monash University, Clayton, Victoria 3168, Australia,
- c. CSIRO Manufacturing, Bayview Avenue, Clayton, Victoria 3169, Australia

*Corresponding Author

Professor Caroline Gargett

Hudson Institute of Medical Research

The Ritchie Centre

Translation Research Facility Level 5

27-31 Wright Street, Clayton, Victoria, 3168

Australia



3.2. Abstract

The immunomodulatory properties of human endometrial mesenchymal stem cells MSC (eMSC) have not been well characterized. Initial studies showed that eMSC modulated the chronic inflammatory response to a non-degradable polyamide/gelatin mesh in a xenogeneic rat skin wound repair model, but the mechanism remains unclear. In this study, we investigated the immunomodulatory effect of eMSC on the macrophage response to polyamide/gelatin composite mesh in an abdominal subcutaneous wound repair model in C57BL6 immunocompetent and NSG (NOD Scid gamma) immunocompromised mice to determine whether responses differed in the absence of an adaptive immune system and NK cells. mCherry lentivirus-labelled eMSC persisted longer in NSG mice, inducing longer term paracrine effects. Inclusion of eMSC in the mesh reduced inflammatory cytokine (Il-1 β , Tnf- α) secretion, and in C57BL6 mice reduced CCR7⁺ M1 macrophages surrounding the mesh on day 3 and increased M2 macrophage marker mRNA (*Arg1*, *Mrc1*, *Il10*) expression at days 3 and 7. In NSG mice, these effects were delayed and only observed at days 7 and 30 in comparison with controls implanted with mesh alone. These results show that the differences in the immune status in the two animals directly affect the survival of xenogeneic eMSC which leads to differences in the short-term and long-term macrophage responses to implanted meshes.

Keywords: endometrium, mesenchymal stem cell, macrophage, tissue engineering

3.3. Introduction

Tissue engineering (TE) combines cells and materials to create implants that improve repair of injured tissues (Langer and Vacanti, 1993, Shafiee and Atala, 2017, Vacanti and Langer, 1999). Huge advances in tissue engineering have occurred over the past two decades with the development of new biomaterials and the use of various adult stem cells, MSC in particular. Tissue engineering has great potential for use in women's urogynaecological health including treatment of stress urinary incontinence (SUI) and pelvic organ prolapse (POP) (Chapple et al., 2015, Gigliobianco et al., 2015, Society, 2017).

Pelvic Organ Prolapse is the herniation of pelvic organs into the vagina. Symptoms include voiding, bowel and sexual dysfunction and incontinence (Maher et al., 2013). POP affects more than 25% of all women and 19% of women undergo reconstructive surgical treatment, often involving surgical mesh to provide mechanical support to damaged tissue (Olsen et al., 1997, Smith et al., 2010a). Monofilament polypropylene mesh with a large pore size allows for greater neo-tissue ingrowth and is the most common type of mesh used in POP surgery (Konstantinovic et al., 2007). However, vaginal insertion of mesh has resulted in complications in approximately 10% of women (Tijdink et al., 2011) including mesh erosion, mesh contracture, infection and pain (de Tayrac R, 2006). The use of tissue engineering constructs may reduce these adverse effects.

Adult mesenchymal stem cells have been used as a cell-based therapy in tissue engineering applications to deliver reparative cells to damaged tissue sites to effect tissue repair and regeneration (Matsushima et al., 2009). A number of tissue engineering

approaches using bone marrow mesenchymal stem cells (bmMSC) have been explored in abdominal wall hernia repair (Dolce et al., 2010, Zhao et al., 2012). More commonly, bmMSC have been administered intravenously, where they home to damaged and injured tissues and exert anti-inflammatory and immunomodulatory effects, without tissue incorporation (Le Blanc and Mougiakakos, 2012). Human endometrial MSC (eMSC) are a recently identified MSC type that are easily accessible by a minimally invasive office-based biopsy procedure without anaesthesia (Ulrich et al., 2013a, Darzi et al., 2016b). Clonogenic eMSC can be purified using co-expression of CD140b and CD146 with a cell sorter or by a single marker, SUSD2 (recognised by the W5C5 antibody) using magnetic bead sorting (Masuda et al., 2012, Schwab and Gargett, 2007). These perivascular eMSC fulfil the International Society for Cellular Therapies minimal MSC criteria, are highly proliferative, self-renew in vitro and reconstitute stromal tissue in vivo (Masuda et al., 2012, Gargett et al., 2016).

We are developing and evaluating a new type of mesh for potential clinical use in POP treatment. In particular, we fabricated a new tissue engineered construct comprising a novel polyamide knitted mesh coated with stabilised gelatin (PA+G) (Edwards et al., 2013, Ulrich et al., 2012). Comparison of the structural characteristic and mechanical properties of the mesh with three commercial PP meshes showed that our PA+G mesh was less stiff and had lower bending rigidity, more desirable properties for POP surgical repair. We have also shown the efficacy of using eMSC in PA+G mesh (Ulrich et al., 2012) to deliver eMSC in a small animal model of wound repair (Ulrich et al., 2014b). In this xenogeneic model, human eMSC exerted a paracrine effect promoting wound healing, angiogenesis

and neo tissue formation. Seeding the mesh with eMSC enhanced the biocompatibility of the mesh by reducing chronic inflammation and promoting the deposition of crimped physiological collagen around mesh filaments resulting in reduced stiffness of the mesh-tissue complex in long term (Edwards et al., 2015). Thus, eMSC-seeded PA+G mesh may provide an alternative treatment option for POP (Ulrich et al., 2013a).

One of the main concerns in tissue engineering is the host response to biomaterials (Anderson et al., 2008). Macrophages play a key role in host response to biomaterials (Xia et al., 1994, Labow et al., 2005) by secreting cytokines and chemokines that impact on tissue repair (Sridharan et al., 2015a). Understanding the exact role of macrophages in host response to implanted biomaterials and the factors that may secrete to regulate this response is important.

Several lines of evidence have demonstrated crosstalk between macrophages and MSC. Macrophages co-cultured with bmMSC expressed higher levels of CD206, the mannose receptor, and secreted anti-inflammatory IL-10 and reduced levels of Tumor Necrosis Factor- α (TNF- α) in the microenvironment (Kim and Hematti, 2009). In a sepsis mouse model, infusion of mouse bmMSC decreased lethality, and the protective effect of the MSC was eliminated by macrophage depletion or by the administration of IL-10 neutralizing antibodies (Nemeth et al., 2009). IL-10 produced by M2 macrophages blocked excessive neutrophil infiltration into the injured tissue and prevented further damage (Nemeth et al., 2009). Similarly, in an endotoxin-induced lung injury model, intrapulmonary delivery of mouse bmMSC decreased the production of Tnf- α and

Chemokine Ligand 2 (CXCL2) and increased alveolar macrophage secretion of IL-10 (Gupta et al., 2007).

To further elucidate the early immune responses to eMSC-seeded PA+G mesh, the aim of the current study was to determine whether eMSC alter macrophage polarization from an M1 inflammatory to an M2 wound healing phenotype in response to implanted mesh in both early and later stages of the host response. We compared two mouse models; immunocompromised (NSG) and immunocompetent (C57BL6) mice. NSG mice lack an adaptive immune system and NK cells, and have a defective innate immunity associated with functionally immature macrophages and deficiencies in several cytokine signalling pathways (Shultz et al., 2007). We compared the anti-inflammatory and immunomodulatory effects of eMSC on macrophage responses between mouse strains with intact (C57BL6) and defective (NSG) immune systems. We also assessed whether xenogeneic, heterologous eMSC persisted longer in the absence of an adaptive and deficient innate immune system.

3.4. Results

3.4.1. eMSC transduction and survival in vivo on PA+G mesh

In order to track the cells in vivo, eMSCs purified by SUSD2 magnetic bead sorting were transduced with mCherry lentiviral vector and the SUSD2⁺mCherry⁺ cells were sorted and cultured in DMEM medium containing 10% FBS. More than 95% of cultured eMSCs were mCherry⁺ (Fig.1A and B) and around 40% of this population were SUSD2⁺. Double positive cells were sorted, expanded and seeded on PA+G mesh (Fig.1C). The persistence of implanted eMSC was assessed by fluorescence microscopy. Three days

after mesh implantation, mCherry⁺ eMSC were found around the mesh filaments and in the gelatin layer in NSG mice (Fig. 1D and E). Fewer mCherry⁺ cells persisted after 7 days (Fig. 1F and G). No mCherry⁺ eMSC were detected in C57BL6 mice after 3 or 7 days implantation.

H&E staining showed the degree of cellularity around the implanted mesh at the later time points (days 14 and 30) in both NSG and C57BL6 mice of the eMSC/mesh and mesh control groups. The gelatin layer coated on the top of the mesh gradually degraded with the time. Visually, there was a higher number of infiltrated cells in immunocompetent mice compared with immunocompromised mice. (Supplementary Fig. 1A-H).

3.4.2. eMSC induce macrophage polarization

Image analysis quantification within the first 100 μ m increment around individual mesh filaments showed that the percentage of total macrophages (F4/80⁺) relative to Hoechst-stained nucleated cells in C57BL6 and NSG mice was relatively constant from day 3 to 30 in both groups; PA+G mesh seeded with and without eMSC (Fig. 2A and C).

To determine the phenotype of F4/80⁺ macrophages accumulating around the eMSC/PA+G (eMSC/mesh) and non-seeded PA+G (mesh control), dual color immunofluorescence staining was performed to quantify M1 (CCR7/F4/80) and M2 (CD206/F4/80) macrophages in sections from C57BL6 and NSG mice at 3, 7, 14 and 30 days. In mesh seeded with eMSCs, the number of M1 expressing macrophages was significantly reduced in comparison to the control implants at day 3 in immune intact

(C57BL6) mice ($P=0.0314$) (Fig. 3A and C). No significant differences between eMSC/mesh and mesh controls were observed at the later time points in C57BL6 mice. In immunocompromised mice (NSG), there was no difference in M1 macrophages from 3 to 30 days between the eMSC/mesh and mesh control groups (Fig. 3B and D).

We next used CD206 to investigate M2 macrophages, a hallmark cell associated with tissue regeneration and healing, around the implanted mesh filaments. There was no significant difference in the proportion of CD206-expressing macrophages between eMSC/mesh and mesh control groups in immunocompetent mice at any time point. (Fig. 4A and C). In the immunocompromised NSG mice, the M2 macrophage proportion gradually increased with time in both mesh control and eMSC/mesh groups with significantly more M2 macrophages present at day 30 compared with day 3, ($P=0.028$) (Fig. 4B and D). However, there was no difference between the density of M2 macrophages around mesh filaments whether eMSC were present or not. The M2/M1 ratio was higher in eMSC/mesh compared to mesh control in NSG and C57BL6 mice. There was a non-significant trend for the M2/M1 ratio to increase from day 3 to day 30 in NSG mice in either eMSC/mesh and mesh control groups ($P=0.9$ and $P=0.2$, respectively) (Supplementary Fig.2A&B).

3.4.3. eMSC modulate inflammatory cytokine mRNA expression

To further assess the inflammatory response to the implanted mesh, the mRNA expression of the inflammatory cytokines, *Il1b* and *Tnfa* was quantified by q-PCR. In C57BL6 mice, no differences were observed in *Il1b* mRNA expression between the groups at any time-point (Fig.5A). *Tnfa* expression was significantly reduced in

eMSC/mesh group at days 14 ($P=0.008$) and 30 ($P=0.01$) compared with mesh control group (Fig.5C).

In NSG mice, there was a significant decrease in *Il1b* gene expression eMSC/mesh group compared with the mesh control group at day 14 ($P=0.0023$) (Fig.5B) with no differences at the other time points. No significant difference was observed in *Tnfa* gene expression between eMSC/mesh and mesh control groups at any time point (Fig.5D) Comparison between immunocompetent and immunocompromised mice showed no significant difference in *Il1b* and *Tnfa* gene expression at any of the four time-points (Fig 5E&F).

3.4.4. eMSC modulate inflammatory cytokine secretion

As the qPCR quantification of inflammatory cytokine mRNA expression was not conclusive, the secretion of $Il-1\beta$ and $Tnf-\alpha$ protein was measured in explanted tissue lysates from C57BL6 and NSG mice. In immunocompetent mice, $Il-1\beta$ and $Tnf-\alpha$ were reduced at the early time points (days 3 and 7) in the eMSC/mesh group compared with the mesh control group (Fig. 6A and C). In the NSG mice, both $Il-1\beta$ and $Tnf-\alpha$ secretion levels were significantly reduced in the eMSC/mesh group compared with the mesh control group at day 7 for both inflammatory cytokines ($Tnf-\alpha$, $P=0.0381$ & $Il-1\beta$, $P=0.0417$), and also at day 30 for $Tnf-\alpha$ ($P=0.0122$) (Fig. 6B and D). The cytokine levels were noticeably lower in the tissues from immunocompromised NSG mice than in immunocompetent C57BL6 mice (Fig.6E and F). There was significantly less $Il-1\beta$ secretion in the mesh control group of NSG mice compared to C57BL6 mice at day 3 ($P=0.0336$) (Fig.6E). $Tnf-\alpha$ was significantly lower in NSG mice in the eMSC/mesh group

compared to the same group in C57BL6 mice after 30 days implantation ($P=0.006$) (Fig.6F).

3.4.5. eMSC induce the expression of M2 macrophage markers

We next assessed whether M2 macrophage marker mRNA expression was altered by the eMSC using q-PCR measurement of *Il10*, Arginase I (*Arg1*) and Mannose Receptor (*Mrc1*). *Arg1*, *Mrc1* and *Il10* mRNAs were significantly higher at day 3 in the eMSC/mesh group compared to the mesh control in immune intact C57BL6 mice ($P=0.032$, 0.0194 , 0.018 , respectively)(Fig. 7A, D and G). Similarly, at day 7, both *Mrc1* and *Il10* were increased in the eMSC/mesh group ($P=0.006$, 0.002 , respectively). In immunodeficient NSG mice *Arg1* expression was significantly increased in the eMSC/mesh group compared to the mesh control group at 30 days ($P=0.0161$) (Fig. 7B). *Mrc1* expression was significantly higher in the eMSC/mesh group at 14 days, compared with the mesh control ($P=0.05$) (Fig. 7E). Over time, *Arg1* expression increased in the eMSC/mesh group from day 7 to day 30 in NSG mice ($P=0.002$) (Fig. 6C). Comparison between C57BL6 and NSG mice showed that *Mrc1* expression was significantly higher in the eMSC/mesh group in C57BL6 mic, compared with same group in NSG mice at day 7 ($P=0.03$) (Fig.7F). Similarly, *Il-10* expression was significantly higher in eMSC/mesh group in C57BL6 mice, compared with NSG mice at days 3 and 7 ($P=0.001$ and $P=0.002$, respectively) (Fig.7J).

3.5. Discussion

The main findings of this study are that human eMSC changed the macrophage phenotype from M1 to M2 in both immunocompromised and immune intact mouse models resulting in a reduction of inflammatory cytokine secretion and an increase in M2 macrophage marker expression. These immunomodulatory effects mediated by eMSC were delayed and weaker in immunocompromised compared to immune intact mice, likely due to the persistence of eMSC and their slower disappearance in NSG mice. It is likely that eMSC exerted these immunomodulatory effects via a paracrine mechanism in both mouse models.

The level of the macrophage infiltration around the mesh was similar in the two animal models and the presence of eMSC had minimal impact on the absolute number of infiltrating macrophages. In the C57BL6 mice, where eMSC were not readily detected even as early as 3 days after eMSC/mesh implantation, there was a significant reduction of the inflammatory CCR7⁺ M1 macrophages. This was accompanied by reduced secretion of Il-1 β and Tnf- α during the first 7 days and reduced gene expression at later time-points, and upregulation of the M2 mRNA markers, *Arg1*, *Mrc1* and *Il10*. These findings indicate for the first time that the eMSC have significant immunomodulatory and anti-inflammatory properties in vivo through their effect on macrophage phenotype in immunocompetent animal models. The effect of eMSC on the macrophage response to implanted mesh was similar in NSG mice, however it was delayed and the cytokine response was blunted even though the eMSC survived longer. This was shown by the prolonged elevation of CD206 M2 macrophages and increased M2 mRNA markers, *Mrc1*

and *Arg1* up to day 30, accompanied by similar and ongoing reductions of pro-inflammatory cytokine secretion and mRNA expression. This persistence of xenogeneic human eMSC in immunocompromised mice suggests that their autologous use in women, where their removal is expected to be delayed, may have greater long term beneficial effects in modulating macrophage responses to foreign mesh materials than an allogeneic source.

Macrophages play a central role in the host response to implanted biomaterials, with both M1 and M2 macrophages having essential roles and the balance of M2/M1 determining the failure or success of implantation(Klopfleisch, 2016). To prevent prolonged detrimental effects of persisting M1 macrophages on implanted non-degradable biomaterials, a timely switch from a M1 to M2 macrophage phenotype can be favourable, a process facilitated by eMSC. Our data shows there was a trend for the M2/M1 ratio to increase over time in the NSG model, suggesting that co-transplantation of eMSC with a non-degradable biomaterial may be beneficial in reducing the chronic inflammatory response.

In this study, we quantified the effect of a recently described MSC on macrophage phenotype after mesh implantation. We showed that eMSC seeded on a synthetic composite mesh significantly reduced inflammation for up to 30 days in immunocompetent mice, despite their rapid disappearance, indicating that their modulatory effects influence the acute and chronic phase of the immune response. Other studies have also shown that injected or implanted MSC (from other sources) do not survive at the site but nevertheless limit tissue injury during their short stay through a

variety of mechanisms (Ionescu et al., 2012, Prockop and Oh, 2012). In an immune intact system as in C57BL6 mice, MSC influence most immune cell types, including those mediating innate immunity; NK cells, dendritic cells, neutrophils, and adaptive immunity cells; T and B lymphocytes (Le Blanc and Mougiakakos, 2012). Our study focused on the effect of eMSC on the macrophage response, showing that they inhibit inflammation by influencing the switching of M1 macrophages to a M2 phenotype, reducing inflammation at early and late time points. While we did not examine which eMSC mediators reduced the inflammatory response to PA+G mesh, it is possible that they operate in a similar manner to other MSC. For example, bmMSC upregulate the expression of Indoleamin2,3 dioxygenase (IDO), which induce the polarization of M1 macrophages to M2 phenotype and promote M2 macrophages secretion of *IL-10* (Le Blanc and Mougiakakos, 2012). Another possibility is the production of PGE2 and TGF- β by eMSC, since these molecules induce M2 phenotype switching (Luz-Crawford et al., 2016). To date there are no studies on the MSC mediators of M2 switching, PGE2 or TGF β , by eMSC. However, we found increased COX1 mRNA expression, a key enzyme involved in PGE2 synthesis, in eMSC treated with A83-01, a TGF β -receptor inhibitor, to prevent differentiation and maintain eMSC stemness, compared with non-treated cells (Gurung S, Werkmeister J, Gargett C, un-published data) suggesting that PGE2 may be involved in eMSC modulatory effects on macrophages. Comparison of eMSC and endometrial stromal fibroblast transcriptomes also showed higher TGF β expression in eMSC (Barragan et al., 2016). These data suggest that eMSC have the potential to function in a similar manner as other immunomodulatory MSC. Our ongoing studies are investigating these possibilities.

In NSG mice, the proportion of CD206⁺ M2 macrophages increased after 30 days in parallel with reduced levels of inflammatory cytokine secretion and mRNA expression. The lack of T, B and NK cells and defective dendritic cells (DC) and macrophages in NSG mice, likely explains the lower cytokine production observed around the mesh filaments compared with C57BL6 mice. In an immunocompromised system, where longer survival of implanted stem/progenitor cells is expected, eMSC may also exert longer-term immunomodulatory effects. In a mouse model of asthma, most of the PKH2-labelled MSC injected IV into BLALB/C mice were phagocytosed by macrophages and these macrophages subsequently acquired an M2 suppressive phenotype (Agrawal et al., 2014). However, it is unknown whether macrophages in NSG mice phagocytose eMSC, and this needs further investigation. One of the limitations of our previous study on the paracrine effects of eMSC on mesh implantation (Ulrich et al., 2014b, Edwards et al., 2015) was the inability to explain the late M1 to M2 switch. In this study only phenotypic CD profiling was used. Macrophages are heterogeneous, and activation and polarization into functional subsets is complex. In our current study, we have complimented the CD phenotype with quantification of more sensitive functional mediators indicative of macrophage status such as inflammatory cytokines and M2 macrophage markers. We detected genetically labelled eMSC surviving for at least 7 days in NSG mice, indicating their potential to have longer term effects as demonstrated by M2 macrophage marker expression and inflammatory cytokine secretion.

Immunofluorescent staining is a qualitative assessment and we did not find significant changes in two groups with this technique. This limitation led us to assess the

macrophage response with mRNA expression (qPCR) and protein secretion (ELISA) techniques which identified the regulatory effects of eMSC. The other limitation of this study which could have been assessed was the effect of macrophages on collagen and elastin synthesis in the area around the mesh fibers and whether the presence of eMSC can affect the tissue regeneration.

In summary, we have characterized some of the immunomodulatory properties of eMSC in vivo for the first time. We showed that eMSC mediate inhibitory effects in both immune intact and immune compromised systems suggesting that immune intact mice are suitable for tissue engineering studies using eMSC, although the implanted cells do not persist in the latter. eMSC exert their modulatory effects-by secretion of anti-inflammatory factors. Our ongoing work will characterize these factors to fully understand the immunoregulatory mechanism of eMSC on innate immune cells, in particular macrophages.

3.6. Material and Methods

3.6.1. Endometrial Tissues

The experimental protocols were performed under the ethical guidelines according to the National Health and Medical Research Council (NHMRC) of Australia's National Statement on Ethical Conduct in Human Research. Endometrial biopsies were obtained from 8 women undergoing laparoscopic surgery for non-endometrial gynaecological conditions and had not taken hormonal treatment for three months before surgery. The

samples were collected during the proliferative or secretory stage and the BMI of these women was not considered in this study. All women gave written informed consent. Our protocol was approved by the Monash Health and Monash University Human Research Ethics committees (09270B). Each patient sample was used to generate an individual eMSC cell line (n=6).

3.6.2. Isolation of SUSD2⁺ eMSC and Culture

Endometrial tissues were minced with scissors and digested using 5% collagenase type II and 40µg/ml deoxyribonuclease type I (DNase I) (Worthington-Biochemical Corporation) at 37°C in Dulbecco's modified Eagle's Medium/F12 medium (DMEM/F12) containing 15 µM Hepes buffer (Invitrogen) in a humidified incubator at 37°C on a rotating MACSmix (Miltenyi Biotec) for 60-90 minutes. Dissociated stromal cells were separated from collagenase resistant epithelial cells (as clumps) using a 40µm sieve (BD Bioscience-Durham) and red blood cells removed by density gradient centrifugation using Ficoll-Paque (GE Healthcare Bioscience-Bio-Sciences AB) as previously described (Chan et al., 2004). Single cell suspensions of stromal cells were incubated with PE-conjugated SUSD2 (formerly W5C5) antibody (2µg/ml) (Biolegend) for 30 minutes at 4°C followed by incubation with anti-PE labelled magnetic beads (Miltenyi Biotec) for 20 minutes and SUSD2⁺ eMSC were selected using a column and magnet (Miltenyi Biotec). SUSD2⁺ eMSC were cultured in DMEM/F12 medium containing 10% Fetal Calf Serum (FCS) (Invitrogen), 1% antibiotic-antimycotic (Life Technologies) and 2 mM glutamine (Life Technologies) for 2-4 passages. We have previously shown that this protocol isolates eMSC which robustly express the typical MSC markers when cultured (ie CD29,

CD44, CD73, CD90, CD105 >90%; CD31, CD34, CD45 <5%). We used cells between passage 2 and 4 for this study to minimize sample variation.

3.6.3. mCherry Lentivirus Transduction of eMSC

To detect eMSC in vivo, the cells were transduced with a mCherry lentivirus. Lentivirus was generated by co-transfection of three plasmids; 10µg pLVX-IRES-mCherry (lentivirus plasmid which contains mCherry gene) (clontech-6312237), packaging plasmids; 9µg pSPAX2 (which encodes capsid) (Addgene 12260) and 1µg pMD2.G (encodes reverse transcriptase for lentivirus replication) (Addgene 12259), into 293 cells. (<https://www.addgene.org/protocols/bacterial-transformation/>) using the TransIT-X2 (Mirus) transfection reagent according to manufacturer's protocols. Transfection was confirmed by monitoring mCherry expression by fluorescence microscopy. Viral containing supernatant was collected and passed through a 0.45µm filter. eMSCs were grown to 70% confluence and transduced with lentiviral supernatant supplemented with polybrene (5ug/ml) (Sigma hexadimethrine bromide, catalogue #[107689](#)). Viral supernatant was replenished after 6 hours.

3.6.4. mCherry⁺ / SUSD2⁺ eMSC Sorting

Following 48-72 hours transduction, eMSC were washed with 2% FBS/PBS, trypsinized with TrypLETM (Life Technologies) and then incubated with APC-conjugated mouse anti-human SUSD2 antibody (2 µg/ml) for 30 minutes in the dark on ice. Cells co-expressing mCherry and SUSD2 were sorted using a Beckman XDP cell sorter (Beckman Coulter, Life Science, Australia) and the data were analysed using Summit Cytomation software version 5.2. Sorted cells were then cultured until confluent for seeding onto the PA+G

mesh. Lentiviral transduction does not affect the expression of the classic MSC markers or SUSD2 (Gurung et al., 2015)

3.6.5. Fabrication of PA+G mesh and seeding with human eMSC

Polyamide (Nylon 6) meshes were warp knitted to a mass per unit area of 42 g/m² using 80 µm monofilament (Wetekam) and coated with gelatin by immersing in 12% sterile porcine type A gelatin, 300g Bloom (G1890, Sigma Aldrich) and cross-linked with 0.0125% glutaraldehyde, as previously described (Su et al., 2014). PA+G meshes were cut into 1x1 cm pieces and gamma sterilized with 25 kGy. Prior to cell seeding, mesh was coated with 10 µg/ml fibronectin for 30 minutes at 37°C. Mesh was then seeded at a density of 125,000 mCherry-labelled SUSD2⁺ cells/cm² in 30-40 µL of medium per mesh and cultured for 48-72 hours. Since the mesh size was only 1 cm² and seeding density of 500,000 cells was not possible (too high for cells to attach), we therefore cultured half of the cells on the mesh (250,000) (125000 per mesh) and then added another 250,000 of the same batch of transfected cells onto the mesh (125000 cells per mesh) on the day of to make sure that enough cells would be delivered to animal. The additional labelled eMSC were delivered in 12% porcine gelatin mixed with 1 mM ruthenium metal complex, (2,2'-bipyridyl) dichloro ruthenium (II) hexahydrate [Ru II(bpy)₃]²⁺ (Sigma-Aldrich) and 20 mM sodium persulfate (SPS) (Sigma-Aldrich) to allow cross linking of the gelatin using a LED dental lamp (460 nm, 1200 mW/cm², 3M Epilar Free Light 2) for 30 seconds (Elvin et al., 2010). Control meshes of PA+G (fibronectin coated) without cells were incubated in culture medium only and on the day of surgery a layer of gelatin without cells was added to the mesh and similarly cross-linked using blue light.

3.6.6. Implantation of eMSC-seeded PA+G Tissue Engineering Constructs

The experimental procedure and mouse husbandry was approved by Monash Medical Centre Animal Ethics Committee A (2014/03). NSG and C57BL6 mice were housed in the animal house at Monash Medical Centre according with the National Health and Medical Research Council of Australia guidelines for the care and use of laboratory animals and were provided sterile food and water under controlled environmental conditions. Mice (48 NSG and 48 C57BL6) were randomly divided into two experimental groups of 24 mice/group and implanted with PA+G mesh seeded with (eMSC/mesh) or without (mesh control) eMSC. The mice were anaesthetized with 3% w/v Isoflurane[®] and carprofen (5 mg/kg body weight) was used as analgesia. The abdomen was shaved and disinfected with 70% ethanol. A longitudinal 1.2 cm skin incision was performed in the lower abdomen and the skin was separated from the fascia by blunt dissection to make two pockets on each side of the midline. Tissue engineering constructs were implanted into two pockets of each animal, which received either eMSC-seeded or unseeded meshes. Meshes were sutured to the abdominal fascial layer using Dysilk 4-0[®] sutures (Dyneck) on two ends. Skin closure was performed with a single intracutaneous Dysilk 4-0[®] suture. Animals were euthanized in a CO₂ chamber and tissue harvested at 3, 7, 14 and 30 days (8 mice/group/time-point using the 8 different eMSC cell lines/group of mice for each time point). Explanted meshes were dissected and divided into 3 parts for immunofluorescence, quantitative RT-PCR and ELISA.

3.6.7. Immunofluorescence

Paraformaldehyde (4% for 24 hours at 4°C) fixed tissue samples frozen in OCT were cut (8 µm) and stained with rat anti-mouse F4/80 antibody (Table 1) to quantify total macrophages, rabbit anti-mouse CCR7 for pro-inflammatory M1 macrophages and rat anti-mouse CD206 for anti-inflammatory M2 macrophages (Table 1). Sections were thawed and blocked with protein block (Dako) for 1 hour at RT. After one wash in PBS, primary antibodies were incubated for 1 hour at RT. Isotype-matched antibodies (rat IgG2b, rat IgG2a and rabbit monoclonal IgG) were used as negative controls and applied at the same concentrations. After washing, Alexa-Fluor-488 and Alexa-Fluor-568-conjugated secondary antibodies were incubated for 30 minutes at RT, respectively. Nuclei were stained with Hoechst 33258 (Molecular Probes) for 3 minutes and the slides were mounted with fluorescent mounting medium (Dako). To avoid the overlap of the red Alexa Fluor 568 and mCherry, all the slides used for CCR7 immunostaining were first checked for the presence of mCherry signal and those containing mCherry⁺ cells were excluded from the immunostaining.

3.6.8. Image analysis

Four images were taken per stained section from one frozen block at each time-point using a FV1200 confocal microscope (Olympus, Life Science) at 20x magnification. mesh knots and the gelatin layer were included and images were taken from the center of the mesh avoiding the sutures. The images were analyzed using Image J software (National Institute of Health, NIH) (Schindelin et al., 2012) to measure positive signals around mesh filaments in 100 µm increments, as described previously (Darzi et al., 2016a). The

percentage of M1 (red) and M2 (white) macrophage immunostaining was calculated as a proportion of total macrophages (green), co-localised in the same sections. Cell numbers were calculated as a ratio of co-localized cells (green-red-blue) and/or (green-white-blue) to total macrophages (green-blue).

3.6.9. Lysate preparation and protein assay

The frozen collected tissues were thawed and cut in half and 300 µl of lysis buffer (Nold et al., 2013) was added and homogenized on ice for one min using a homogenizer (IKA T 10 basic ULTRA-TURRAX). The supernatant was collected following centrifugation at 13,000 rpm for 10 minutes. Then 3 µl of the supernatant was used to quantify total protein content using a bicinchoninic acid assay (BCA) according to the manufacturer's directions (Thermo Scientific) and read at 562 nm using a plate reader (Biotek). Lysate were stored in -80°C prior to use in ELISAs.

3.6.10. ELISAs

The inflammatory cytokines, Il-1 β and Tnf- α , were assessed by ELISA using mouse commercial kits (BD Bioscience OptEIA). The plates were coated with capture antibodies and incubated overnight at 4°C. The following day the plates were blocked with assay diluent (10% FBS in PBS) for one hour. The samples were diluted 1/10 in assay diluent and 50 µl of each of the samples and standards were loaded into the wells of 96 well plates. After 2 hours incubation at room temperature (RT), the plates were washed three times and incubated with biotinylated detection antibody for 1 hour followed with washing; then streptavidin-HRP was added to each well and incubated for 30 minutes at RT. Finally, a stop solution was added and the plates were read at 450 nm using a plate

reader (Biotek). The cytokine concentration of the samples was obtained from the four-parameter logistic standard curve and normalized to total protein for each sample.

3.6.11. qRT-PCR

RNA was extracted from explanted tissue using a RNA extraction mini kit (Qiagen-Life Technologies) according to manufacturer's protocol and the quality and yield determined by 260/280 and 230/260 absorbance in a Nanodrop (Lab Gear). The extracted RNA was stored at -80°C until use. First-strand cDNA was synthesized using SuperScript III first-strand synthesis system (Invitrogen). 100 ng of cDNA was then measured and assessed by quantitative PCR. M2 macrophage markers including Mannose receptor, Arginase and *Il10* mRNA and M1 macrophage markers including *Il1b* and *Tnfa* expression using SYBR Green Super Mix. Primer sets are detailed in Table 2. The PCR conditions consisted of initial denaturation at 95°C for 10 minutes, followed by 40 cycles of denaturation at 95°C for 15 seconds and annealing/polymerization at 60°C for 60 seconds. To determine the relative expression of target mRNA, the expression level of each gene was normalized to the expression level of GAPDH mRNA as an endogenous control and relative expression was reported as ΔCt .

3.6.12. Statistics

Statistical analysis was performed using GraphPad Prism v7 and data were normally distributed and analyzed with unpaired parametric two-tailed t-Test, one way and three-way ANOVA followed by Tukey posthoc test. Data are presented as mean +/- SEM.

Acknowledgements

The authors would like to thank Kellie Woodclarke for collecting tissue, Mina Khalaji and Jingyuan Shi for performing the ELISAs, Dr Kirstin Elgass, Monash Micro Imaging, for helping with confocal microscope and image analysis and MHTP histology for processing tissues for sectioning.

This work was supported by National Health and Medical Research Council (NHMRC) of Australia Project Grant 1081944 (C.E.G., J.A.W.), an NHMRC Senior Research Fellowship (1042298) (C.E.G.), Monash University International Research Postgraduate Scholarship (S.D.), Monash Graduate Scholarship (S.D.), and the Victorian government's Operational Infrastructure Support Program.

Authors contribution

Study conception and design: SD, CEG, JW, JD

Experimental designs: CEG, JD, SD, JW, CN

Perform experiments, SD, JD, SM, KST

Assistance with and provision of essential materials: SLE, AV, SG, DG

Statistical analysis: SD, CEG

Manuscript writing and editing: SD, CEG, J

Additional information

The Authors declare that there is no conflict of interest

References

- 1 Langer, R. & Vacanti, J. P. Tissue engineering. *Science* **260**, 920-926 (1993).
- 2 Shafiee, A. & Atala, A. Tissue Engineering: Toward a New Era of Medicine. *Annu Rev Med* **68**, 29-40, doi:10.1146/annurev-med-102715-092331 (2017).
- 3 Vacanti, J. P. & Langer, R. Tissue engineering: the design and fabrication of living replacement devices for surgical reconstruction and transplantation. *Lancet* **354** **Suppl 1**, S132-34 (1999).
- 4 Chapple, C. R. *et al.* Application of Tissue Engineering to Pelvic Organ Prolapse and Stress Urinary Incontinence. *Lower urinary tract symptoms* **7**, 63-70, doi:10.1111/luts.12098 (2015).
- 5 Gigliobianco, G. *et al.* Biomaterials for pelvic floor reconstructive surgery: how can we do better? *BioMed research international* **2015**, 968087, doi:10.1155/2015/968087 (2015).
- 6 Society, T. R. *Obstract: interpreting the abstraction of tissue regeneration and re-engineering of female pelvic floor disorders in clinical practice*, <<https://royalsociety.org/science-events-and-lectures/2017/10/pelvic-floor/>> (2017).
- 7 Maher, C., Feiner, B., Baessler, K. & Schmid, C. Surgical management of pelvic organ prolapse in women. *Cochrane Database Syst Rev* **4**, Cd004014, doi:10.1002/14651858.CD004014.pub5 (2013).

- 8 Olsen, A. L., Smith, V., Bergstrom, J., Colling, J. & Clark, A. L. Epidemiology of surgically managed pelvic organ prolapse and urinary incontinence. *Obstet. Gynecol.* **89**, 501-506 (1997).
- 9 Smith, F. J., Holman, C. D., Moorin, R. E. & Tsokos, N. Lifetime risk of undergoing surgery for pelvic organ prolapse. *Obstetrics and gynecology* **116**, 1096-1100, doi:10.1097/AOG.0b013e3181f73729 (2010).
- 10 Konstantinovic, M. L. *et al.* Tensile strength and host response towards different polypropylene implant materials used for augmentation of fascial repair in a rat model. *International urogynecology journal and pelvic floor dysfunction* **18**, 619-626, doi:10.1007/s00192-006-0202-y (2007).
- 11 Tijdink, M. M., Vierhout, M. E., Heesakkers, J. P. & Withagen, M. I. Surgical management of mesh-related complications after prior pelvic floor reconstructive surgery with mesh. *Int Urogynecol J* **22**, 1395-1404, doi:10.1007/s00192-011-1476-2 (2011).
- 12 de Tayrac R, D. X., Gervaise A *et al.* Long-term anatomical and functional assessment of trans-vaginal cystocele repair using a tension-free polypropylene mesh. *Int Urogynecol J* **17**, 483-488, doi:10.1007/s00192-005-0046-x (2006).
- 13 Matsushima, A. *et al.* In vivo osteogenic capability of human mesenchymal cells cultured on hydroxyapatite and on beta-tricalcium phosphate. *Artif Organs* **33**, 474-481, doi:10.1111/j.1525-1594.2009.00749.x (2009).

- 14 Dolce, C. J. *et al.* Pushing the envelope in biomaterial research: initial results of prosthetic coating with stem cells in a rat model. *Surg Endosc* **24**, 2687-2693, doi:10.1007/s00464-010-1026-x (2010).
- 15 Zhao, Y. *et al.* Abdominal hernia repair with a decellularized dermal scaffold seeded with autologous bone marrow-derived mesenchymal stem cells. *Artif Organs* **36**, 247-255, doi:10.1111/j.1525-1594.2011.01343.x (2012).
- 16 Le Blanc, K. & Mougiakakos, D. Multipotent mesenchymal stromal cells and the innate immune system. *Nature reviews. Immunology* **12**, 383-396, doi:10.1038/nri3209 (2012).
- 17 Ulrich, D., Muralitharan, R. & Gargett, C. E. Toward the use of endometrial and menstrual blood mesenchymal stem cells for cell-based therapies. *Expert Opinion on Biological Therapy* **13**, 1387-1400, doi:10.1517/14712598.2013.826187 (2013).
- 18 Darzi, S., Werkmeister, J. A., Deane, J. A. & Gargett, C. E. Identification and Characterization of Human Endometrial Mesenchymal Stem/Stromal Cells and Their Potential for Cellular Therapy. *Stem Cells Transl Med* **5**, 1127-1132, doi:10.5966/sctm.2015-0190 (2016).
- 19 Masuda, H., Anwar, S. & HJ, B. A Novel Marker of Human Endometrial Mesenchymal Stem-Like Cells. *Cell Transplantation* (2012).
- 20 Schwab, K. E. & Gargett, C. E. Co-expression of two perivascular cell markers isolates mesenchymal stem-like cells from human endometrium. *Hum Reprod* **22**, 2903-2911, doi:dem265 [pii]

10.1093/humrep/dem265 (2007).

- 21 Gargett, C. E., Schwab, K. E. & Deane, J. A. Endometrial stem/progenitor cells: the first 10 years. *Human reproduction update* **22**, 137-163, doi:10.1093/humupd/dmv051 (2016).
- 22 Edwards, S. L. *et al.* Characterisation of clinical and newly fabricated meshes for pelvic organ prolapse repair. *Journal of the mechanical behavior of biomedical materials* **23**, 53-61, doi:10.1016/j.jmbbm.2013.04.002 (2013).
- 23 Ulrich, D. *et al.* A preclinical evaluation of alternative synthetic biomaterials for fascial defect repair using a rat abdominal hernia model. *PLoS One* **7**, e50044, doi:10.1371/journal.pone.0050044 (2012).
- 24 Ulrich, D. *et al.* Human Endometrial Mesenchymal Stem Cells Modulate the Tissue Response and Mechanical Behavior of Polyamide Mesh Implants for Pelvic Organ Prolapse Repair. *Tissue Eng. Part A* **20**, 785-798 (2014).
- 25 Edwards, S. L. *et al.* Temporal changes in the biomechanical properties of endometrial mesenchymal stem cell seeded scaffolds in a rat model. *Acta Biomater* **13**, 286-294, doi:10.1016/j.actbio.2014.10.043 (2015).
- 26 Anderson, J. M., Rodriguez, A. & Chang, D. T. Foreign body reaction to biomaterials. *Semin Immunol* **20**, 86-100, doi:10.1016/j.smim.2007.11.004 (2008).
- 27 Xia, Z. D. *et al.* Macrophages in degradation of collagen/hydroxylapatite(CHA), beta-tricalcium phosphate ceramics (TCP) artificial bone graft. An in vivo study. *Chinese medical journal* **107**, 845-849 (1994).

- 28 Labow, R. S., Sa, D., Matheson, L. A. & Santerre, J. P. Polycarbonate-urethane hard segment type influences esterase substrate specificity for human-macrophage-mediated biodegradation. *Journal of biomaterials science. Polymer edition* **16**, 1167-1177 (2005).
- 29 Sridharan, R., Cameron, A. R., Kelly, D. J., Kearney, C. J. & O'Brien, F. J. Biomaterial based modulation of macrophage polarization: a review and suggested design principles. *Materials Today* **18**, 313 (2015).
- 30 Kim, J. & Hematti, P. Mesenchymal stem cell-educated macrophages: a novel type of alternatively activated macrophages. *Exp Hematol* **37**, 1445-1453, doi:10.1016/j.exphem.2009.09.004 (2009).
- 31 Nemeth, K. *et al.* Bone marrow stromal cells attenuate sepsis via prostaglandin E(2)-dependent reprogramming of host macrophages to increase their interleukin-10 production. *Nat Med* **15**, 42-49, doi:10.1038/nm.1905 (2009).
- 32 Gupta, N. *et al.* Intrapulmonary delivery of bone marrow-derived mesenchymal stem cells improves survival and attenuates endotoxin-induced acute lung injury in mice. *J Immunol* **179**, 1855-1863 (2007).
- 33 Shultz, L. D., Ishikawa, F. & Greiner, D. L. Humanized mice in translational biomedical research. *Nature reviews. Immunology* **7**, 118-130, doi:10.1038/nri2017 (2007).
- 34 Klopffleisch, R. Macrophage reaction against biomaterials in the mouse model - Phenotypes, functions and markers. *Acta Biomater* **43**, 3-13, doi:10.1016/j.actbio.2016.07.003 (2016).

- 35 Ionescu, L. I. *et al.* Airway delivery of soluble factors from plastic-adherent bone marrow cells prevents murine asthma. *Am J Respir Cell Mol Biol* **46**, 207-216, doi:10.1165/rcmb.2010-0391OC (2012).
- 36 Prockop, D. J. & Oh, J. Y. Medical therapies with adult stem/progenitor cells (MSCs): a backward journey from dramatic results in vivo to the cellular and molecular explanations. *J Cell Biochem* **113**, 1460-1469, doi:10.1002/jcb.24046 (2012).
- 37 Luz-Crawford, P. *et al.* The immunosuppressive signature of menstrual blood mesenchymal stem cells entails opposite effects on experimental arthritis and graft versus host diseases. *Stem Cells* **34**, 456-469, doi:10.1002/stem.2244 (2016).
- 38 Barragan, F. *et al.* Human Endometrial Fibroblasts Derived from Mesenchymal Progenitors Inherit Progesterone Resistance and Acquire an Inflammatory Phenotype in the Endometrial Niche in Endometriosis. *Biol Reprod* **94**, 118, doi:10.1095/biolreprod.115.136010 (2016).
- 39 Agrawal, H. *et al.* Human adipose-derived stromal/stem cells demonstrate short-lived persistence after implantation in both an immunocompetent and an immunocompromised murine model. *Stem Cell Res Ther* **5**, 142, doi:10.1186/scrt532 (2014).
- 40 Chan, R. W., Schwab, K. E. & Gargett, C. E. Clonogenicity of human endometrial epithelial and stromal cells. *Biol Reprod* **70**, 1738-1750, doi:10.1095/biolreprod.103.024109
biolreprod.103.024109 [pii] (2004).

- 41 Gurung, S., Werkmeister, J. A. & Gargett, C. E. Inhibition of Transforming Growth Factor-beta Receptor signaling promotes culture expansion of undifferentiated human Endometrial Mesenchymal Stem/stromal Cells. *Scientific reports* **5**, 15042, doi:10.1038/srep15042 (2015).
- 42 Su, K. *et al.* Induction of endometrial mesenchymal stem cells into tissue-forming cells suitable for fascial repair. *Acta Biomater* **10**, 5012-5020, doi:10.1016/j.actbio.2014.08.031 (2014).
- 43 Elvin, C. M. *et al.* A highly elastic tissue sealant based on photopolymerised gelatin. *Biomaterials* **31**, 8323-8331, doi:10.1016/j.biomaterials.2010.07.032 (2010).
- 44 Schindelin, J. *et al.* Fiji: an open-source platform for biological-image analysis. *Nature methods* **9**, 676-682, doi:10.1038/nmeth.2019 (2012).
- 45 Darzi, S. *et al.* Tissue response to collagen containing polypropylene meshes in an ovine vaginal repair model. *Acta Biomater* **39**, 114-123, doi:10.1016/j.actbio.2016.05.010 (2016).
- 46 Nold, M. F. *et al.* Interleukin-1 receptor antagonist prevents murine bronchopulmonary dysplasia induced by perinatal inflammation and hyperoxia. *Proceedings of the National Academy of Sciences of the United States of America* **110**, 14384-14389, doi:10.1073/pnas.1306859110 (2013).

Figures

Figure 1. eMSC transduction and survival of eMSC on PA+G mesh in NSG mice. (A) cultured mCherry transduced eMSC showing red fluorescence, (B) more than 95% of transduced and cultured eMSC were mCherry⁺ by flow cytometry and about 40% of this population were SUSD2⁺. Representative trace of n=6 patient samples, (C) PA+G mesh seeded and cultured with eMSC. (D, E) mCherry⁺ eMSC were observed after 3 and (F,G) 7 days implantation around the mesh filaments in immunocompromised NSG mice. Arrows, representative mCherry⁺ eMSC; m, mesh filament; g, gelatin. Scale Bars 100µm

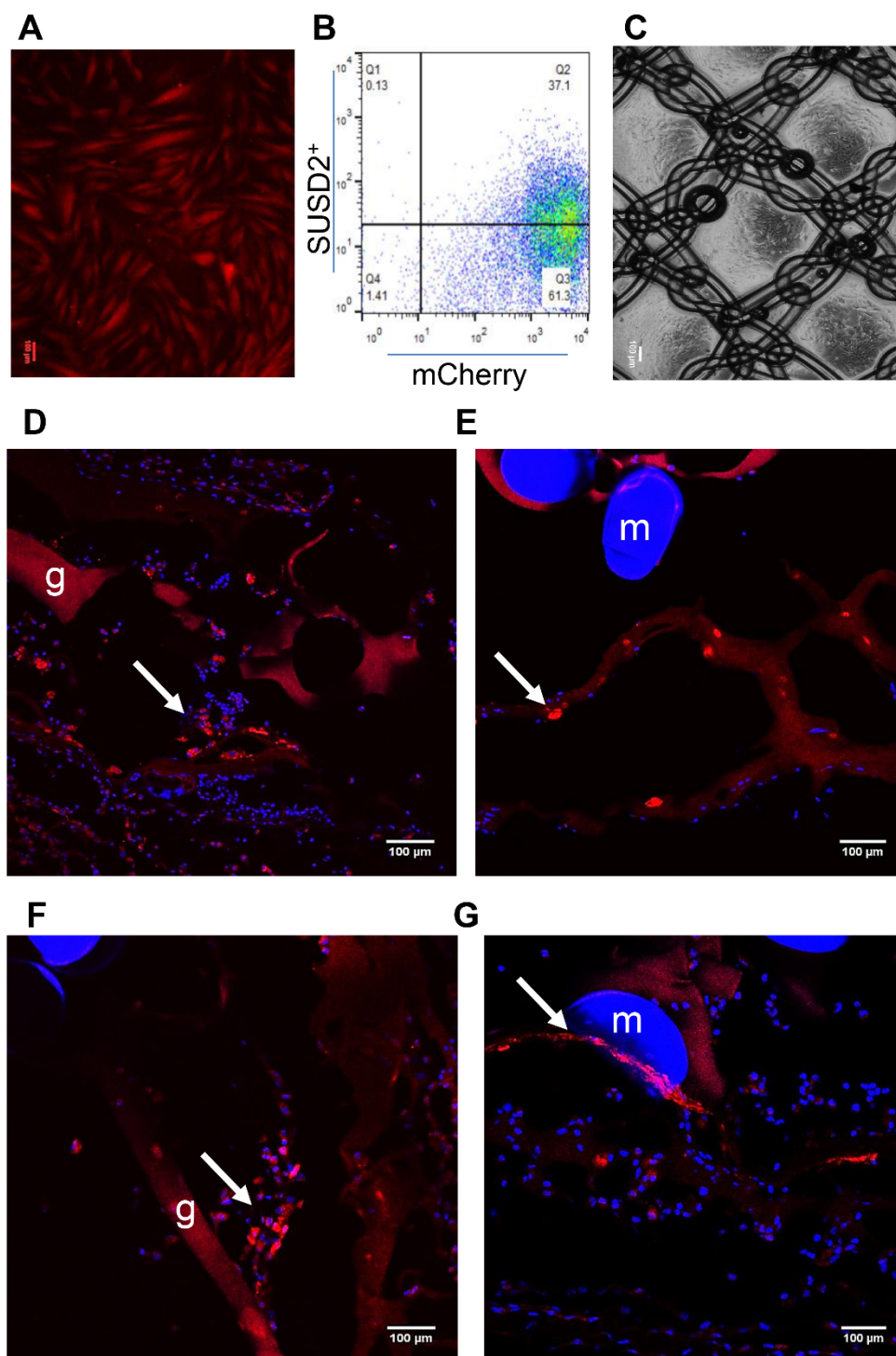


Figure 2. Macrophages surround implanted mesh with or without eMSC. Representative images of F4/80 immunostaining in (A) C57BL/6 mice implanted with eMSC/PA+G mesh (upper panel) and PA+G mesh control (lower panel) for 3 - 30 days and similarly implanted (B) NSG mice. Macrophages (F4/80⁺, green) as a percentage of total nucleated cells in the first 100 μ m increment around mesh filament in (C) C57BL/6 mice and (D) NSG mice. Data are mean \pm SEM of n=8 animals/group. m, mesh, g, gelatin, white dashed lines, outline of PA+G mesh, yellow dotted lines, 100 μ m increment around mesh analyzed eg in (A, D7). Arrowheads, representative F4/80 macrophages both within and outside the 100 μ m increment around PA+G mesh. Scale bars 100 μ m.

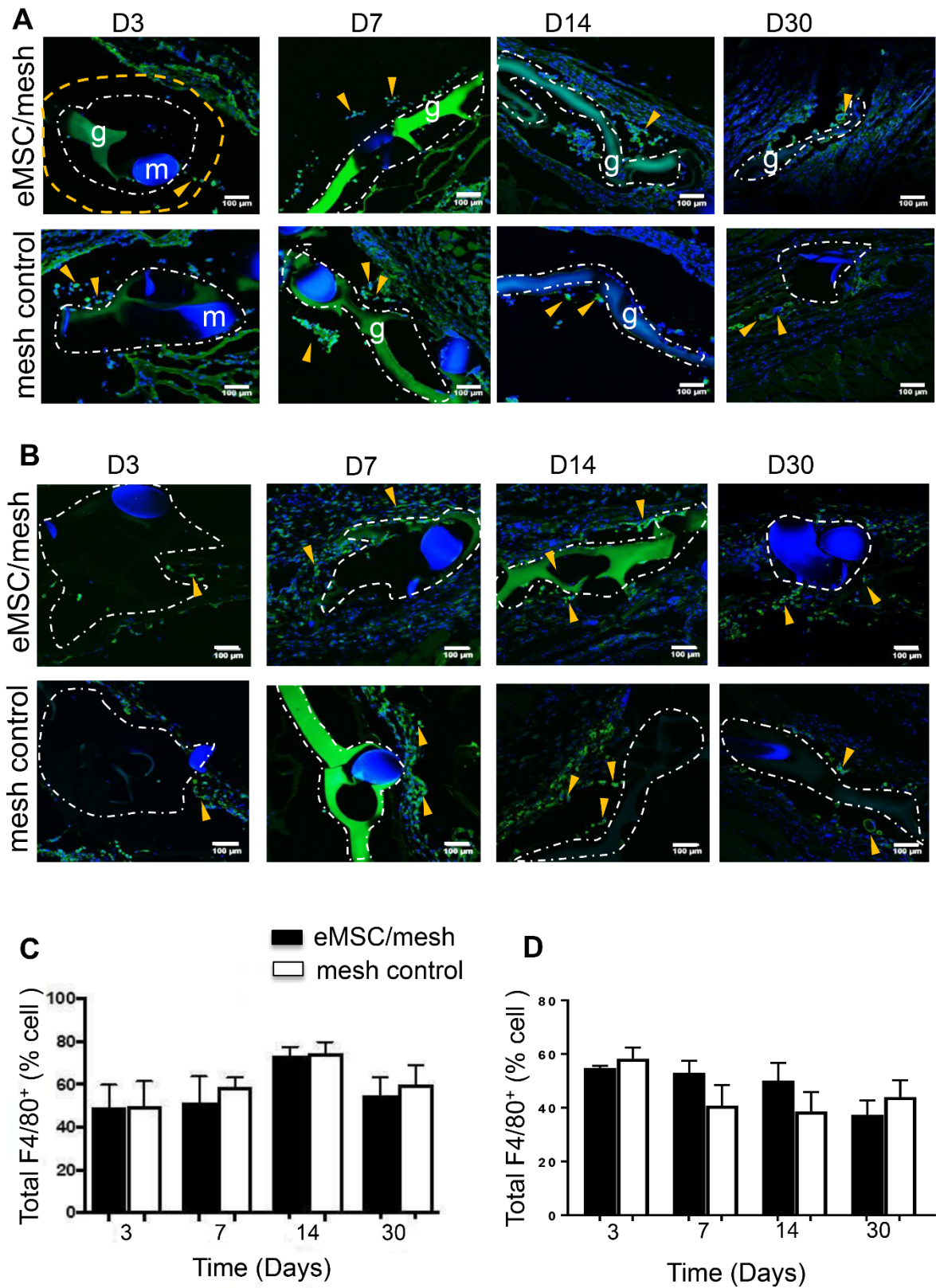


Figure 3. M1 macrophage quantification around implanted mesh in C57BL/6 and NSG mice. CCR7 M1 macrophage (red) and F4/80 macrophage (green) co-localized (yellow) around implanted mesh in mesh/eMSC and mesh control groups from day 3 to day 30 in (A) C57BL6 mice and (B) NSG mice. Ratio of macrophages with co-localized markers in the first 100 μ m around mesh filament in (C) immunocompetent mice and (D) immunocompromised mice. Data are mean \pm SEM of n=8 animals/group. *P < 0.05. Arrows show representative CCR7⁺F4/80⁺ macrophages both within and outside the 100 μ m increment around PA+G mesh, m, mesh filament; g, gelatin. Scale Bars 100 μ m.

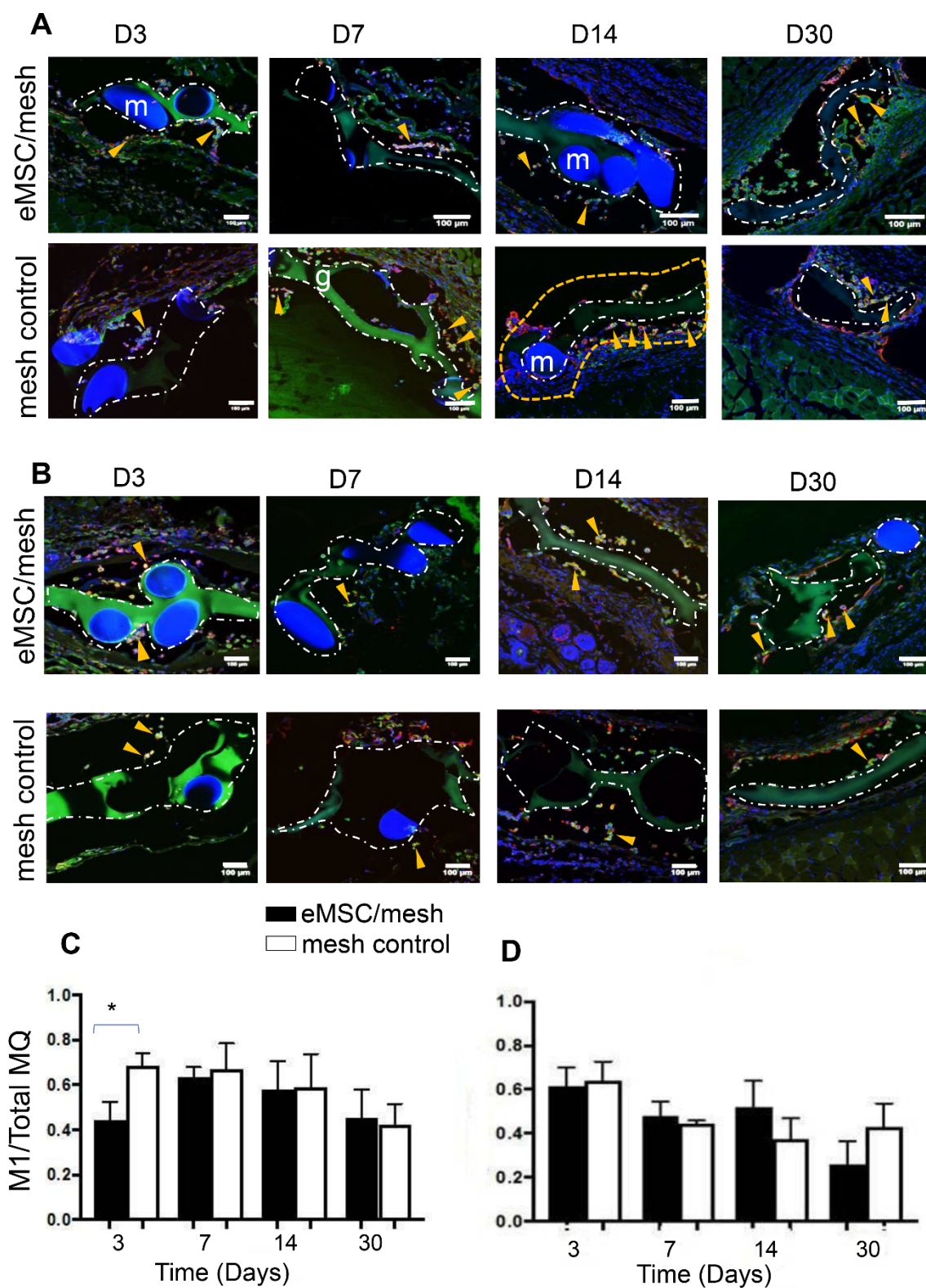


Figure 4. M2 macrophage quantification around implanted mesh in C57BL/6 and NSG mice. CD206 M2 macrophage (white) and macrophage F4/80 (green) co-localization around implanted mesh at day 3 to 30 in (A) C57BL/6 mice and (B) NSG mice. C and D ratio of macrophages with co-localized markers to total macrophages (MQ) in the first 100 μ m around mesh filament in (C) C57BL/6 Immunocompetent mice and (D) NSG Immunocompromised mice. Data are mean \pm SEM of n=8 animals/group. *P < 0.05. Arrows show representative CD206⁺F4/80⁺ macrophages within and outside the 100 μ m increment around PA+G mesh, m, mesh filament; g, gelatin. Scale Bars 100 μ m.

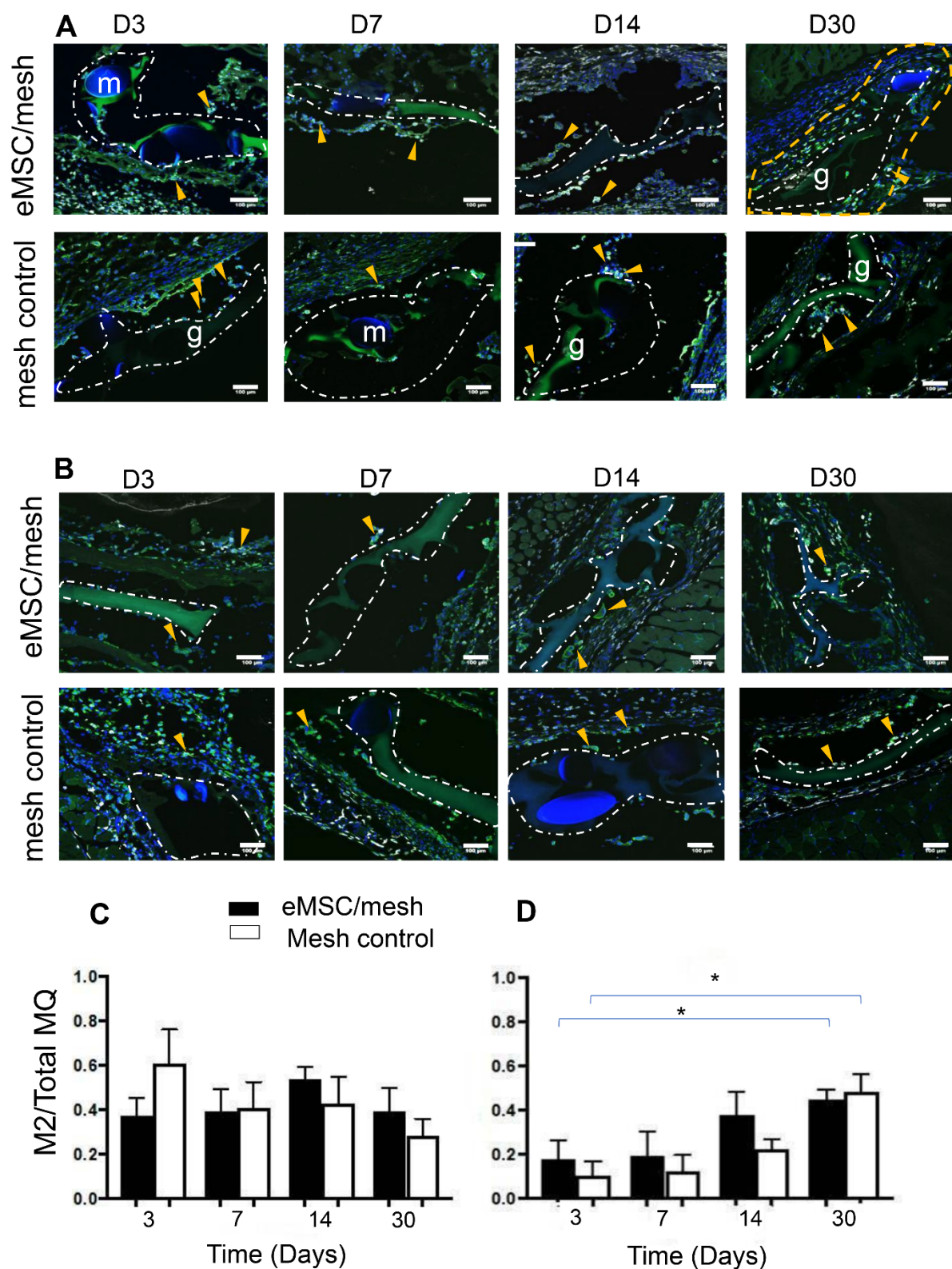


Figure 5. mRNA expression of M1 macrophage markers by Quantitative PCR.

I11b and *Tnfa* mRNA expression in eMSC/mesh and mesh control groups in (A and C) C57BL6 and (B and D) NSG mice. (E and F) total comparison of *I11b* and *Tnfa* mRNA expression between two types of mice, two groups and four time-points. Error bars mean +/- SEM. *P <0.05

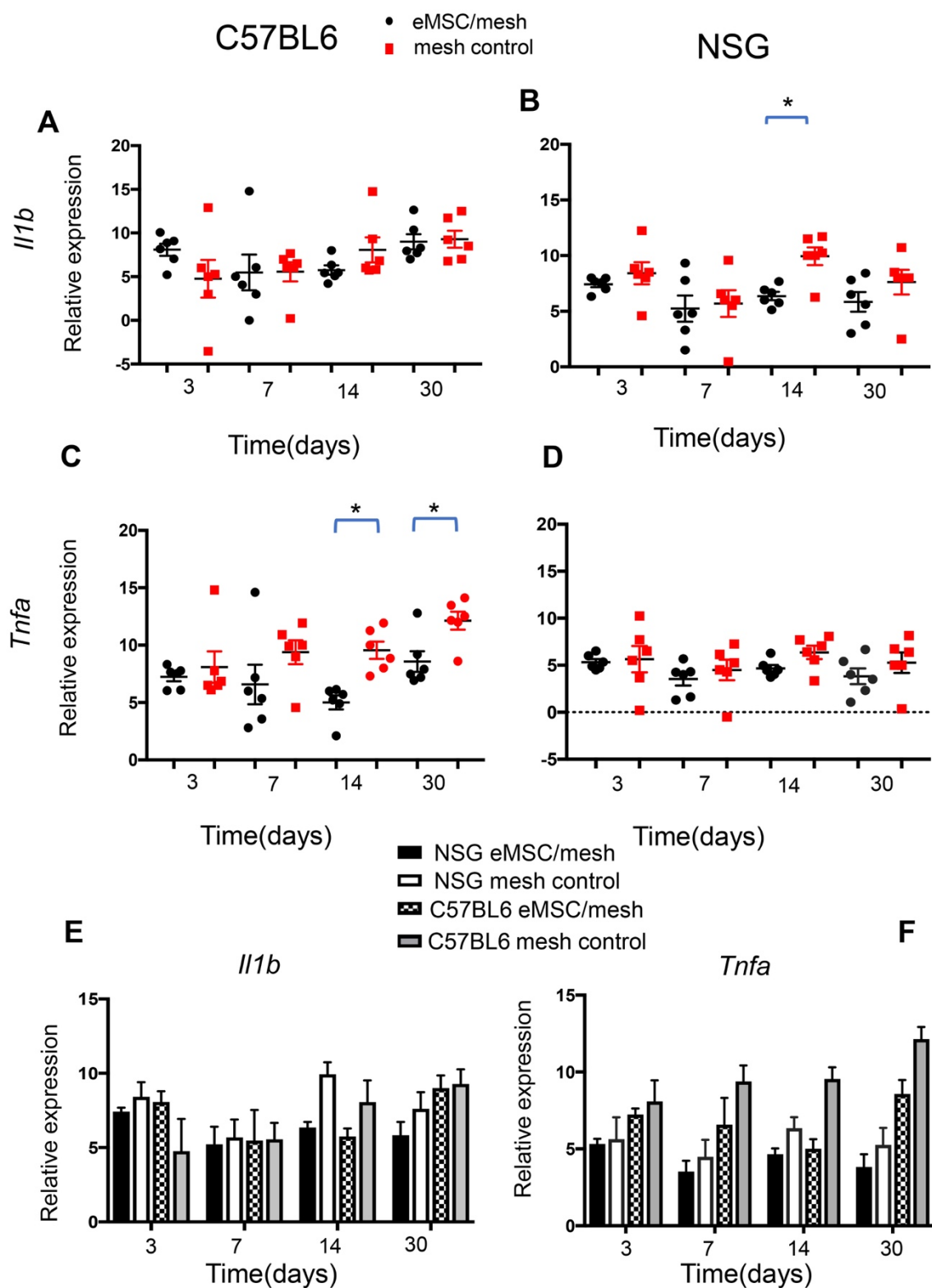


Figure 6. Inflammatory M1 macrophage cytokine secretion assayed by ELISA. Il-1 β and Tnf- α secretion in eMSC/mesh and mesh control group implants in (A,C) immunocompetent C57BL/6 mice and (B,D) immunocompromised NSG mice. (E,F) comparison of cytokine expression between the two mouse models for eMSC/mesh and mesh control. Data are mean \pm SEM of n=8 animals/group. *P <0.05

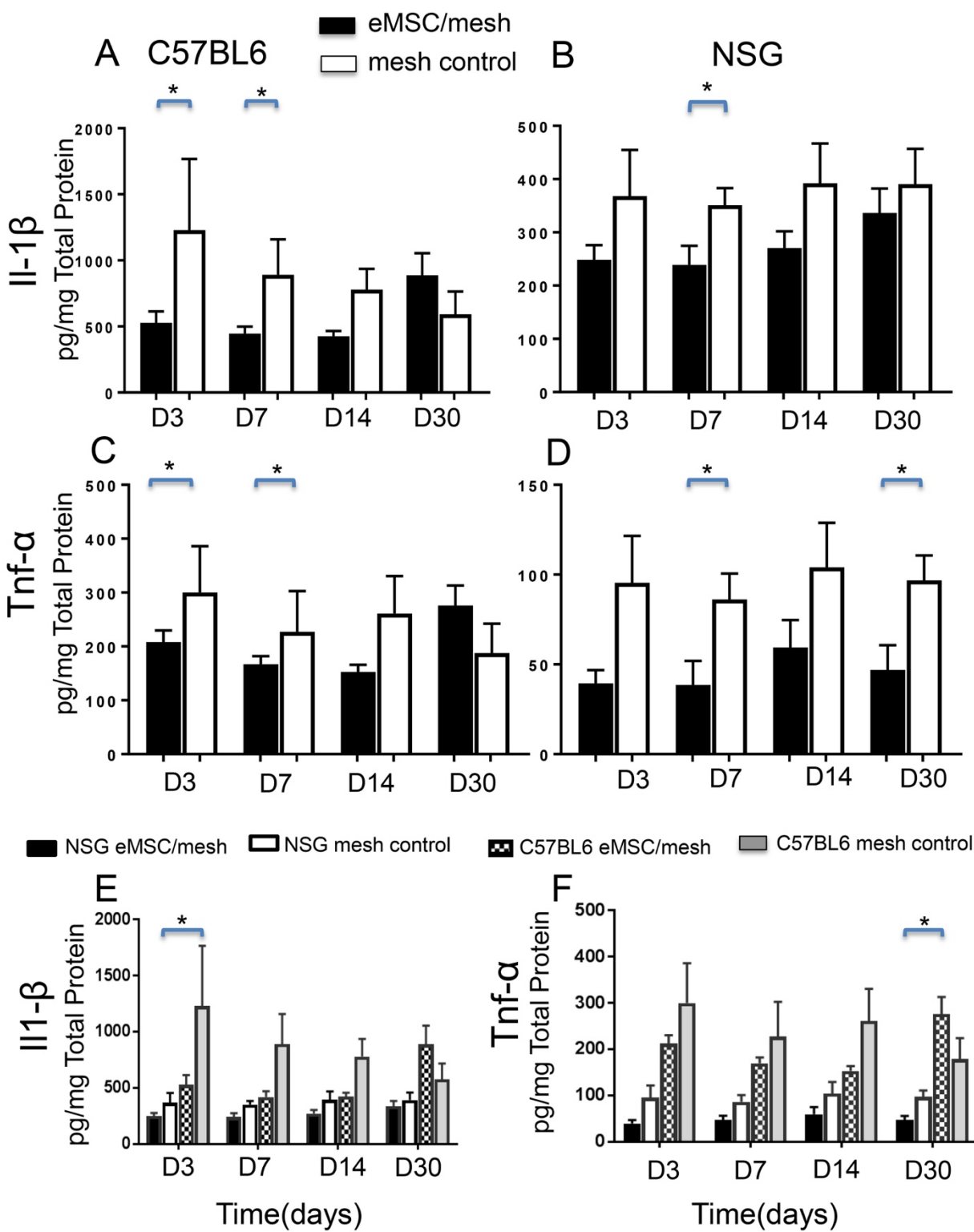
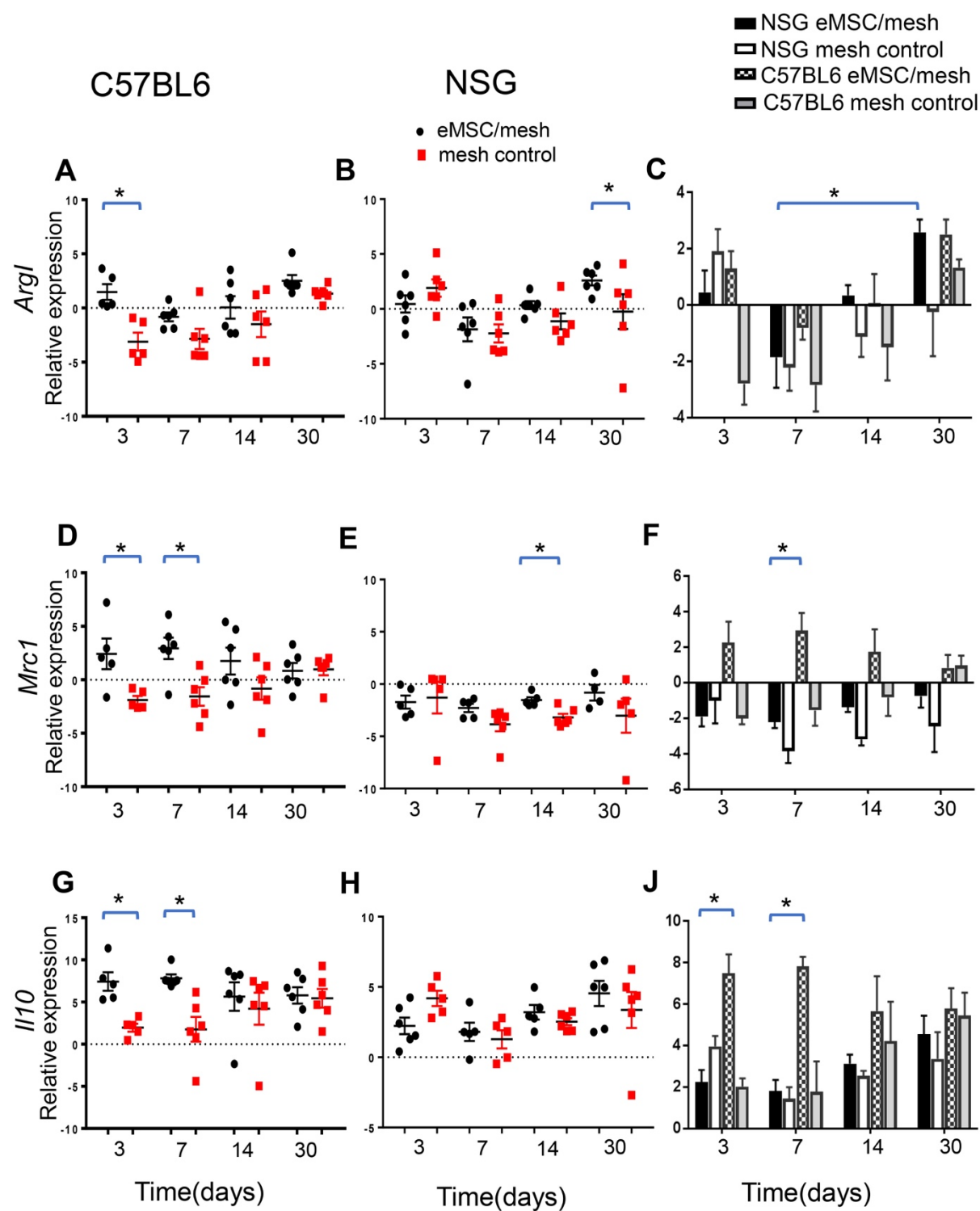
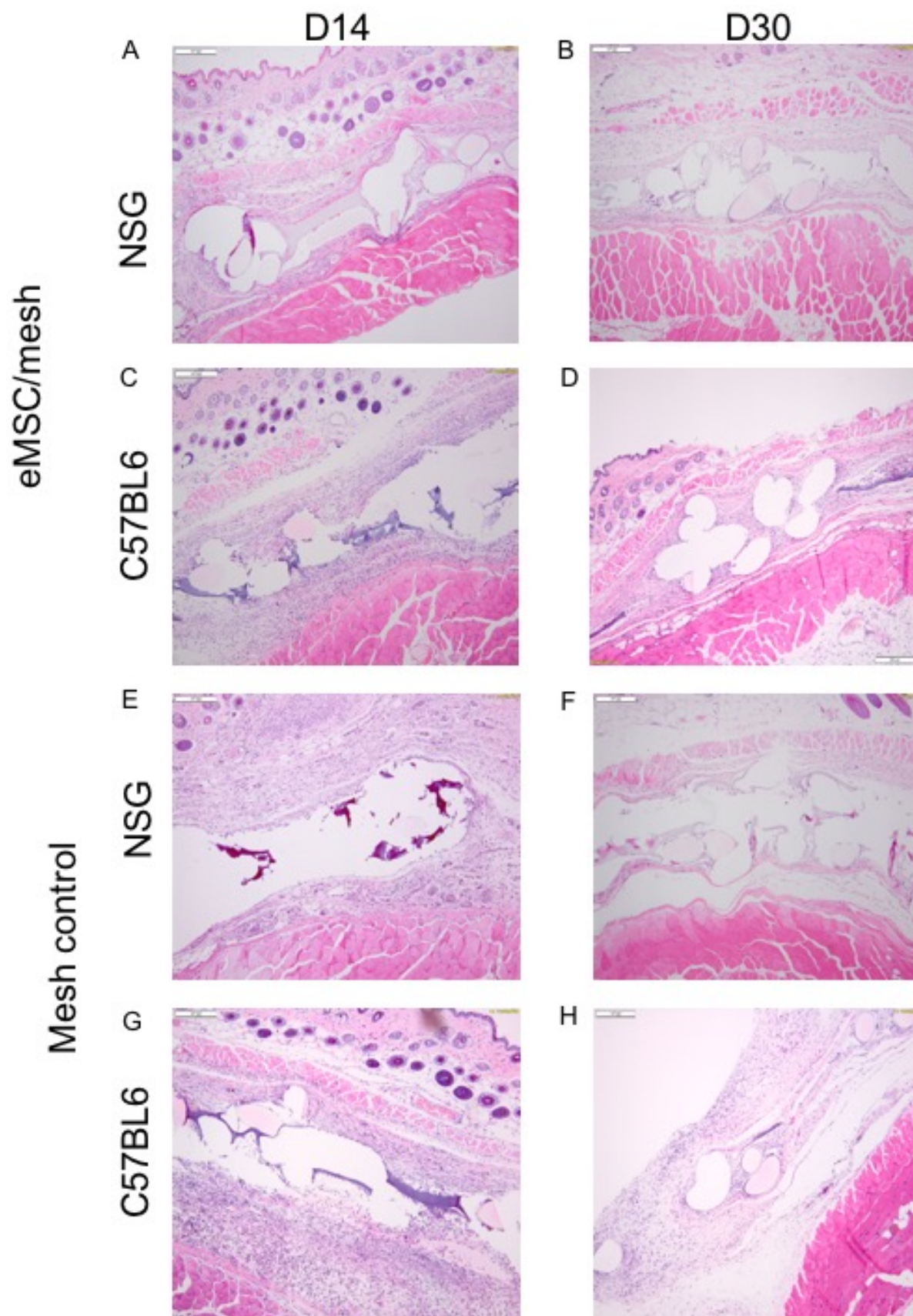


Figure 7. mRNA expression of M2 macrophage markers by Quantitative PCR. *Argl*, *Mrc1* and *Il10* in eMSC/mesh and mesh control groups in (A,D and G) C57BL6 and (B,E and H) NSG mice. (C,F and J) comparison of *Argl*, *Mrc1* and *Il10* expression between the two types of mice, eMSC/mesh and mesh control. Error bars mean +/- SEM. *P <0.05



Supplementary Figure 1. **H&E staining of explanted tissue at day 14 and 30.** eMSC/mesh group in NSG (A,B) and in C57BL6 (C,D). Mesh control group in NSG (E,F) and C57BL6 (G,H).



Supplementary Figure 2. **M2/M1 ratio in eMSC/mesh and mesh control groups.**

(A) C57BL6 and (B) NSG mice.

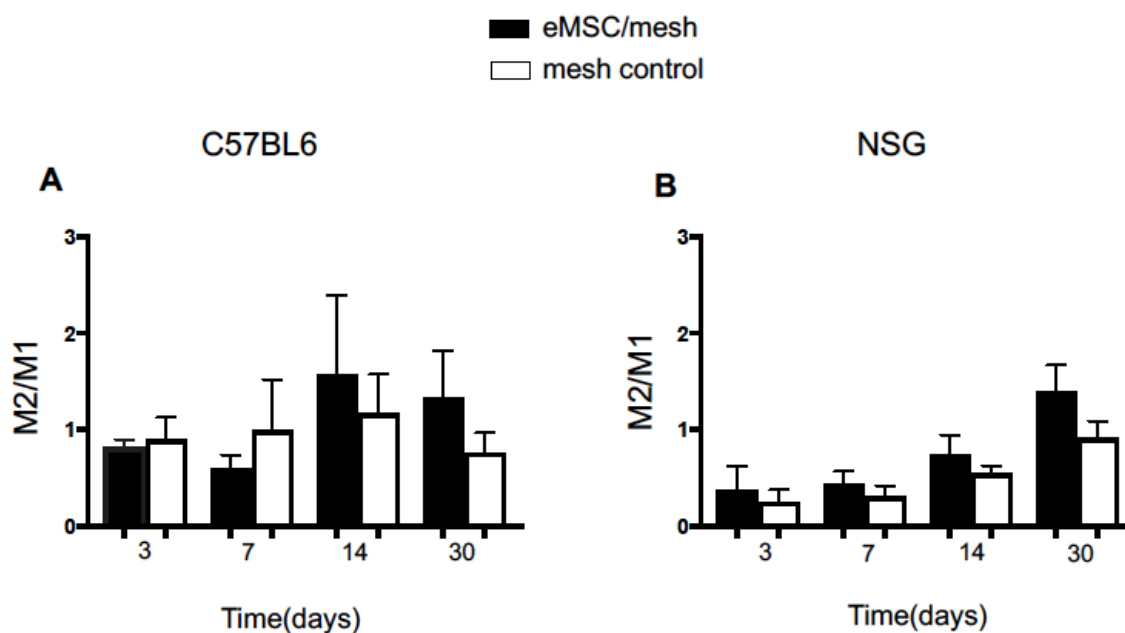


Table 1

Details of antibodies used in immunostaining

Primary antibody	Isotype	Supplier	Dilution (Concentration)	Secondary Ab	Concentration	Supplier
CCR7	Rabbit monoclonal	Abcam	1/200 (1µg/ml)	Donkey anti rabbit IgG	1/500	Life Technologies
CD206	Rat IgG2a-Alexa Fluor 647 conjugated	Biolegend	1/100 (1µ/ml)	-	-	-
F4/80	Rat IgG2b	BioRad	1/200 (1µg/ml)	Chicken anti rat IgG	1/500	Life Technologies

Table 2

Primer sequences

Primer sequences	Forward	Reverse
Arginase I (<i>ArgI</i>)	5' CATGAGCTCGCCAAAGT 3'	5' TTTTCCAGCAGACCAGCTT 3'
Mannose Receptor (<i>Mrc1</i>)	5' TGGCATGTCCTGGAATGAT 3'	5' CAGGTGTGGGCTCAGGTAGT 3'
Interleukin 10 (<i>Il10</i>)	5' TTTGAATTCCCTGGGTGAGA 3'	5' AGACACCTTGGTCTTGGAGC 3'
<i>Il1b</i>	5' TCACCCAAGACTCTGCCTTTAC 3'	5' CCATGGTGGCAGTGAGGTTT 3'
<i>Tnfa</i>	5' CCCTCACACTCAGATCATCTTCT 3'	5' GCTACGACGTGGGCTACAG 3'
<i>GAPDH</i>	5' AACTTTGGCATTGTGGAAGG 3'	5' ACACATTGGGGGTAGGAACA 3'

Chapter 4

Resident macrophages mediate the host response to implanted mesh and impact the survival of eMSC

4.1. Introductory statement

In Chapter 3 I noticed a considerable accumulation of macrophages around mesh filaments and a rapid disappearance of mCherry transduced eMSC. In this Chapter I wanted to further investigate the source of accumulated macrophages and determine whether eMSC would have a longer survival in the absence of accumulated macrophages. For this Chapter, I established a systemic macrophage depletion model using clodronate injections. I assessed the survival of mCherry transduced eMSC as well as the source of responding macrophages to the implanted mesh. eMSC isolation, culture, transduction and mouse surgery was the same as described in Chapter 3. I thank Dr James Deane for doing the clodronate IV injections and scientific inputs. I also thank Prof. David Nikolic Paterson for his advice on macrophage depletion and Dr Sharon Edwards for mesh preparation.

Chapter 4- Resident macrophages mediate the host response to implanted mesh and impact the survival of eMSC

Declaration

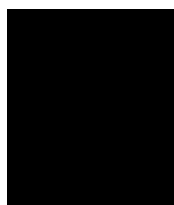
Monash University

Declaration for Thesis Chapter 4

In the case of Chapter 4 my contribution to the work involved the following:

Name	Nature of Contribution	Extent of contribution (%) for student co-authors only
Saeedeh Darzi	Cell culture and transduction, Mouse surgery Immunofluorescence, Flow cytometry, Manuscript writing	75%
James Deane	Clodronate injection, scientific input and manuscript revision	N
Caroline Gargett	Conception and design of the study, manuscript revision	N
Jerome Werkmeister	Conception and design of the study, manuscript revision	N
Sharon Edwards	PA+G mesh fabrication	N

Student signature:



Date: 12.08.2017

4.2. Abstract

The tissue response to implantation of a tissue engineering construct comprising a biomaterial seeded with MSC involves macrophages, which play key roles in the inflammatory response, tissue regeneration and fibrosis. Macrophages can behave as pro or anti-inflammatory cells and the balance between these two states results in tissue remodelling and avoids the extended inflammation and fibrosis following biomaterial implantation.

Continuing from the previous study (Chapter 3), in this study I further explored the source of responding macrophages to implanted PA+G mesh seeded with mCherry-labelled eMSC. To understand the role of macrophages, recruited monocytes were systemically depleted by clodronate injections. After the last injection, PA+G mesh seeded with mCherry-labelled eMSC was implanted between the skin and abdominal fascial layer in C57BL6 mice and tissues were collected and assessed for mCherry eMSC and macrophages after 3 and 7 days.

Results revealed that 1). Macrophage depletion did not result in longer survival of eMSC, 2). While systemic monocytes were effectively depleted with clodronate, resident macrophages were not impacted and migrated to the implanted mesh but did not proliferate. 3). The majority of resident migrating macrophages around the mesh in systemic monocyte depleted animals were uncommitted M0 macrophages compared with M1 macrophage accumulation around mesh in untreated animals. However, while our results demonstrate for the first time the importance of the resident macrophage response to implanted mesh, further work is required to understand the interplay between

Chapter 4- Resident macrophages mediate the host response to implanted mesh and impact the survival of eMSC

circulating monocyte migration and the local macrophage response to foreign materials in a larger number of replicates in animal groups. Inclusion of a further control group of saline-only treated animals are also required.

4.3. Introduction

Tissue engineering (TE) is an emerging alternative and complementary solution for treating tissue failure and organ loss. Tissue engineering refers to a combination of scaffolds or biomaterials, cells and bioactive molecules which aims to restore, maintain and improve the normal function of tissue (Langer and Vacanti, 2016). Huge advances in tissue engineering using biomaterials have occurred over the past two decades. The basic strategy in TE uses scaffolds with cells that can be sourced from a variety of tissues and can include autologous or allogeneic differentiated cells or stem cells (Shafiee and Atala, 2017). Bone marrow mesenchymal stem cells are nonspecific multipotent cells which are able to differentiate to a specific cell and display the function of that cell (Demirbag et al., 2011).

Macrophages play a key role in the response to implanted tissue engineered constructs containing cells. Studies have shown the robust recruitment of macrophages around the implanted material along with rapid disappearance of MSC, implying a role for macrophages in MSC disappearance (Braza et al., 2016, Ulrich et al., 2014b). Macrophages originate from two distinct sources; circulatory monocyte-derived and tissue resident. Local macrophages sustain their population by rapid proliferation during tissue injury and bone marrow-derived monocytes circulate in peripheral blood for several days before entering inflamed tissues by extravasation through the endothelium (Davies et al., 2013, Klopffleisch, 2016)

Following our previous study in which I assessed the role of eMSC on macrophage polarization and response to implanted mesh, in this study I aimed to further understand

the role of circulating monocytes as well as tissue resident macrophages in response to implanted PA+G mesh seeded with mCherry-labelled eMSC.

4.4. Material and Methods

4.4.1. Human samples

Endometrial biopsies were obtained from 8 pre-menopausal women undergoing laparoscopic surgery for gynaecological conditions for non-endometrial pathological conditions (endometriosis and adenomyosis), who had not taken hormonal treatment for three months before surgery. All women gave written informed consent. Our protocol was approved by the Monash Health and Monash University Human Research Ethics committees.

4.4.2. eMSC isolation, culture and transduction

eMSC were isolated as previously described (Ulrich et al., 2014b). Briefly, endometrial tissues were mechanically minced and digested using collagenase type II and deoxyribonuclease type I (DNase I) at 37°C in DMEM/F12 containing 15µM Hepes buffer. Using a 40µm sieve (BD Bioscience-Durham), stromal and epithelial cells (as clumps) were separated and the red blood cells were then removed using Ficoll-Paque density gradient from the stromal fraction. Single cell suspensions of stromal cells were then incubated with PE-conjugated SUSD2 antibody (2µg/ml) (Biolegend) for 30 minutes at 4°C followed by incubation with anti-PE labeled magnetic beads (Miltenyi Biotec) for 20 minutes and SUSD2⁺ eMSC were selected using a column and magnet (Miltenyi Biotec). SUSD2⁺ eMSC were cultured in DMEM/F12 medium containing 10% Fetal Bovine Serum

(FBS) (Invitrogen), 1% antibiotic-antimycotic (Life Technologies) and 2mM glutamine (Life Technologies) for 2-4 passages.

To track the cells in-vivo, eMSC were transduced with mCherry lentivirus plasmids (<https://www.addgene.org/protocols/bacterial-transformation/>) and mCherry⁺ cells were sorted using a Beckman XDP cell sorter (Beckman Coulter, Life Science) as described in Chapter 3. Sorted cells were cultured until confluency for seeding onto PA+G mesh.

4.4.3. PA+G mesh fabrication

Polyamide meshes were prepared and coated with 12% gelatin as previously described and crosslinked with 0.0125 % glutaraldehyde (Ulrich et al., 2014b). Mesh pieces (1 x 1 cm) were seeded at a density of 125,000 mCherry-labelled SUSD2⁺ eMSC/cm² in 30-40μL of medium per mesh and cultured for 48-72 h. To increase the cell dose, on the day of surgery, additional eMSC (125,000 cells/mesh) were added to individual mesh pieces, together with 1mM ruthenium metal complex, (2,2'-bipyridyl) dichloro ruthenium (II) hexahydrate [Ru II(bpy)₃]²⁺ (Sigma-Aldrich) and 20mM sodium persulfate (SPS) (Sigma-Aldrich), to increase cell dosage to 500,000 eMSCs/mesh. The gelatin was then cross-linked using a LED dental lamp (460 nm, 1200 mW/cm², 3M Epilar Free Light 2) for 30 seconds.

4.4.4. Macrophage depletion

Liposome encapsulated clodronate and PBS liposomes (5mg/ml) were purchased from <http://www.clodronateliposomes.org> (Nico van Rooijen company). PBS liposomes were injected as a negative control for depletion of macrophages. 200μL clodronate liposomes were injected intravenously (IV) every three days for up to three injections (Fig1A and B).

Chapter 4- Resident macrophages mediate the host response to implanted mesh and impact the survival of eMSC

24 hours after the last injection, the eMSC-seeded mesh was implanted subcutaneously on the flank as previously described (Chapter 3).

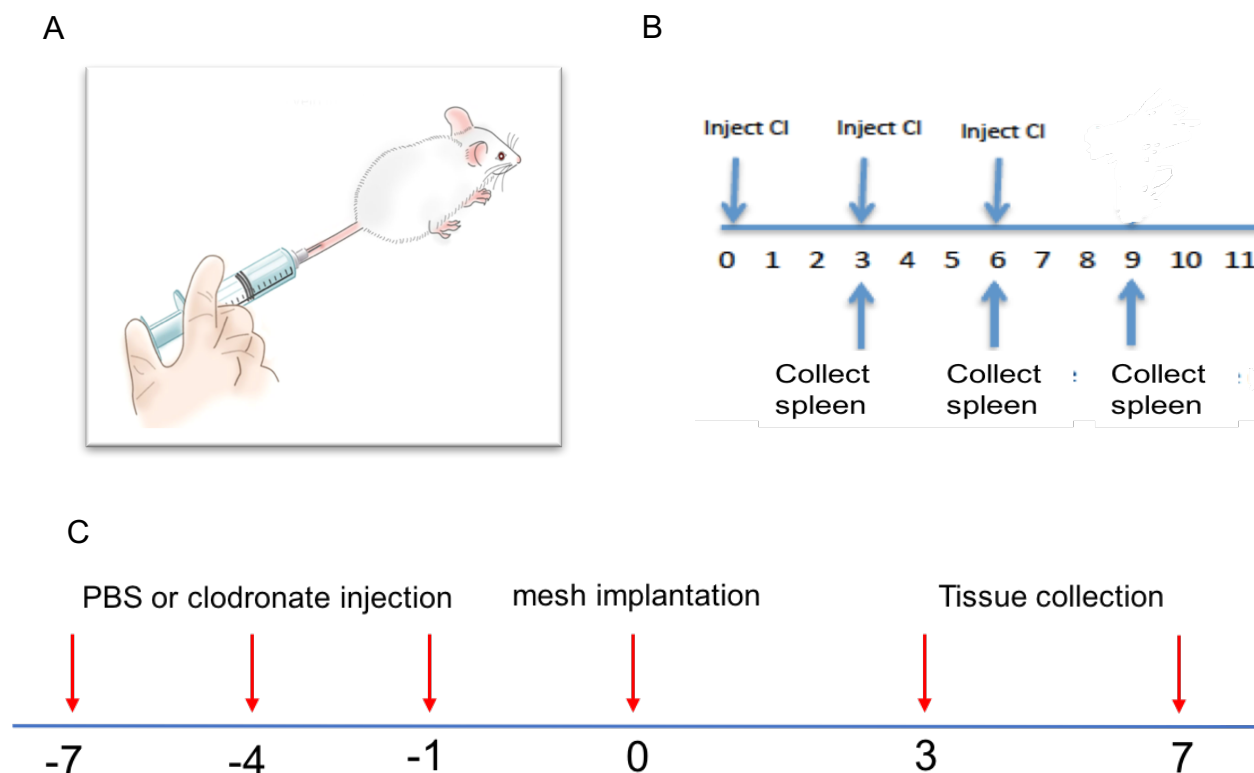


Figure 1. (A). schematic of IV injection. (B). experimental plan showing optimising the number of clodronate injections. (C). IV injection, eMSC/mesh implantation and tissue collection diagram.

4.4.5. Animal surgery and tissue collection

The experimental procedure and mouse husbandry was approved by Monash Medical Centre Animal Ethics Committee A (2016/43). C57BL6 mice were housed in the animal house at Monash Medical Centre in accordance with the National Health and Medical Research Council of Australia guidelines for the care and use of laboratory animals and were provided sterile food and water ad libitum under controlled environmental conditions.

C57BL6 mice (n = 8) were randomly divided into two experimental groups to receive PBS-liposomes or clodronate liposomes with 4 mice/group. Mice were implanted with PA+G mesh seeded with mCherry⁺SUSD2⁺ eMSC.

The surgery procedure was previously described (Chapter 3). Briefly, a longitudinal 1.2 cm skin incision was created on the midline and two pockets were made on each side of the midline by blunt dissection of skin from fascia. Meshes were implanted into two pockets of each animal and sutured in place with Dysilk 4-0[®] sutures (Dyneck). Tissues were harvested 3 and 7 days post implantation and assessed by immunostaining.

Sample size for this study was determined from our previous studies. There was insufficient time to complete the study for this thesis and only n=2/animals per group could be done in the time frame available.

4.4.6. Flow cytometry

To assess the efficiency of clodronate- induced macrophage depletion in the C57BL6 mice, spleens were collected every three days after each clodronate injection to detect macrophages using two markers CD11b and F4/80 (Fig 1B).

To check the repopulation of macrophages, the spleen was collected 3 and 7 days after eMSC/mesh implantation (last injection) (Fig 1C). Collected spleens were mashed through a 70µm strainer, washed with 1% PBS/FBS and the red blood cells were lysed in red cell lysis buffer (Biolegend) for 1 minute at room temperature. The cells were washed and stained with anti-mouse Alexa Fluor 450-conjugated CD11b (1µg/ml) (Thermofisher) and APC-conjugated anti-mouse F4/80 (1µg/ml) (Biolegend) for one hour on ice, washed and analyzed by a flow cytometer (Beckman Coulter, Life Science).

4.4.7. Immunostaining

Collected mesh/tissue complexes were fixed in 4% paraformaldehyde embedded in 30% sucrose and then frozen in OCT. Cryo sections were cut (8µm) and stained with APC or Alexa Fluor 488 rat anti-mouse F4/80 antibody, rabbit anti-mouse CCR7 for pro-inflammatory M1 macrophages and Alexa Fluor 647 rat anti-mouse CD206 for anti-inflammatory M2 macrophages, unconjugated rabbit monoclonal Ki67 and Alexa Fluor 594 rat anti mouse CD11b antibodies (Table 1). Sections were thawed and blocked with protein block (Dako) for 1 hour at RT. After one wash in PBS, the primary antibodies were incubated for 1 hour at RT. Isotype-matched antibodies (rat IgG2b and IgG2a, rabbit monoclonal IgG) were used as negative controls and applied at the same concentrations. After washing, secondary conjugated antibodies were applied for 30 minutes at RT. Nuclei were stained with Hoechst 33258 (Molecular Probes) for 3 minutes and the slides were mounted with a fluorescent mounting medium (Dako).

Table 1. Details of antibodies used in immunostaining

Primary antibody	Isotype	Supplier	Dilution (Concentration)	Secondary Antibody	Concentration	Supplier
CCR7	Rabbit monoclonal	Abcam	1/200 (1µg/ml)	Donkey anti rabbit IgG	1/500	Life Technologies
CD206	Rat IgG2a-Alexa Fluor 647 conjugated	Biolegend	1/100 (1µ/ml)	-	-	-
F4/80	Rat IgG2b APC conjugated	Biolegend	1/200 (1µg/ml)			
F4/80	Rat IgG2a-Alexa Fluor 488 conjugated	Biolegend	1/200 (1µg/ml)			
Ki67	Rabbit monoclonal	Biolegend	1/100	Chicken anti rat IgG	1/500	Life Technologies
CD11b	Rat IgG2b Alexa Four 594 conjugated	Biolegend	1/100			

4.4.8. Image analysis

Three images were taken per stained section from one frozen block from each animal at each time-point (D3 and D7) using a FV1200 confocal microscope (Olympus, Life Science) at 20x magnification. The images were analyzed using Image J software (National Institute of Health, NIH) to measure positive signals around mesh filaments in 100µm increments. The percentage of M1 (red) and M2 (white) macrophages was calculated as a proportion of total macrophages (green), co-localized in the same sections. Cell numbers were calculated as a ratio of co-localized cell (green-red-blue) and/or (green-white-blue) to total macrophages (green-blue).

4.5. Results

4.5.1. Labelling eMSC for cell tracking in vivo

To track the cells *in vivo*, SUSD2⁺ eMSCs were transduced with mCherry lentivirus vector. More than 95% of eMSC transduced with mCherry and about 40 ± 5 % (n=2) of this population were SUSD2⁺. (refer to Chapter 3, Fig1A and B).

4.5.2. Clodronate depletes macrophage from the spleen

To assess the role of recruited monocytes to the implanted eMSC/PA+G construct on eMSC survival, monocytes and macrophages were systemically depleted by clodronate IV injection. To optimize the efficiency of clodronate in macrophage depletion, clodronate and PBS liposomes were injected every three days (Fig 1B). The depletion efficiency of clodronate was assessed in spleen tissue every three days for CD11b⁺/F4/80⁺, CD11b⁻/F4/80⁺, and CD11b⁺/F4/80⁻ cells. Following each of the three clodronate injections, the

number of CD11b⁺F4/80⁺ and CD11b⁻/F4/80⁺ cells decreased in clodronate injected mice compared with PBS injection. However, the percentage of CD11b⁺ F4/80⁻ cells did not decrease after each injection (Fig 2 A-F) (Table2) and I realized that three injections were sufficient to deplete approximately 90% of macrophages. It should be noted that PBS-Liposomes also reduced the various macrophage populations after the first and second injection. Repopulation of splenic macrophages following the final clodronate injection did not occur at 3 or 7days post implantation as shown by flow cytometry. (Fig 3A-D).

Table 2. Percentage of CD11b⁺ F4/80⁻, CD11b⁻ F4/80⁺, and CD11b⁺F4/80⁺ cells after 1, 2 and 3 injections of clodronate or PBS liposomes.

	First injection			Second injection			Third injection		
	CD11b ⁺ F4/80 ⁻	CD11b ⁺ F480 ⁺	CD11b ⁻ F4/80 ⁺	CD11b ⁺ F4/80 ⁻	CD11b ⁺ F480 ⁺	CD11b ⁻ F4/80 ⁺	CD11b ⁺ F4/80 ⁻	CD11b ⁺ F4/80 ⁻	CD11b ⁻ F4/80 ⁺
PBS	9.63	5.42	3.01	3.65	1.33	1.52	1.87	1.90	2.96
CI	6.95	4.00	1.12	4.47	0.76	0.22	2.28	1.80	0.60

NB: Results are from the spleen of single mouse for each injection.

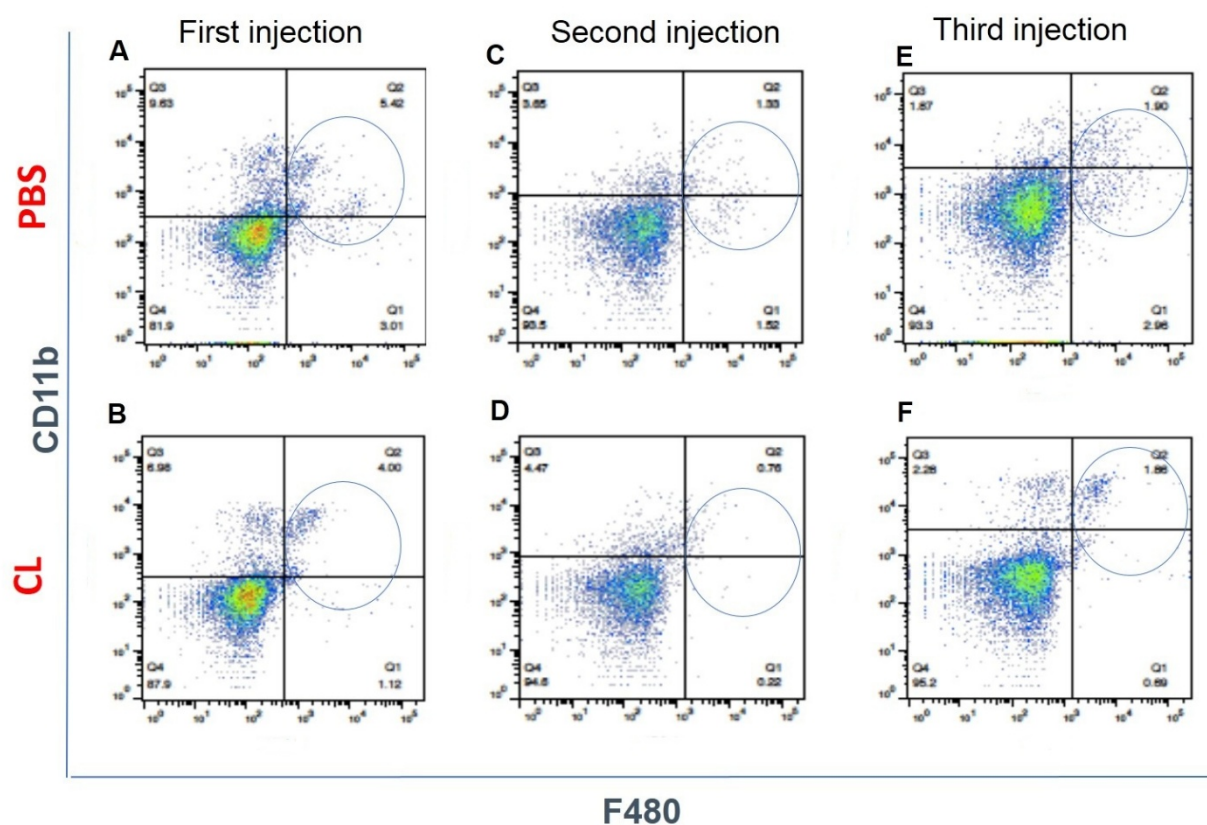


Figure 2. Macrophage detection in mouse spleen after IV injection of 1mg/20gr body weight clodronate. (A,B) first injection, (C,D) second injection, and (E,F) third injection.

Detection of $CD11b^+F4/80^+$, $CD11b^-F480^+$ and $CD11b^+F4/80^-$ cells after PBS-Liposome injection (A, C and E) and (B,D and F) Clodronate-Liposome (CL) injection. Results are from a single mouse/injection.

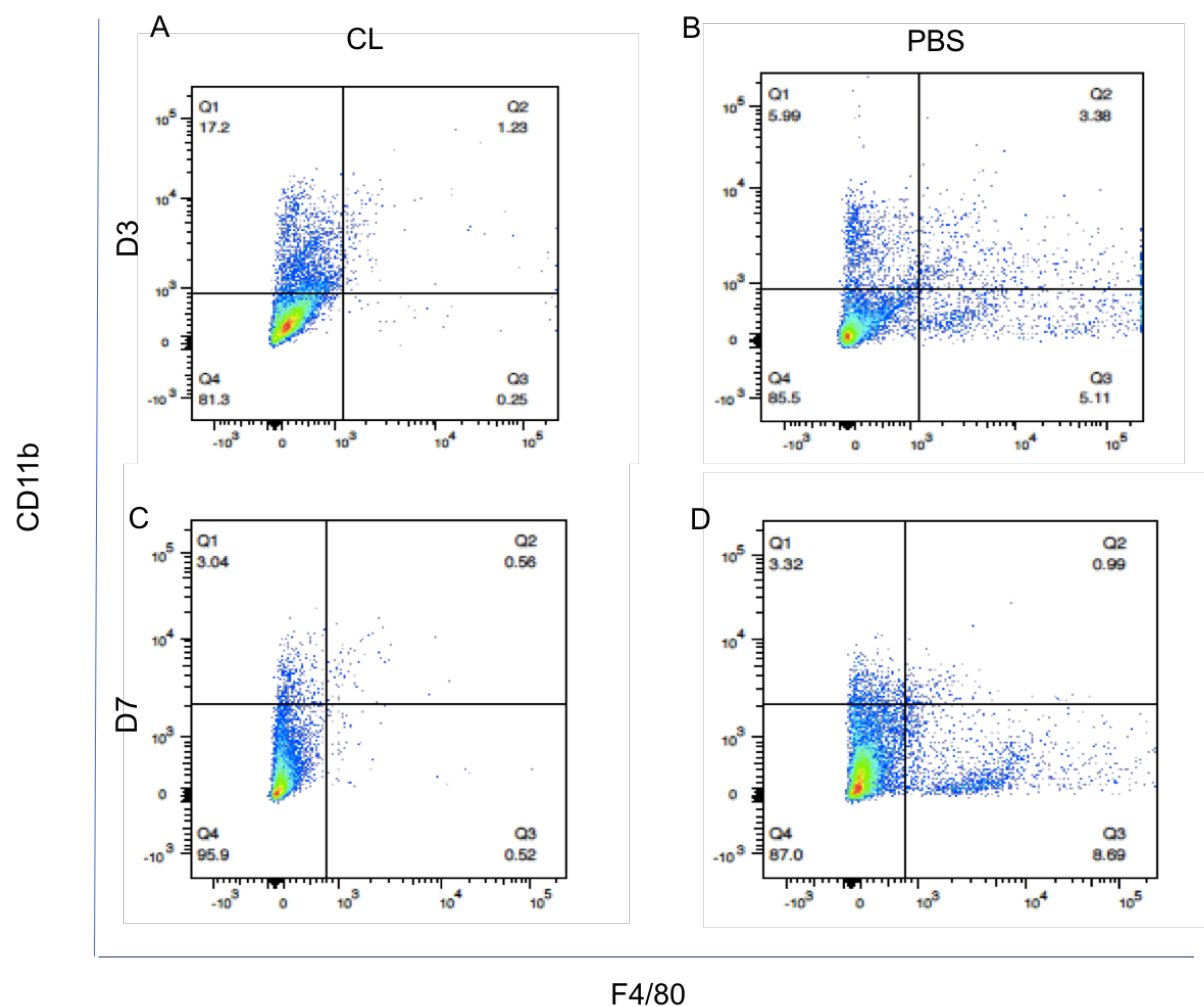


Figure 3. Macrophage detection in mouse spleen 3 and 7 days post eMSC/PA+G implantation. (A,C) Clodronate-Liposome (CL) injected mice (B,D) PBS-Liposome injected mice.

4.5.3. eMSC survival in implanted mesh in the absence of macrophages

To determine the effect of systemic macrophage depletion on eMSC survival, fluorescence microscopy was used to identify m-Cherry labelled eMSC in and around mesh filaments. However, no mCherry labelled eMSC were found around the mesh

implanted area 3 and 7 days post implantation in both clodronate injected and PBS control mice.

4.5.4. Macrophage presence around mesh filament in clodronate and PBS injected mice

The presence and phenotype of macrophages around mesh filaments was investigated by immunofluorescence staining. Considerable numbers of F4/80 immunostained macrophages accumulated around mesh filaments in both control as expected (PBS liposome injected) (Fig 4A and B) but also in clodronate injected mice (Fig 4C and D) mice, particularly at day 3. The number of F4/80 macrophages around mesh filaments was quantified at 3 and 7 days after implantation of eMSC seeded mesh in PBS and Cl injected mice. There was a higher percentage of macrophages in the first 100µm around mesh filaments in PBS injected mice compared with clodronate injected mice (Fig 4E). ~~although sample size needs increasing to determine statistical significant of this result.~~

The presence of M1 and M2 macrophages was assessed by double staining for macrophage (F4/80) and/or M1 marker (CCR7) and M2 marker (CD206). The number of M1 macrophages was higher in the PBS injected group after 3 and 7 days compared with the CL injected group (Fig 5A-D and E). More samples are required to determine if this finding is significant. M2 macrophages were less prominent in both groups as expected at these early time points. (Fig 6A-D and E). Interestingly, at least 50% of F4/80 macrophages around the mesh filaments in CL-treated animals were uncommitted M0 macrophages (M1 and M2 negative).

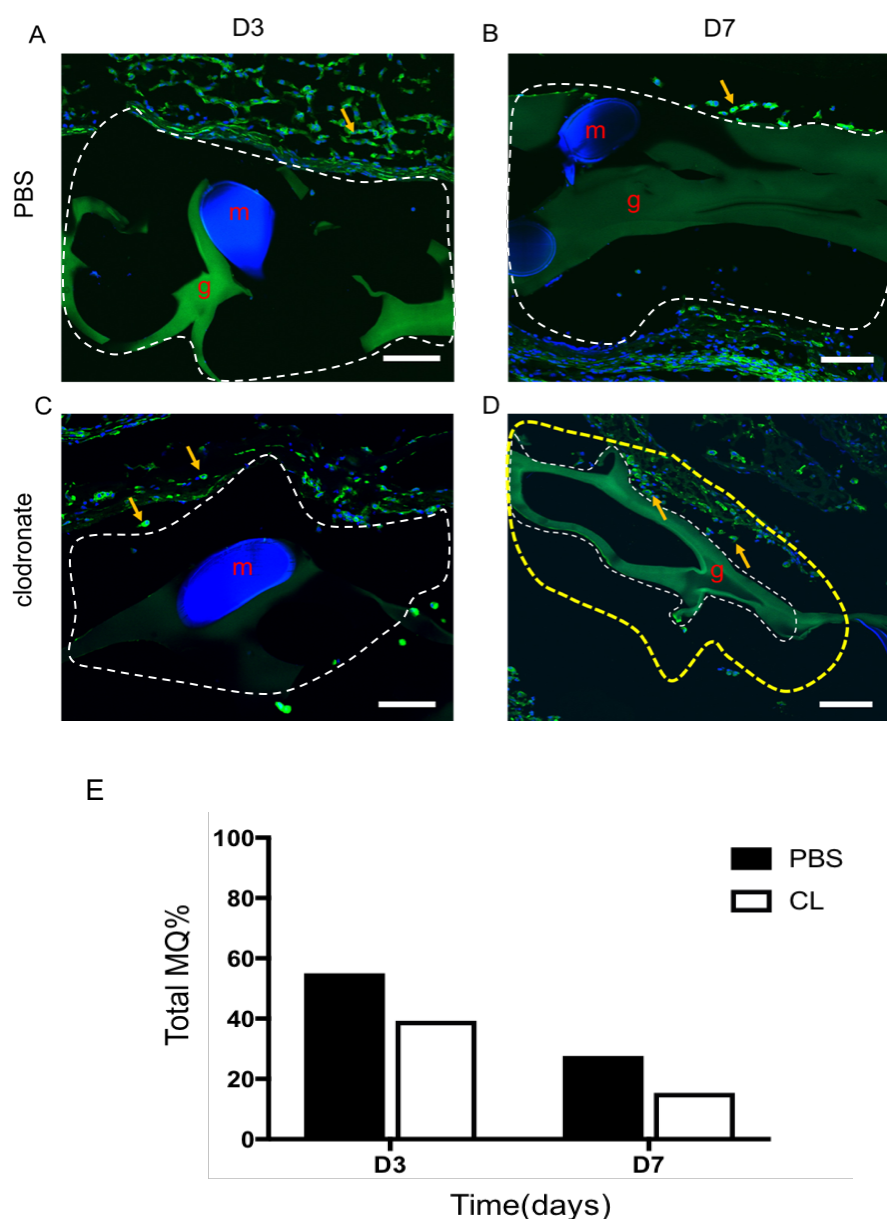


Figure 4. Macrophages surround implanted m-Cherry-labelled eMSC/mesh in clodronate and PBS treated mice. (A) F4/80⁺ macrophages (green) after 3 and (B) 7 days post implantation in PBS injected mice and (C,D) F4/80⁺ macrophages after 3 and 7 days post implantation in clodronate injected mice, respectively. Arrows show representative macrophages. Scale bar 100 μ m. (E) quantified macrophages (F4/80⁺, green) as a percentage of total nucleated cells in the first 100 μ m increment around mesh filament in PBS and clodronate injected mice. Data are mean \pm SEM of n=2

animals/group. m, mesh, g, gelatin, white dashed lines, outline of PA+G mesh, yellow dotted lines, 100µm increment around mesh analyzed eg in (D). MQ, macrophages

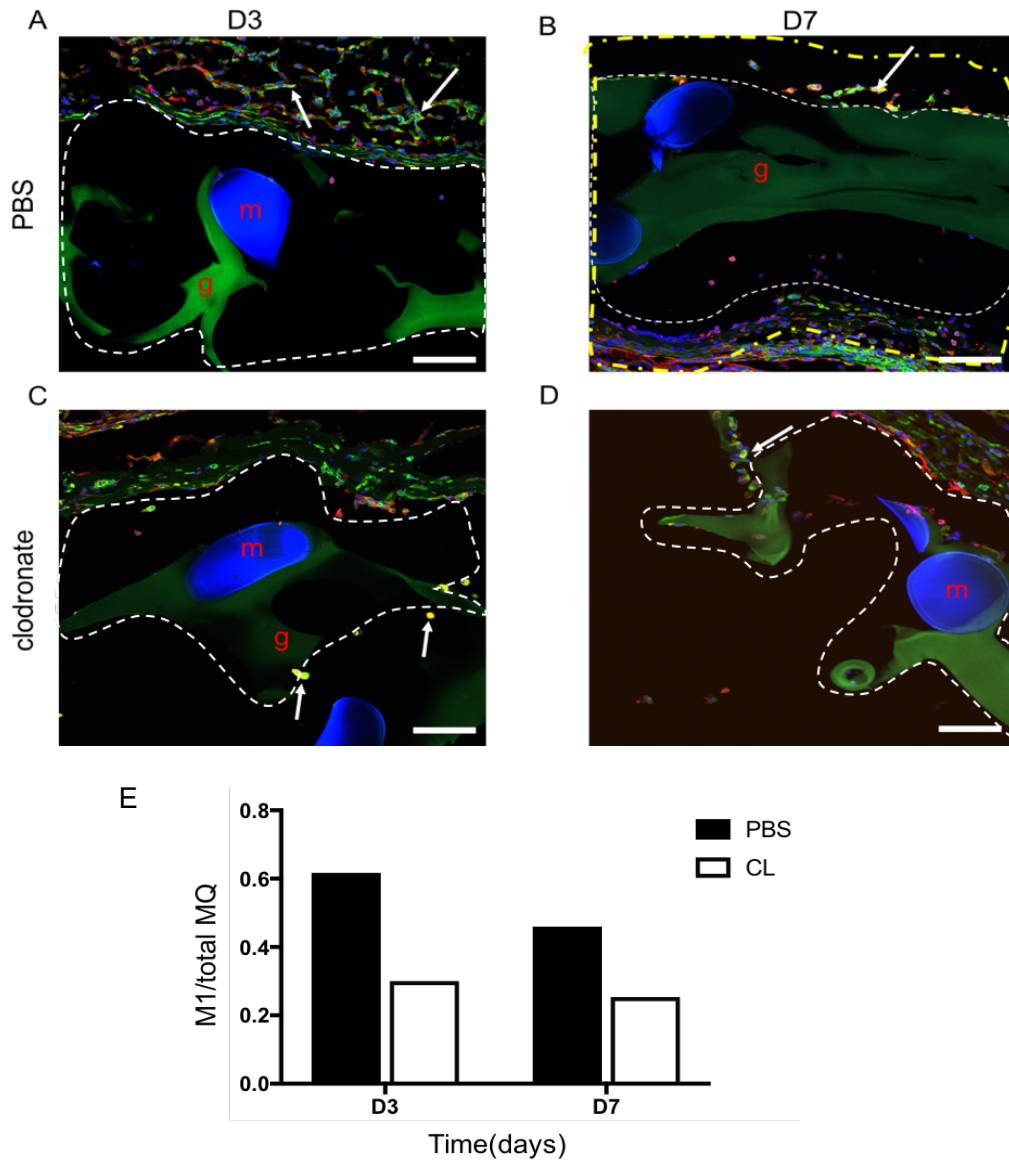


Figure 5. M1 Macrophage quantification around implanted mesh in clodronate and PBS treated mice. (A) CCR7 M1 macrophage (red) and F4/80 macrophage (green) co-localized (yellow) around implanted mesh after 3 and 7 days in (A,B), PBS injected mice and (C,D) clodronate injected mice. Arrows show representative M1 macrophages. Scale

bar 100 μ m. (E) Ratio of macrophages with co-localized markers in the first 100 μ m around mesh. Data are mean \pm SEM of n=2 animals/group. m, mesh, g, gelatin, white dashed lines, outline of PA+G mesh, yellow dotted lines, 100 μ m increment around mesh analyzed eg in (B).

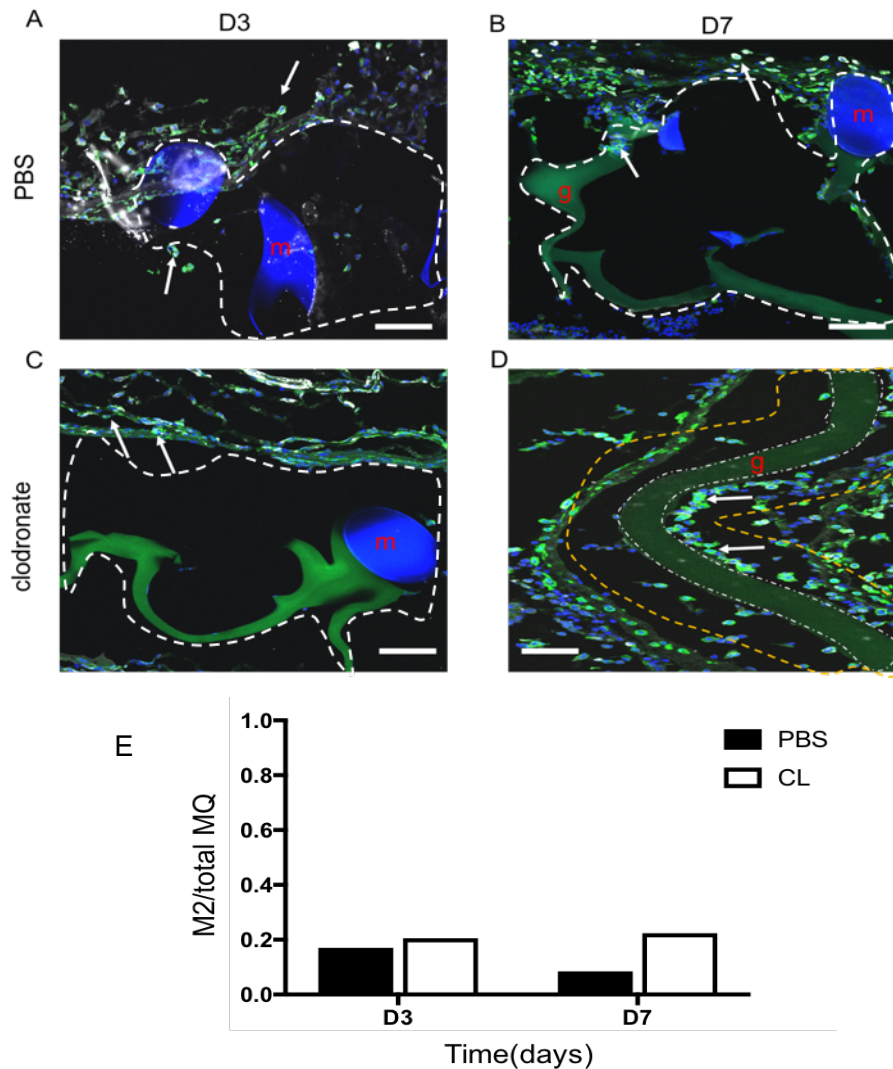


Figure 6. M2 Macrophage quantification around implanted mesh in clodronate and PBS treated mice. (A) CD206 M2 macrophage (white) and F4/80 macrophage (green) co-localized around implanted mesh after 3 and 7 days in (A,B), PBS injected mice and (C,D) clodronate injected mice. Arrows show representative M2 macrophages. Scale bar 100 μ m. (E) Ratio of macrophages with co-localized markers in the first 100 μ m around

mesh. Data are mean \pm SEM of n=2 animals/group. m, mesh, g, gelatin, white dashed lines, outline of PA+G mesh, yellow dotted lines, 100 μ m increment around mesh analyzed eg in (D).

4.5.5. Absence of immature monocytes in tissue around mesh

The presence of immature monocytes (CD11b⁺F4/80⁺) in PBS and clodronate injected mice was also investigated. CD11b⁺F4/80⁺ immature monocytes were not detected 3 and 7 days post implantation in PBS and clodronate injected mice (Fig 8A and B).

4.5.6. Lack of local macrophage proliferation in implanted mesh of clodronate treated mice

I next determined whether the resident responding macrophages observed around the PA+G mesh resulted from proliferation of local resident macrophages. Dual color immunofluorescence staining with F4/80 and Ki67 (proliferation marker) was performed in sections obtained from C57BL6 mice injected with clodronate and PBS and implanted with eMSC seeded mesh. The accumulated macrophages around mesh filaments did not proliferate as no F4/80⁺ macrophages showed nuclear Ki67 immunostaining (Fig. 7A and B).

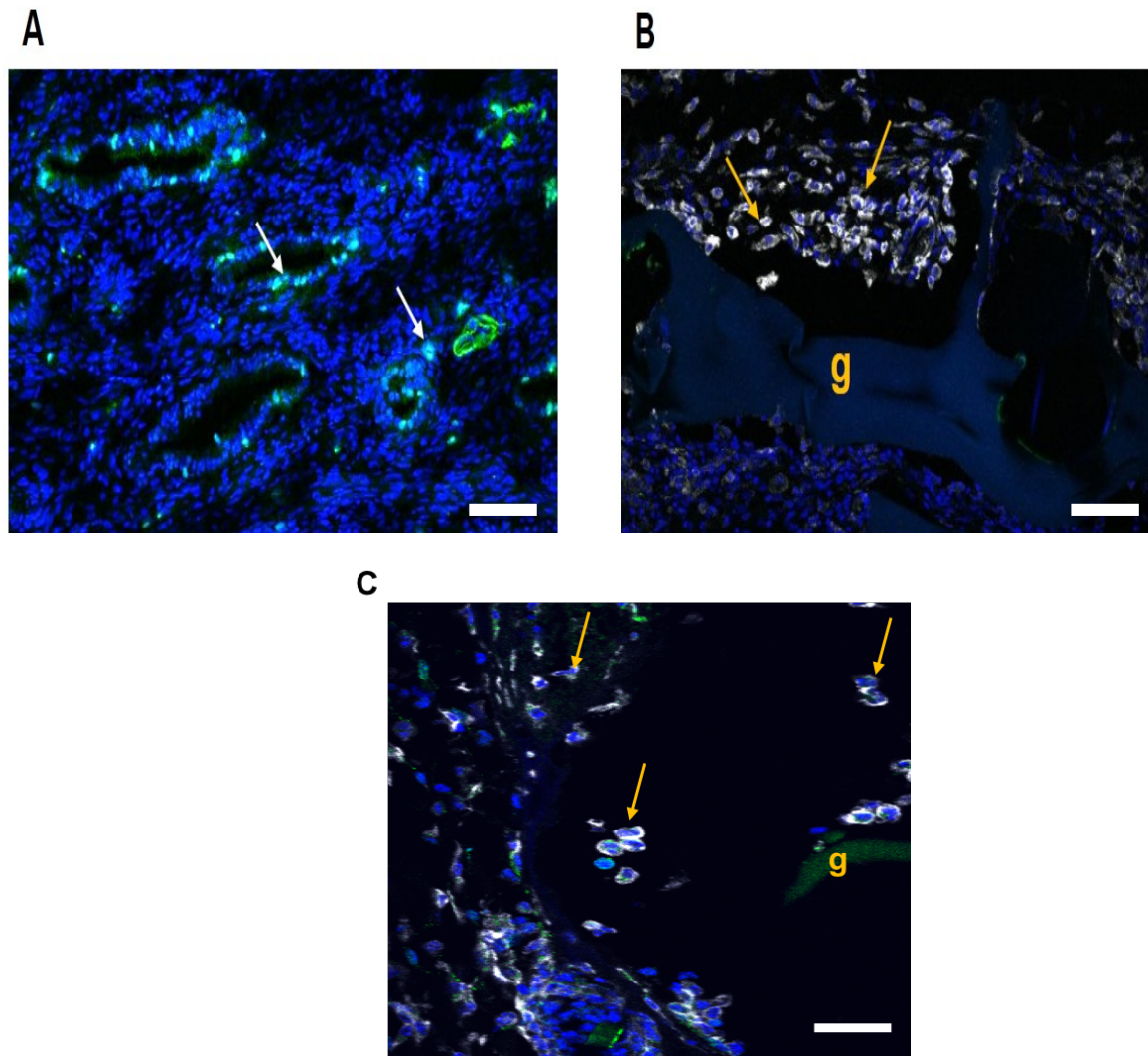


Fig.7. Macrophage proliferation around implanted eMSC/mesh in clodronate and PBS treated mice. (A) Ki67⁺ (green nuclei) mouse endometrial cells (positive control) (white arrows) and (B,C) co-localization of F4/80 (white) and Ki67 (green) in tissue around implanted eMSC/mesh in (B) clodronate injected and (C) PBS injected mice Yellow arrow show representative macrophages Scale bars 100 μm

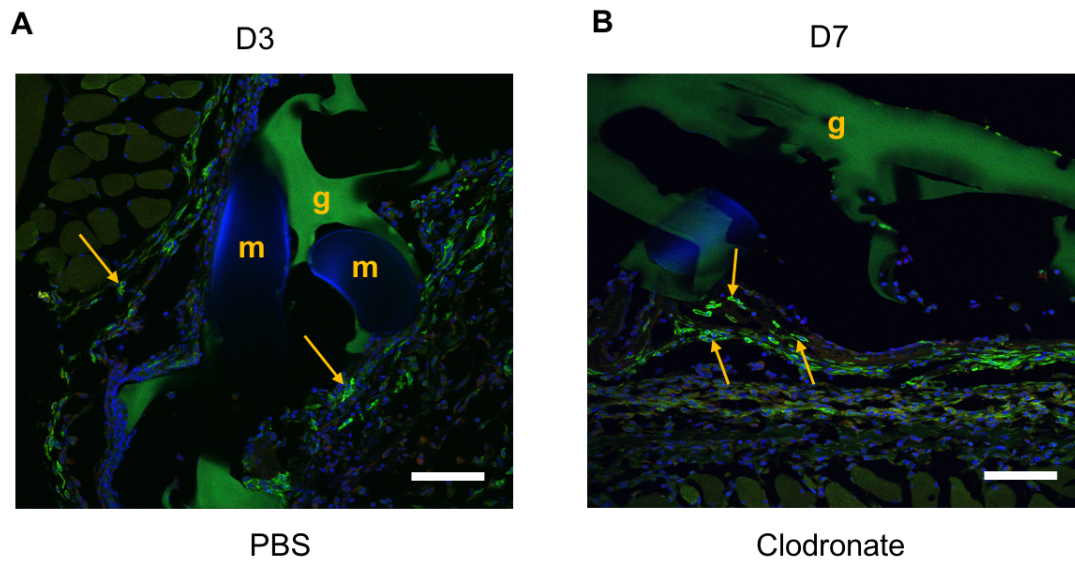


Fig.8. Lack of immature macrophages around implanted eMSC/mesh in clodronate and PBS treated mice. (A) co-localization of F4/80 (green) and CD11b (red) in PBS injected mice 3 days after mesh implantation and (B) in clodronate injected mouse 7 days post implantation. Yellow arrow show CD11b⁻F4/80⁺ macrophages. No CD11b⁺F4/80⁺ were observed. Scale bars 100 μ m

4.6. Discussion

The main findings of this study are firstly, resident macrophages, independently of recruited monocytes, are responding to mesh implantation and responsible for clearance of implanted eMSC. Secondly, I found that local macrophages do not proliferate in response to the implanted eMSC/mesh tissue engineering construct suggesting that migrating macrophages are one of the sources of accumulated macrophages. Thirdly, the majority of resident migrating macrophages around the mesh in systemic monocyte depleted animals were uncommitted M0 macrophages.

Macrophages are the key cells which determine the success or failure outcome of implanted biomaterials. I previously showed that eMSC affected macrophage polarization in response to implanted mesh. I found less inflammatory cytokines including IL1 β and TNF- α and higher expression of M2 macrophage markers including Arginase I, Mannose receptor and IL-10 in mice implanted with eMSC seeded mesh (Chapter 3). Due to considerable accumulation of macrophages around mesh filaments and rapid disappearance of eMSC in C57BL6 mice, I was interested to investigate whether macrophage depletion resulted in longer survival of eMSC.

I found fewer macrophages in clodronate compared with PBS injected mice which may indicate that in control animals, recruitment of circulating monocytes was still operating. However, further replicates are needed to allow statistical comparison between the two groups. CD11b immature monocytes/macrophages, were not detected around the mesh which confirms that the source of recruited macrophages was from the local resident population. This result indicates two possibilities; 1. Recruited circulating monocytes do not participate in the macrophage response to the implanted mesh or 2. PBS-liposome

(control) caused some macrophage depletion as suggested (Table 1). The effect of route of clodronate administration on macrophage depletion in PBS injected mice has not been studied before and whether macrophage depletion in PBS group is related to the site of injection or the liposome might be toxic for macrophages, need to be studied.

Several previous studies have investigated the source of macrophages responding to injured tissues. In a muscle injury rat model, there was a 50% decrease in macrophages at the site of injury following IV clodronate injection (Cote et al., 2013). Local macrophage proliferation increased after this systemic depletion of monocytes, contributing to the 50% of macrophages found at the site. The authors concluded that both recruited and local macrophages contributed in macrophage accumulation at the muscle injury site (Cote et al., 2013). In a mouse model of parasitic infection macrophages accumulated in the pleural cavity of nematode infected mice despite the removal of blood monocytes with clodronate and about 40% of accumulated macrophages were proliferation (Ki67⁺). This result indicates that macrophage accumulation in inflammation occurs independently of blood monocytes (Jenkins et al., 2011). Indeed, blood recruited monocytes and resident macrophages maintain different populations during inflammation (Davies et al., 2013).

This together with our findings suggest that the local resident macrophage population plays a significant role in the foreign body response to subcutaneously implanted mesh. IV injection of clodronate depletes spleen and liver macrophages but not completely in bone marrow (Sunderkotter et al., 2004). In our study, due to limited time, the clodronate efficiency on reducing bone marrow recruited macrophage progenitors (monocytes) was not assessed, an important limitation of the present study. The other limitations in this study are the insufficient replicates and lack of liposome control which could have showed

the effect of liposomes on macrophage depletion, which was reported previously (Weisser et al., 2011, Qualls et al., 2006, Weisser et al., 2012).

There is no report on the source of responding macrophages following MSC-seeded biomaterial implantation. Given that our preliminary findings showing a lack of local macrophage proliferation and depleted splenic macrophages, there is likely an alternative mechanism involved in the macrophage accumulation around mesh filaments. In the physiological process of wound healing, macrophages migrate to site of injury from the bone marrow (Davies et al., 2013). Given that local macrophage proliferation was not seen in the F4/80⁺ population around mesh filaments, it is possible that they migrate along a chemoattractant gradient of CCL3 and CCL5 secreted by other immune cells such as dendritic and NK cells. This new hypothesis of tissue resident macrophages migration needs to be further assessed and confirmed by increasing sample size in the present study.

In this study, for the first time, in a limited number of replicates due to time constraints, I showed that the source of responding macrophages to an eMSC-seeded mesh *in vivo* was neither due to monocyte recruitment, nor to proliferation of local macrophages and that macrophage response was dominated by M0 macrophages. Although sample size needs increasing to determine statistical significant of this result and further work needs to be performed to examine the independent roles of circulating and resident macrophage recruitment and efficiency of clodronate injection on bone marrow recruited monocytes and tissue macrophage migration.

Chapter 5
Overall discussion

The main goal of this thesis was to examine different approaches to minimize the inflammation and host response to implanted meshes. I assessed two alternative options including collagen-coating a conventional polypropylene (PP) mesh and seeding eMSC onto a novel mesh. To reduce an excessive host inflammatory response, various mesh modifications have been investigated, including pore size and mesh weight. Another alteration is coating the mesh with extracellular matrix to provide a biological interface of the mesh with the tissue. This approach results in less inflammation and reduced leukocyte accumulation for ECM coated meshes. (Wolf et al., 2014, Valentin et al., 2009). An entirely new approach is to seed immunomodulatory cells (ie MSC) onto meshes to modulate the inflammatory response. Both of these approaches were investigated in my thesis.

In the first aim of my thesis I assessed how different formats of collagen coating impacted the host response to PP mesh. Collagen is the most common protein in the ECM and structurally it is classified into fibrillar and non-fibrillar collagen. Accordingly, I assessed commercially available PP meshes either incorporated with a sheet of natural tissue based fibrillar collagen that was further cross-linked (Avaulta plus) or coated with tissue-solubilized monomeric collagen (Ugytex) which has physical and biological properties similar to native collagen. Sheep vaginal surgery was used as a model to evaluate the role of collagen tertiary structure in modifying the host response. This ovine model has similarities with the human reproductive system including size of vagina, the pelvic structure and biomechanics (Urbankova et al., 2017). Furthermore, sheep spontaneously develop POP. Our results revealed that despite a vigorous leukocyte response around

both collagen-containing meshes and unmodified control PP meshes, the soluble collagen-coated mesh resulted in higher numbers of favored M2 macrophages which promote tissue healing. This, together with an increased number of vWF⁺ blood vessels around the implanted mesh, suggests enhanced healing around the soluble collagen-coated filament mesh and better integration of the mesh into the tissue. In the soluble monomeric collagen coated mesh, each mesh filament is coated with soluble non-cross-linked, highly resorbing, collagen allowing rapid penetration of capillaries and greater vascularization. This finding supports the beneficial effects of collagen incorporation into PP mesh designs but indicates that the collagen format and rate of degradation can itself be a critical factor in promoting these outcomes.

One of the limitations of this study is the lack of elastin measurement. Elastin is one of the important proteins in connective tissue and plays a role in preserving the connective tissue structure following stretch or contraction.

One innovation our group brought to the field is to use an objective method of cell or matrix quantification in a defined increment around individual mesh filaments using Metamorph software to improve on subjective scoring. Using our quantitative morphometric analysis, I examined Sirius Red birefringence of newly synthesized collagen fibers and identified the density and maturation of collagen fibers at the tissue filament interface. I found that the total birefringent collagen deposited in animals vaginally implanted with collagen-coated mesh was more similar to uninjured tissue than those implanted with an unmodified control PP mesh.

Macrophages are one of the main immune cells involved in the inflammatory response to implanted mesh, playing a central role in determining the success or failure of implanted

mesh. It is both their finely controlled pro- and anti-inflammatory functions that is a major determinant in the outcomes of tissue engineering and cell transplantation. Apart from the physical properties of the biomaterial which affects the host macrophage response, any incorporated cells used in tissue engineered constructs or biomaterials may also modulate the immune cell response, particularly macrophage responses (Klopffleisch, 2016). M1 pro-inflammatory and M2 anti-inflammatory macrophages orchestrate the processes associated with the foreign body reaction by producing cytokines and other bioactive molecules which affect the early (innate) and late (adaptive) immune responses. While both the M1 and M2 macrophages are temporally important in the response to non-degradable biomaterial implantation, the M2 macrophage response is more beneficial in the long-term as it facilitates tissue remodeling and stable integration of material, by promoting angiogenesis and superior healing.

Mesenchymal stem/stromal cells are being explored for their immunomodulatory properties and their ability to facilitate the switching of M1 macrophages to M2 macrophages (Eggenhofer and Hoogduijn, 2012). In the second result chapter of this thesis I used a newly identified source of MSC from the endometrium. Endometrial mesenchymal stem cells (eMSC) are highly proliferative, differentiate to mesodermal lineages and we have developed methodology for their purification using SUSD2 magnetic bead sorting. We previously reported the beneficial effects of xenogeneic eMSC in promoting new tissue growth and minimizing fibrosis in a wound repair model using mesh augmentation (Ulrich et al., 2014b). In Aim 2, I found that eMSC modulated the inflammatory response to PA+G mesh. Inflammation was reduced, together with increased M2 macrophage expression markers and cytokine activity in mice with an intact

immune system several days post implantation. This suggests an immunomodulatory effect of eMSC on early responding NK, Dendritic Cell (DC) and macrophages. However, this came at the expense of eMSC survival, as these disappeared in less than three days in immune intact mice. Activated MSC secrete regulatory factors such as IL10 which inhibit the production of inflammatory cytokines by DC and macrophages and induce the generation of regulatory T cells (Kyurkchiev et al., 2014). I did not examine the effects of eMSC on early responding immune cells including neutrophils and DC but the reduction in inflammatory response soon after mesh implantation in C57BL6 mice is likely due to eMSC-induced reduction in inflammatory mediators produced by DCs, neutrophils and macrophages.

In an NSG immunocompromised mouse system, the adaptive immune system is defective, as well as some innate immune cells including DC and NK cells. Fewer innate immune cells responded to the implanted mesh resulting in a reduced acute inflammatory response in NSG compared with C57BL6 mice. The regulatory effects of eMSC was subsequently delayed and weaker in NSG mice.

The modulatory effects of MSC on immune cells *in vitro* and *in vivo* have been reported before. MSC decreased the activation of lymphocytes and DC and secreted the inhibitory cytokines, IL-10 and TGF β in co-culture with these immune cells (Aggarwal and Pittenger, 2005, Singer and Caplan, 2011). Human adipose-derived cells decreased inflammatory cytokines and chemokines, and increased IL-10 following systemic infusion in acute and chronic colitis in C57BL6 mouse models. In this study, I used a xenogeneic heterologous source of adult stem cells and assessed their immunomodulatory activity in both immunocompetent and immunocompromised mice as I was interested to determine

whether xenogeneic heterologous MSC differ in their persistence in the absence of an adaptive immune system and NK cells (immunocompromised mice). Another question I wished to answer was whether the interaction between eMSC and macrophages differs in the presence or absence of an intact immune system. In this thesis, I found longer survival of eMSC in the absence of an intact immune system. However, the shorter survival of eMSC in an intact immune system, did not affect their modulatory effects. Assuming that xenogeneic cells may be similar in effect to allogeneic cells, my findings suggest that there may be similar benefits when using allogeneic compared to autologous MSC for cell therapies and tissue engineering studies.

Others have also shown that systemic or locally delivered MSC (from other sources) do not survive at the site but nevertheless limit tissue injury during their short stay through their immunomodulatory effects via paracrine factor secretion (Braza et al., 2016, Agrawal et al., 2014). Activated MSC from bone marrow produce COX2 and increase PGE2 secretion which results in switching of M1 macrophages to an M2 phenotype (Prockop, 2013).

In an immunocompromised system, eMSC survived longer as has been shown by others using different sources of MSC (Bai et al., 2011, Vilalta et al., 2008, Meyerrose et al., 2007). Intramuscular and intravenous implantation of human adipose derived stem cells in nude mice showed that 75% of the injected MSC were lost in the first week but the number of surviving cells (5000 cells in thigh muscle and 3000 cells in lung) remained stable up to 8 months (Vilalta et al., 2008). In another study, the engraftment and distribution of injected human adipose derived stem cells (ASC) following acute myocardial infarction showed that injected ASC survived in infarcted hearts of SCID mice

during the 10 weeks follow-up (Bai et al., 2011). In my study, irrespective of differing eMSC survival, eMSC showed regulatory effects in both immune intact and immune compromised systems suggesting that immune intact mice are an equally suitable if not better model to study immunomodulatory effects of MSC.

Following the rapid disappearance of mCherry-labelled eMSC in mesh implanted C57BL6 mice, I became interested in understanding whether macrophages, as the major type of cell accumulating around the mesh, phagocytose the eMSC and contribute to their short survival *in vivo*. I also questioned whether eMSC survive longer in the absence of macrophages. As a first step in investigating this goal in Aim 3, I sought to determine the source of macrophages accumulating at the site of the mesh, whether they were from circulating monocytes or tissue resident macrophages. I investigated the role of recruited monocytes to the injury site and developed a systemic macrophage depletion mouse model using clodronate IV injection. Macrophage accumulation around mesh filaments was not affected by systemic macrophage depletion, despite the removal of macrophages from the spleen, suggesting a role for tissue resident macrophages in the tissue response to mesh. Furthermore, mCherry-labelled eMSC failed to survive longer in the absence of macrophages. However, local macrophage proliferation does not appear to have a role in the tissue response to implanted mesh. My thesis shows for the first time, albeit with limited sample numbers, that the source of responding macrophages to implanted biomaterial seeded with eMSC *in vivo* does not involve local macrophage proliferation. In contrast, in infectious injury models both recruited monocytes and local macrophage proliferation played a role in mitigating muscle injury or infections (Jenkins et al., 2011, Cote et al., 2013). While my result with eMSC supports previous studies regarding the

role of macrophages, my study found for the first time an alternative mechanism for macrophage accumulation involving resident macrophages.

Tissue engineering using mesenchymal stem cells, is an emerging alternative solution for tissue replacement in organ failure and tissue loss. However, when biomaterials are implanted, the host response should be considered as one of the main factors responsible for the failure or success of the biomaterial implant. Macrophages are the main cell type involved in the inflammatory response and its resolution during the wound healing process. Precise understanding of their role and the factors that might affect the macrophage responses will improve the outcomes of tissue engineering approaches in terms of designing improved biocompatible mesh to promote better tissue integration with less inflammation. The results of this project provide a basis for ongoing studies on the host response to implanted biomaterials.

References

- ABED, H., RAHN, D. D., LOWENSTEIN, L., BALK, E. M., CLEMONS, J. L. & ROGERS, R. G. 2011. Incidence and management of graft erosion, wound granulation, and dyspareunia following vaginal prolapse repair with graft materials: a systematic review. *Int Urogynecol J*, 22, 789-98.
- ABRAMOWITCH, S. D., FEOLA, A., JALLAH, Z. & MOALLI, P. A. 2009. Tissue mechanics, animal models, and pelvic organ prolapse: a review. *Eur J Obstet Gynecol Reprod Biol*, 144 Suppl 1, S146-58.
- AGGARWAL, S. & PITTENGER, M. F. 2005. Human mesenchymal stem cells modulate allogeneic immune cell responses. *Blood*, 105, 1815-22.
- AGRAWAL, H., SHANG, H., SATTAH, A. P., YANG, N., PEIRCE, S. M. & KATZ, A. J. 2014. Human adipose-derived stromal/stem cells demonstrate short-lived persistence after implantation in both an immunocompetent and an immunocompromised murine model. *Stem Cell Res Ther*, 5, 142.
- ALTMAN, D., ZETTERSTROM, J., LOPEZ, A., ANZEN, B., FALCONER, C., HJERN, F. & MELLGREN, A. 2005. Functional and anatomic outcome after transvaginal rectocele repair using collagen mesh: a prospective study. *Dis Colon Rectum*, 48, 1233-41; discussion 1241-2; author reply 1242.
- ANDERSON, J. M., RODRIGUEZ, A. & CHANG, D. T. 2008. Foreign body reaction to biomaterials. *Semin Immunol*, 20, 86-100.
- ASHTON-MILLER, J. A. & DELANCEY, J. O. 2007. Functional anatomy of the female pelvic floor. *Ann N Y Acad Sci*, 1101, 266-96.

- ASHTON-MILLER, J. A. & DELANCEY, J. O. 2009. On the biomechanics of vaginal birth and common sequelae. *Annu Rev Biomed Eng*, 11, 163-76.
- AUGELLO, A., TASSO, R., NEGRINI, S. M., AMATEIS, A., INDIVERI, F., CANCEDDA, R. & PENNESI, G. 2005. Bone marrow mesenchymal progenitor cells inhibit lymphocyte proliferation by activation of the programmed death 1 pathway. *Eur J Immunol*, 35, 1482-90.
- AYELE, T., ZUKI, A. B., NOORJAHAN, B. M. & NOORDIN, M. M. 2010. Tissue engineering approach to repair abdominal wall defects using cell-seeded bovine tunica vaginalis in a rabbit model. *J Mater Sci Mater Med*, 21, 1721-30.
- BAI, X., YAN, Y., COLEMAN, M., WU, G., RABINOVICH, B., SEIDENSTICKER, M. & ALT, E. 2011. Tracking long-term survival of intramyocardially delivered human adipose tissue-derived stem cells using bioluminescence imaging. *Mol Imaging Biol*, 13, 633-45.
- BARBER, M. D. & MAHER, C. 2013. Epidemiology and outcome assessment of pelvic organ prolapse. *Int Urogynecol J*, 24, 1783-90.
- BARRAGAN, F., IRWIN, J. C., BALAYAN, S., ERIKSON, D. W., CHEN, J. C., HOUSHDARAN, S., PILTONEN, T. T., SPITZER, T. L., GEORGE, A., RABBAN, J. T., NEZHAT, C. & GIUDICE, L. C. 2016. Human Endometrial Fibroblasts Derived from Mesenchymal Progenitors Inherit Progesterone Resistance and Acquire an Inflammatory Phenotype in the Endometrial Niche in Endometriosis. *Biol Reprod*, 94, 118.
- BARRETT, A. J. & LE BLANC, K. 2008. Prophylaxis of acute GVHD: manipulate the graft or the environment? *Best Pract Res Clin Haematol*, 21, 165-76.

- BARTHOLOMEW, A., STURGEON, C., SIATSKAS, M., FERRER, K., MCINTOSH, K., PATIL, S., HARDY, W., DEVINE, S., UCKER, D., DEANS, R., MOSELEY, A. & HOFFMAN, R. 2002. Mesenchymal stem cells suppress lymphocyte proliferation in vitro and prolong skin graft survival in vivo. *Exp Hematol*, 30, 42-8.
- BIANCO, P., CAO, X., FRENETTE, P. S., MAO, J. J., ROBEY, P. G., SIMMONS, P. J. & WANG, C. Y. 2013. The meaning, the sense and the significance: translating the science of mesenchymal stem cells into medicine. *Nature Medicine*, 19, 35-42.
- BIANCO, P., RIMINUCCI, M., GRONTHOS, S. & ROBEY, P. G. 2001. Bone marrow stromal stem cells: nature, biology, and potential applications. *Stem Cells*, 19, 180-92.
- BOENNELYCKE, M., GRAS, S. & LOSE, G. 2013. Tissue engineering as a potential alternative or adjunct to surgical reconstruction in treating pelvic organ prolapse. *Int Urogynecol J*, 24, 741-7.
- BRAEKKEN, I. H., MAJIDA, M., ENGH, M. E. & BO, K. 2010. Can pelvic floor muscle training reverse pelvic organ prolapse and reduce prolapse symptoms? An assessor-blinded, randomized, controlled trial. *Am J Obstet Gynecol*, 203, 170.e1-7.
- BRANCH, M. J., HASHMANI, K., DHILLON, P., JONES, D. R., DUA, H. S. & HOPKINSON, A. 2012. Mesenchymal stem cells in the human corneal limbal stroma. *Invest Ophthalmol Vis Sci*, 53, 5109-16.
- BRAZA, F., DIROU, S., FOREST, V., SAUZEAU, V., HASSOUN, D., CHESNE, J., CHEMINANT-MULLER, M. A., SAGAN, C., MAGNAN, A. & LEMARCHAND, P.

2016. Mesenchymal Stem Cells Induce Suppressive Macrophages Through Phagocytosis in a Mouse Model of Asthma. *Stem Cells*, 34, 1836-45.
- BROOKE, G., ROSSETTI, T., PELEKANOS, R., ILIC, N., MURRAY, P., HANCOCK, S., ANTONENAS, V., HUANG, G., GOTTLIEB, D., BRADSTOCK, K. & ATKINSON, K. 2009. Manufacturing of human placenta-derived mesenchymal stem cells for clinical trials. *Br. J. Haematol.*, 144, 571-579.
- BROWN, B. N., MANI, D., NOLFI, A. L., LIANG, R., ABRAMOWITCH, S. D. & MOALLI, P. A. 2015. Characterization of the host inflammatory response following implantation of prolapse mesh in rhesus macaque. *Am J Obstet Gynecol*, 213, 668.e1-10.
- BROWN, B. N., VALENTIN, J. E., STEWART-AKERS, A. M., MCCABE, G. P. & BADYLAK, S. F. 2009. Macrophage phenotype and remodeling outcomes in response to biologic scaffolds with and without a cellular component. *Biomaterials*, 30, 1482-91.
- BUMP, R. C., MATTIASSON, A., BO, K., BRUBAKER, L. P., DELANCEY, J. O., KLARSKOV, P., SHULL, B. L. & SMITH, A. R. 1996. The standardization of terminology of female pelvic organ prolapse and pelvic floor dysfunction. *Am J Obstet Gynecol*, 175, 10-7.
- CAPLAN, A. I. 2007. Adult mesenchymal stem cells for tissue engineering versus regenerative medicine. *J Cell Physiol*, 213, 341-7.
- CAPLAN, A. I. 2008. All MSCs are pericytes? *Cell Stem Cell*, 3, 229-30.
- CAPLAN, A. I. 2009. Why are MSCs therapeutic? New data: new insight. *J Pathol*, 217, 318-24.

- CAPLAN, A. I. 2010. Mesenchymal Stem Cells: The Past, the Present, the Future. *Cartilage*, 1, 6-9.
- CAREY, M., HIGGS, P., GOH, J., LIM, J., LEONG, A., KRAUSE, H. & CORNISH, A. 2009. Vaginal repair with mesh versus colporrhaphy for prolapse: a randomised controlled trial. *Bjog*, 116, 1380-6.
- CHAMPLIN, A. K., DORR, D. L. & GATES, A. H. 1973. Determining the stage of the estrous cycle in the mouse by the appearance of the vagina. *Biol Reprod*, 8, 491-4.
- CHAN, R., KAITU'U-LINO, T. & GARGETT, C. E. 2012. Role of Label-Retaining Cells in Estrogen-Induced Endometrial Regeneration. *Reprod. Sci.*, 19, 102-114.
- CHAN, R. W., SCHWAB, K. E. & GARGETT, C. E. 2004. Clonogenicity of human endometrial epithelial and stromal cells. *Biol Reprod*, 70, 1738-50.
- CHAN, R. W. S. & GARGETT, C. 2006. Identification of label-retaining cells in mouse endometrium. *Stem Cells*, 24, 1529-1538.
- CHAPPLE, C. R., OSMAN, N. I., MANGERA, A., HILLARY, C., ROMAN, S., BULLOCK, A. & MACNEIL, S. 2015. Application of Tissue Engineering to Pelvic Organ Prolapse and Stress Urinary Incontinence. *Low Urin Tract Symptoms*, 7, 63-70.
- CHOE, J. M. 2003. The use of synthetic materials in pubovaginal sling. *Adv Exp Med Biol*, 539, 481-92.
- CHOW, B. F. & AGUSTIN, C. E. 1965. Induction of premature birth in rats by a methionine antagonist. *J Nutr*, 87, 293-6.
- CLAERHOUT, F., DE RIDDER, D., VAN BECKEVOORT, D., COREMANS, G., VELDMAN, J., LEWI, P. & DEPREST, J. 2010. Sacrocolpopexy using xenogenic

- acellular collagen in patients at increased risk for graft-related complications. *Neurourol Urodyn*, 29, 563-7.
- COMOLI, P., GINEVRI, F., MACCARIO, R., AVANZINI, M. A., MARCONI, M., GROFF, A., COMETA, A., CIONI, M., PORRETTI, L., BARBERI, W., FRASSONI, F. & LOCATELLI, F. 2008. Human mesenchymal stem cells inhibit antibody production induced in vitro by allostimulation. *Nephrol Dial Transplant*, 23, 1196-202.
- CORCIONE, A., BENVENUTO, F., FERRETTI, E., GIUNTI, D., CAPPIELLO, V., CAZZANTI, F., RISSO, M., GUALANDI, F., MANCARDI, G. L., PISTOIA, V. & UCCELLI, A. 2006. Human mesenchymal stem cells modulate B-cell functions. *Blood*, 107, 367-72.
- COTE, C. H., BOUCHARD, P., VAN ROOIJEN, N., MARSOLAIS, D. & DUCHESNE, E. 2013. Monocyte depletion increases local proliferation of macrophage subsets after skeletal muscle injury. *BMC Musculoskelet Disord*, 14, 359-370.
- COURI, B. M., LENIS, A. T., BORAZJANI, A., PARAISO, M. F. & DAMASER, M. S. 2012. Animal models of female pelvic organ prolapse: lessons learned. *Expert Rev Obstet Gynecol*, 7, 249-260.
- CRISAN, M., YAP, S., CASTEILLA, L., CHEN, C. W., CORSELLI, M., PARK, T., ANDRIOLO, G., SUN, B., ZHENG, B., ZHANG, L., NOROTTE, C., TENG, P., TRAAS, J., SCHUGAR, R., DEASY, B. M., BADYLAK, S., BUHRING, H., GIACOBINO, J. P., LAZZARI, L., HUARD, J. & PEAULT, B. 2008. A perivascular origin for mesenchymal stem cells in multiple human organs. *Cell Stem Cell*, 3, 301-313.

- CUI CH, U. T., MIYADO K ET AL 2007. Menstrual blood-derived cells confer human dystrophin expression in the murine model of Duchenne muscular dystrophy via cell fusion and myogenic transdifferentiation. *Molecular Biology Of the Cell*, 18, 1586-1594.
- DARZI, S., URBANKOVA, I., SU, K., WHITE, J., LO, C., ALEXANDER, D., WERKMEISTER, J. A., GARGETT, C. E. & DEPREST, J. 2016a. Tissue response to collagen containing polypropylene meshes in an ovine vaginal repair model. *Acta Biomater*, 39, 114-23.
- DARZI, S., WERKMEISTER, J. A., DEANE, J. A. & GARGETT, C. E. 2016b. Identification and Characterization of Human Endometrial Mesenchymal Stem/Stromal Cells and Their Potential for Cellular Therapy. *Stem Cells Transl Med*, 5, 1127-32.
- DARZI, S., ZARNANI, A. H. & M, J.-T. 2012. Osteogenic Differentiation of Stem Cells Derived from Menstrual Blood Versus Bone Marrow in the Presence of Human Platelet Releasate. *Tissue Engineering Part A*, 120625132319008.
- DAVID-MONTEFIORE, E., BARRANGER, E., DUBERNARD, G., DETCHEV, R., NIZARD, V. & DARAI, E. 2005. Treatment of genital prolapse by hammock using porcine skin collagen implant (Pelvicol). *Urology*, 66, 1314-8.
- DAVIES, L. C., JENKINS, S. J., ALLEN, J. E. & TAYLOR, P. R. 2013. Tissue-resident macrophages. *Nat Immunol*, 14, 986-95.
- DAYAN, V., YANNARELLI, G., BILLIA, F., FILOMENO, P., WANG, X. H., DAVIES, J. E. & KEATING, A. 2011. Mesenchymal stromal cells mediate a switch to alternatively activated monocytes/macrophages after acute myocardial infarction. *Basic Res Cardiol*, 106, 1299-310.

- DE BARI, C., DELL'ACCIO, F., VANDENABEELE, F., VERMEESCH, J. R., RAYMACKERS, J. M. & LUYTEN, F. P. 2003. Skeletal muscle repair by adult human mesenchymal stem cells from synovial membrane. *J Cell Biol*, 160, 909-18.
- DE MIGUEL, M. P., FUENTES-JULIAN, S., BLAZQUEZ-MARTINEZ, A., PASCUAL, C. Y., ALLER, M. A., ARIAS, J. & ARNALICH-MONTIEL, F. 2012. Immunosuppressive properties of mesenchymal stem cells: advances and applications. *Curr Mol Med*, 12, 574-91.
- DE TAYRAC, R., ALVES, A. & THERIN, M. 2007. Collagen-coated vs noncoated low-weight polypropylene meshes in a sheep model for vaginal surgery. A pilot study. *Int Urogynecol J Pelvic Floor Dysfunct*, 18, 513-20.
- DE TAYRAC, R., DEFFIEUX, X., GERVAISE, A., CHAUVEAUD-LAMBLING, A. & FERNANDEZ, H. 2006a. Long-term anatomical and functional assessment of trans-vaginal cystocele repair using a tension-free polypropylene mesh. *Int Urogynecol J Pelvic Floor Dysfunct*, 17, 483-8.
- DE TAYRAC R, D. X., GERVAISE A ET AL 2006. Long-term anatomical and functional assessment of trans-vaginal cystocele repair using a tension-free polypropylene mesh. *Int Urogynecol J*, 17, 483-488.
- DE TAYRAC, R., PICONE, O., CHAUVEAUD-LAMBLING, A. & FERNANDEZ, H. 2006b. A 2-year anatomical and functional assessment of transvaginal rectocele repair using a polypropylene mesh. *Int Urogynecol J Pelvic Floor Dysfunct*, 17, 100-5.
- DEANS, R. J. & MOSELEY, A. B. 2000. Mesenchymal stem cells: biology and potential clinical uses. *Exp Hematol*, 28, 875-84.

- DEMIRBAG, B., HURI, P. Y., KOSE, G. T., BUYUKSUNGUR, A. & HASIRCI, V. 2011. Advanced cell therapies with and without scaffolds. *Biotechnol J*, 6, 1437-53.
- DENMAN, M. A., GREGORY, W. T., BOYLES, S. H., SMITH, V., EDWARDS, S. R. & CLARK, A. L. 2008. Reoperation 10 years after surgically managed pelvic organ prolapse and urinary incontinence. *Am J Obstet Gynecol*, 198, 555.e1-5.
- DEPREST, J., DE RIDDER, D., ROOVERS, J. P., WERBROUCK, E., COREMANS, G. & CLAERHOUT, F. 2009. Medium term outcome of laparoscopic sacrocolpopexy with xenografts compared to synthetic grafts. *J Urol*, 182, 2362-8.
- DEPREST, J. & FEOLA, A. 2013. The need for preclinical research on pelvic floor reconstruction. *Bjog*, 120, 141-3.
- DEPREST, J., ZHENG, F., KONSTANTINOVIC, M., SPELZINI, F., CLAERHOUT, F., STEENSMA, A., OZOG, Y. & DE RIDDER, D. 2006. The biology behind fascial defects and the use of implants in pelvic organ prolapse repair. *Int Urogynecol J Pelvic Floor Dysfunct*, 17 Suppl 1, S16-25.
- DI NICOLA, M., CARLO-STELLA, C., MAGNI, M., MILANESI, M., LONGONI, P. D., MATTEUCCI, P., GRISANTI, S. & GIANNI, A. M. 2002. Human bone marrow stromal cells suppress T-lymphocyte proliferation induced by cellular or nonspecific mitogenic stimuli. *Blood*, 99, 3838-43.
- DIAS, M. M., DE, A. C. R., BORTOLINI, M. A., DELROY, C. A., MARTINS, P. C., GIRAO, M. J. & SARTORI, M. G. 2016. Two-years results of native tissue versus vaginal mesh repair in the treatment of anterior prolapse according to different success criteria: A randomized controlled trial. *Neurourol Urodyn*, 35, 509-14.

- DIETZ, H. P. 2008. Prolapse worsens with age, doesn't it? *Aust N Z J Obstet Gynaecol*, 48, 587-91.
- DIETZ, H. P., SHEK, K. L., CHANTARASORN, V. & LANGER, S. E. 2012. Do women notice the effect of childbirth-related pelvic floor trauma? *Aust N Z J Obstet Gynaecol*, 52, 277-81.
- DIMARINO, A. M., CAPLAN, A. I. & BONFIELD, T. L. 2013. Mesenchymal stem cells in tissue repair. *Front Immunol*, 4, 201-212.
- DOLCE, C. J., STEFANIDIS, D., KELLER, J. E., WALTERS, K. C., NEWCOMB, W. L., HEATH, J. J., NORTON, H. J., LINCOURT, A. E., KERCHER, K. W. & HENIFORD, B. T. 2010. Pushing the envelope in biomaterial research: initial results of prosthetic coating with stem cells in a rat model. *Surg Endosc*, 24, 2687-93.
- DOMINICI, M., LE BLANC, K., MUELLER, I., SLAPER-CORTENBACH, I., MARINI, F., KRAUSE, D., DEANS, R., KEATING, A., PROCKOP, D. & HORWITZ, E. 2006. Minimal criteria for defining multipotent mesenchymal stromal cells. The International Society for Cellular Therapy position statement. *Cytotherapy*, 8, 315-7.
- DREWA, T., GALAZKA, P., PROKURAT, A., WOLSKI, Z., SIR, J., WYSOCKA, K. & CZAJKOWSKI, R. 2005. Abdominal wall repair using a biodegradable scaffold seeded with cells. *J Pediatr Surg*, 40, 317-21.
- DREWES, P. G., YANAGISAWA, H., STARCHER, B., HORNSTRA, I., CSISZAR, K., MARINIS, S. I., KELLER, P. & WORD, R. A. 2007. Pelvic organ prolapse in fibulin-5 knockout mice: pregnancy-induced changes in elastic fiber homeostasis in mouse vagina. *Am J Pathol*, 170, 578-89.

- DRUTZ, H. P. & ALARAB, M. 2006. Pelvic organ prolapse: demographics and future growth prospects. *Int Urogynecol J Pelvic Floor Dysfunct*, 17 Suppl 1, S6-9.
- EDWARDS, S. L., ULRICH, D., WHITE, J. F., SU, K., ROSAMILIA, A., RAMSHAW, J. A., GARGETT, C. E. & WERKMEISTER, J. A. 2015. Temporal changes in the biomechanical properties of endometrial mesenchymal stem cell seeded scaffolds in a rat model. *Acta Biomater*, 13, 286-94.
- EDWARDS, S. L., WERKMEISTER, J. A., ROSAMILIA, A., RAMSHAW, J. A., WHITE, J. F. & GARGETT, C. E. 2013. Characterisation of clinical and newly fabricated meshes for pelvic organ prolapse repair. *J Mech Behav Biomed Mater*, 23, 53-61.
- EGGENHOFER, E. & HOOGDUIJN, M. J. 2012. Mesenchymal stem cell-educated macrophages. *Transplant Res*, 1, 12.
- ELFENBEIN, G. J. & SACKSTEIN, R. 2004. Primed marrow for autologous and allogeneic transplantation: a review comparing primed marrow to mobilized blood and steady-state marrow. *Exp Hematol*, 32, 327-39.
- ELLINGTON, D. R. & RICHTER, H. E. 2013a. Indications, contraindications, and complications of mesh in surgical treatment of pelvic organ prolapse. *Clin Obstet Gynecol*, 56, 276-88.
- ELLINGTON, D. R. & RICHTER, H. E. 2013b. The role of vaginal mesh procedures in pelvic organ prolapse surgery in view of complication risk. *Obstet Gynecol Int*, 2013, 356960.
- ELVIN, C. M., VUOCOLO, T., BROWNLEE, A. G., SANDO, L., HUSON, M. G., LIYOU, N. E., STOCKWELL, P. R., LYONS, R. E., KIM, M., EDWARDS, G. A., JOHNSON, G., MCFARLAND, G. A., RAMSHAW, J. A. & WERKMEISTER, J. A. 2010. A highly

- elastic tissue sealant based on photopolymerised gelatin. *Biomaterials*, 31, 8323-31.
- FALCO, E. E., ROTH, J. S. & FISHER, J. P. 2008. Skeletal muscle tissue engineering approaches to abdominal wall hernia repair. *Birth Defects Res C Embryo Today*, 84, 315-21.
- FDA 2008. FDA Public Health Notification: Serious Complications Associated with Transvaginal Placement of Surgical Mesh in Repair of Pelvic Organ Prolapse and Stress Urinary Incontinence.
- FDA. 2011. *UPDATE on Serious Complications Associated with Transvaginal Placement of Surgical Mesh for Pelvic Organ Prolapse: FDA Safety Communication* [Online]. Available: <https://www.fda.gov/medicaldevices/safety/alertsandnotices/ucm262435.htm> [Accessed].
- FEOLA, A., ENDO, M., URBANKOVA, I., VLACIL, J., DEPREST, T., BETTIN, S., KLOSTERHALFEN, B. & DEPREST, J. 2015. Host reaction to vaginally inserted collagen containing polypropylene implants in sheep. *Am J Obstet Gynecol*, 212, 474.e1-8.
- FISHER, M. B. & MAUCK, R. L. 2013. Tissue engineering and regenerative medicine: recent innovations and the transition to translation. *Tissue Eng Part B Rev*, 19, 1-13.
- FRANZ, S., RAMMELT, S., SCHARNWEBER, D. & SIMON, J. C. 2011. Immune responses to implants - a review of the implications for the design of immunomodulatory biomaterials. *Biomaterials*, 32, 6692-709.

- FRIEDENSTEIN, A. J., PETRAKOVA, K. V., KUROLESOVA, A. I. & FROLOVA, G. P. 1968. Heterotopic of bone marrow. Analysis of precursor cells for osteogenic and hematopoietic tissues. *Transplantation*, 6, 230-47.
- FUKANO, Y., USUI, M. L., UNDERWOOD, R. A., ISENHATH, S., MARSHALL, A. J., HAUCH, K. D., RATNER, B. D., OLERUD, J. E. & FLECKMAN, P. 2010. Epidermal and dermal integration into sphere-templated porous poly(2-hydroxyethyl methacrylate) implants in mice. *J Biomed Mater Res A*, 94, 1172-86.
- GARCIA-URENA, M. A., VEGA RUIZ, V., DIAZ GODOY, A., BAEZ PEREA, J. M., MARIN GOMEZ, L. M., CARNERO HERNANDEZ, F. J. & VELASCO GARCIA, M. A. 2007. Differences in polypropylene shrinkage depending on mesh position in an experimental study. *Am J Surg*, 193, 538-42.
- GARGETT, C. E. 2007a. Review article: stem cells in human reproduction. *Reproductive sciences (Thousand Oaks, Calif.)*, 14, 405.
- GARGETT, C. E. 2007b. Uterine stem cells: What is the evidence?
- GARGETT, C. E. & MASUDA, H. 2010. Adult stem cells in the endometrium. *Mol Hum Reprod*, 16, 818-34.
- GARGETT, C. E., SCHWAB, K., ZILLWOOD, R. M., NGUYEN, H. & WU, D. 2009. Isolation and Culture of Epithelial Progenitors and Mesenchymal Stem Cells from Human Endometrium. *Biology of Reproduction*, 80, 1136-1145.
- GARGETT, C. E., SCHWAB, K. E. & DEANE, J. A. 2016. Endometrial stem/progenitor cells: the first 10 years. *Hum Reprod Update*, 22, 137-63.

- GIGLIOBIANCO, G., REGUEROS, S. R., OSMAN, N. I., BISSOLI, J., BULLOCK, A. J., CHAPPLE, C. R. & MACNEIL, S. 2015. Biomaterials for pelvic floor reconstructive surgery: how can we do better? *Biomed Res Int*, 2015, 968087.
- GONZALEZ, R., FUGATE, K., MCCLUSKY, D., 3RD, RITTER, E. M., LEDERMAN, A., DILLEHAY, D., SMITH, C. D. & RAMSHAW, B. J. 2005. Relationship between tissue ingrowth and mesh contraction. *World J Surg*, 29, 1038-43.
- GRONTHOS, S., FRANKLIN, D. M., LEDDY, H. A., ROBEY, P. G., STORMS, R. W. & GIMBLE, J. M. 2001. Surface protein characterization of human adipose tissue-derived stromal cells. *J Cell Physiol*, 189, 54-63.
- GRONTHOS, S., MANKANI, M., BRAHIM, J., ROBEY, P. G. & SHI, S. 2000. Postnatal human dental pulp stem cells (DPSCs) in vitro and in vivo. *Proc. Natl. Acad. Sci. U. S. A.*, 97, 13625-13630.
- GUPTA, N., SU, X., POPOV, B., LEE, J. W., SERIKOV, V. & MATTHAY, M. A. 2007. Intrapulmonary delivery of bone marrow-derived mesenchymal stem cells improves survival and attenuates endotoxin-induced acute lung injury in mice. *J Immunol*, 179, 1855-63.
- GURUNG, S., WERKMEISTER, J. A. & GARGETT, C. E. 2015. Inhibition of Transforming Growth Factor-beta Receptor signaling promotes culture expansion of undifferentiated human Endometrial Mesenchymal Stem/stromal Cells. *Sci Rep*, 5, 15042.
- HANDEL, L. N., FRENKL, T. L. & KIM, Y. H. 2007. Results of cystocele repair: a comparison of traditional anterior colporrhaphy, polypropylene mesh and porcine dermis. *J Urol*, 178, 153-6; discussion 156.

- HAYLEN, B. T., FREEMAN, R. M., SWIFT, S. E., COSSON, M., DAVILA, G. W., DEPREST, J., DWYER, P. L., FATTON, B., KOCJANCIC, E., LEE, J., MAHER, C., PETRI, E., RIZK, D. E., SAND, P. K., SCHAEER, G. N. & WEBB, R. 2011. An International Urogynecological Association (IUGA)/International Continence Society (ICS) joint terminology and classification of the complications related directly to the insertion of prostheses (meshes, implants, tapes) and grafts in female pelvic floor surgery. *Neurourol Urodyn*, 30, 2-12.
- HIDA, N., NISHIYAMA, N., MIYOSHI, S., KIRA, S., SEGAWA, K., UYAMA, T., MORI, T., MIYADO, K., IKEGAMI, Y., CUI, C., KIYONO, T., KYO, S., SHIMIZU, T., OKANO, T., SAKAMOTO, M., OGAWA, S. & UMEZAWA, A. 2008. Novel cardiac precursor-like cells from human menstrual blood-derived mesenchymal cells. *Stem Cells*, 26, 1695-704.
- HILTUNEN, R., NIEMINEN, K., TAKALA, T., HEISKANEN, E., MERIKARI, M., NIEMI, K. & HEINONEN, P. K. 2007. Low-weight polypropylene mesh for anterior vaginal wall prolapse: a randomized controlled trial. *Obstet Gynecol*, 110, 455-62.
- HINOUL, P., OMBELET, W. U., BURGER, M. P. & ROOVERS, J. P. 2008. A prospective study to evaluate the anatomic and functional outcome of a transobturator mesh kit (prolifix anterior) for symptomatic cystocele repair. *J Minim Invasive Gynecol*, 15, 615-20.
- HO, M. H., HEYDARKHAN, S., VERNET, D., KOVANECH, I., FERRINI, M. G., BHATIA, N. N. & GONZALEZ-CADAVID, N. F. 2009. Stimulating vaginal repair in rats through skeletal muscle-derived stem cells seeded on small intestinal submucosal scaffolds. *Obstet Gynecol*, 114, 300-9.

- HUEBNER, M., HSU, Y. & FENNER, D. E. 2006. The use of graft materials in vaginal pelvic floor surgery. *Int J Gynaecol Obstet*, 92, 279-88.
- HUFFAKER, R. K., MUIR, T. W., RAO, A., BAUMANN, S. S., KUEHL, T. J. & PIERCE, L. M. 2008. Histologic response of porcine collagen-coated and uncoated polypropylene grafts in a rabbit vagina model. *Am J Obstet Gynecol*, 198, 582.e1-7.
- IONESCU, L. I., ALPHONSE, R. S., ARIZMENDI, N., MORGAN, B., ABEL, M., EATON, F., DUSZYK, M., VLIAGOFTIS, H., APRAHAMIAN, T. R., WALSH, K. & THEBAUD, B. 2012. Airway delivery of soluble factors from plastic-adherent bone marrow cells prevents murine asthma. *Am J Respir Cell Mol Biol*, 46, 207-16.
- JABBOUR, H. N., KELLY, R. W., FRASER, H. M. & CRITCHLEY, H. O. D. 2006. Endocrine regulation of menstruation. *Endocrine reviews*, 27, 17-46.
- JELOVSEK, J. E., MAHER, C. & BARBER, M. D. 2007. Pelvic organ prolapse. *Lancet*, 369, 1027-38.
- JENKINS, S. J., RUCKERL, D., COOK, P. C., JONES, L. H., FINKELMAN, F. D., VAN ROOIJEN, N., MACDONALD, A. S. & ALLEN, J. E. 2011. Local macrophage proliferation, rather than recruitment from the blood, is a signature of TH2 inflammation. *Science*, 332, 1284-8.
- KIM, J. & HEMATTI, P. 2009. Mesenchymal stem cell-educated macrophages: a novel type of alternatively activated macrophages. *Exp Hematol*, 37, 1445-53.
- KLINGE, U., JUNGE, K., STUMPF, M., AP, A. P. & KLOSTERHALFEN, B. 2002. Functional and morphological evaluation of a low-weight, monofilament polypropylene mesh for hernia repair. *J Biomed Mater Res*, 63, 129-36.

- KLOPFLEISCH, R. 2016. Macrophage reaction against biomaterials in the mouse model - Phenotypes, functions and markers. *Acta Biomater*, 43, 3-13.
- KNIGHT, K. M., MOALLI, P. A., NOLFI, A., PALCSEY, S., BARONE, W. R. & ABRAMOWITCH, S. D. 2016. Impact of parity on ewe vaginal mechanical properties relative to the nonhuman primate and rodent. *Int Urogynecol J*, 27, 1255-63.
- KOHLI, N. 2012. Controversies in utilization of transvaginal mesh. *Curr Opin Obstet Gynecol*, 24, 337-42.
- KOHLI, N. & MIKLOS, J. R. 2003. Dermal graft-augmented rectocele repair. *Int Urogynecol J Pelvic Floor Dysfunct*, 14, 146-9.
- KONSTANTINOVIC, M. L., LAGAE, P., ZHENG, F., VERBEKEN, E. K., DE RIDDER, D. & DEPREST, J. A. 2005. Comparison of host response to polypropylene and non-cross-linked porcine small intestine serosal-derived collagen implants in a rat model. *Bjog*, 112, 1554-60.
- KONSTANTINOVIC, M. L., PILLE, E., MALINOWSKA, M., VERBEKEN, E., DE RIDDER, D. & DEPREST, J. 2007. Tensile strength and host response towards different polypropylene implant materials used for augmentation of fascial repair in a rat model. *Int Urogynecol J Pelvic Floor Dysfunct*, 18, 619-26.
- KYURKCHIEV, D., BOCHEV, I., IVANOVA-TODOROVA, E., MOURDJEVA, M., ORESHKOVA, T., BELEMEZOVA, K. & KYURKCHIEV, S. 2014. Secretion of immunoregulatory cytokines by mesenchymal stem cells. *World J Stem Cells*, 6, 552-70.

- LABOW, R. S., SA, D., MATHESON, L. A. & SANTERRE, J. P. 2005. Polycarbonate-urethane hard segment type influences esterase substrate specificity for human-macrophage-mediated biodegradation. *J Biomater Sci Polym Ed*, 16, 1167-77.
- LANGER, R. & VACANTI, J. 2016. Advances in tissue engineering. *J Pediatr Surg*, 51, 8-12.
- LANGER, R. & VACANTI, J. P. 1993. Tissue engineering. *Science*, 260, 920-6.
- LE BLANC, K. & DAVIES, L. C. 2015. Mesenchymal stromal cells and the innate immune response. *Immunol Lett*, 168, 140-6.
- LE BLANC, K. & MOUGIAKAKOS, D. 2012. Multipotent mesenchymal stromal cells and the innate immune system. *Nat Rev Immunol*, 12, 383-96.
- LE BLANC, K., TAMMIK, L., SUNDBERG, B., HAYNESWORTH, S. E. & RINGDEN, O. 2003. Mesenchymal stem cells inhibit and stimulate mixed lymphocyte cultures and mitogenic responses independently of the major histocompatibility complex. *Scand J Immunol*, 57, 11-20.
- LIU, X., ZHAO, Y., PAWLYK, B., DAMASER, M. & LI, T. 2006. Failure of elastic fiber homeostasis leads to pelvic floor disorders. *Am J Pathol*, 168, 519-28.
- LO, T. S., CORTES, E. F., WU, P. Y., TAN, Y. L., AL-KHARABSHEH, A. & PUE, L. B. 2016. Assessment of collagen versus non collagen coated anterior vaginal mesh in pelvic reconstructive surgery: prospective study. *Eur J Obstet Gynecol Reprod Biol*, 198, 138-44.
- LUKACZ, E. S., LAWRENCE, J. M., CONTRERAS, R., NAGER, C. W. & LUBER, K. M. 2006. Parity, mode of delivery, and pelvic floor disorders. *Obstet Gynecol*, 107, 1253-60.

- LUZ-CRAWFORD, P., TORRES, M. J., NOEL, D., FERNANDEZ, A., TOUPET, K., ALCAYAGA-MIRANDA, F., TEJEDOR, G., JORGENSEN, C., ILLANES, S. E., FIGUEROA, F. E., DJOUAD, F. & KHOURY, M. 2016. The immunosuppressive signature of menstrual blood mesenchymal stem cells entails opposite effects on experimental arthritis and graft versus host diseases. *Stem Cells*, 34, 456-69.
- MADDEN, L. R., MORTISEN, D. J., SUSSMAN, E. M., DUPRAS, S. K., FUGATE, J. A., CUY, J. L., HAUCH, K. D., LAFLAMME, M. A., MURRY, C. E. & RATNER, B. D. 2010. Proangiogenic scaffolds as functional templates for cardiac tissue engineering. *Proc Natl Acad Sci U S A*, 107, 15211-6.
- MAGGINI, J., MIRKIN, G., BOGNANNI, I., HOLMBERG, J., PIAZZON, I. M., NEPOMNASCHY, I., COSTA, H., CANONES, C., RAIDEN, S., VERMEULEN, M. & GEFFNER, J. R. 2010. Mouse bone marrow-derived mesenchymal stromal cells turn activated macrophages into a regulatory-like profile. *PLoS One*, 5, e9252.
- MAHER, C., FEINER, B., BAESSLER, K. & SCHMID, C. 2013. Surgical management of pelvic organ prolapse in women. *Cochrane Database Syst Rev*, 4, Cd004014.
- MALGIERI, A., KANTZARI, E., PATRIZI, M. P. & GAMBARDELLA, S. 2010. Bone marrow and umbilical cord blood human mesenchymal stem cells: state of the art. *Int J Clin Exp Med*, 3, 248-69.
- MASUDA, H., ANWAR, S. & HJ, B. 2012. A Novel Marker of Human Endometrial Mesenchymal Stem-Like Cells. *Cell Transplantation*.
- MATSUSHIMA, A., KOTOBUKI, N., TADOKORO, M., KAWATE, K., YAJIMA, H., TAKAKURA, Y. & OHGUSHI, H. 2009. In vivo osteogenic capability of human

- mesenchymal cells cultured on hydroxyapatite and on beta-tricalcium phosphate. *Artif Organs*, 33, 474-81.
- MECHAM, R. P., BROEKELMANN, T. J., FLISZAR, C. J., SHAPIRO, S. D., WELGUS, H. G. & SENIOR, R. M. 1997. Elastin degradation by matrix metalloproteinases. Cleavage site specificity and mechanisms of elastolysis. *J Biol Chem*, 272, 18071-6.
- MEI, S. H., HAITSMA, J. J., DOS SANTOS, C. C., DENG, Y., LAI, P. F., SLUTSKY, A. S., LILES, W. C. & STEWART, D. J. 2010. Mesenchymal stem cells reduce inflammation while enhancing bacterial clearance and improving survival in sepsis. *Am J Respir Crit Care Med*, 182, 1047-57.
- MENG, X., ICHIM, T. E., ZHONG, J., ROGERS, A., YIN, Z., JACKSON, J., WANG, H., GE, W., BOGIN, V., CHAN, K. W., THEBAUD, B. & RIORDAN, N. H. 2007. Endometrial regenerative cells: a novel stem cell population. *J Transl Med*, 5, 57.
- MESCHIA, M., PIFAROTTI, P., BERNASCONI, F., MAGATTI, F., RIVA, D. & KOCJANCIC, E. 2007. Porcine skin collagen implants to prevent anterior vaginal wall prolapse recurrence: a multicenter, randomized study. *J Urol*, 177, 192-5.
- MEYERROSE, T. E., DE UGARTE, D. A., HOFLING, A. A., HERRBRICH, P. E., CORDONNIER, T. D., SHULTZ, L. D., EAGON, J. C., WIRTHLIN, L., SANDS, M. S., HEDRICK, M. A. & NOLTA, J. A. 2007. In vivo distribution of human adipose-derived mesenchymal stem cells in novel xenotransplantation models. *Stem Cells*, 25, 220-7.

- MIEDEL, A., TEGERSTEDT, G., MORLIN, B. & HAMMARSTROM, M. 2008. A 5-year prospective follow-up study of vaginal surgery for pelvic organ prolapse. *Int Urogynecol J Pelvic Floor Dysfunct*, 19, 1593-601.
- MILANI, A. L., HINOUL, P., GAULD, J. M., SIKIRICA, V., VAN DRIE, D. & COSSON, M. 2011. Trocar-guided mesh repair of vaginal prolapse using partially absorbable mesh: 1 year outcomes. *Am J Obstet Gynecol*, 204, 74.e1-8.
- MILANI, R., SALVATORE, S., SOLIGO, M., PIFAROTTI, P., MESCHIA, M. & CORTESE, M. 2005. Functional and anatomical outcome of anterior and posterior vaginal prolapse repair with prolene mesh. *Bjog*, 112, 107-11.
- MOALLI, P. A., HOWDEN, N. S., LOWDER, J. L., NAVARRO, J., DEBES, K. M., ABRAMOWITCH, S. D. & WOO, S. L. 2005a. A rat model to study the structural properties of the vagina and its supportive tissues. *Am J Obstet Gynecol*, 192, 80-8.
- MOALLI, P. A., JONES IVY, S., MEYN, L. A. & ZYCZYNSKI, H. M. 2003. Risk factors associated with pelvic floor disorders in women undergoing surgical repair. *Obstet Gynecol*, 101, 869-74.
- MOALLI, P. A., SHAND, S. H., ZYCZYNSKI, H. M., GORDY, S. C. & MEYN, L. A. 2005b. Remodeling of vaginal connective tissue in patients with prolapse. *Obstet Gynecol*, 106, 953-63.
- MORRISON, S. J., SHAH, N. M. & ANDERSON, D. J. 1997. Regulatory mechanisms in stem cell biology. *Cell*, 88, 287-98.

- MURPHY, M. B., MONCIVAIS, K. & CAPLAN, A. I. 2013. Mesenchymal stem cells: environmentally responsive therapeutics for regenerative medicine. *Exp Mol Med*, 45, e54.
- MURPHY, M. P., WANG, H., PATEL, A. N., KAMBHAMPATI, S., ANGLE, N., CHAN, K., MARLEAU, A. M., PYSZNIAK, A., CARRIER, E., ICHIM, T. E. & RIORDAN, N. H. 2008. Allogeneic endometrial regenerative cells: an "Off the shelf solution" for critical limb ischemia? *J Transl Med*, 6, 45.
- NEMETH, K., LEELAHAVANICHKUL, A., YUEN, P. S., MAYER, B., PARMELEE, A., DOI, K., ROBEY, P. G., LEELAHAVANICHKUL, K., KOLLER, B. H., BROWN, J. M., HU, X., JELINEK, I., STAR, R. A. & MEZEY, E. 2009. Bone marrow stromal cells attenuate sepsis via prostaglandin E(2)-dependent reprogramming of host macrophages to increase their interleukin-10 production. *Nat Med*, 15, 42-9.
- NIEMINEN, K., HILTUNEN, R., TAKALA, T., HEISKANEN, E., MERIKARI, M., NIEMI, K. & HEINONEN, P. K. 2010. Outcomes after anterior vaginal wall repair with mesh: a randomized, controlled trial with a 3 year follow-up. *Am J Obstet Gynecol*, 203, 235.e1-8.
- NOLD, M. F., MANGAN, N. E., RUDLOFF, I., CHO, S. X., SHARIATIAN, N., SAMARASINGHE, T. D., SKUZA, E. M., PEDERSEN, J., VELDMAN, A., BERGER, P. J. & NOLD-PETRY, C. A. 2013. Interleukin-1 receptor antagonist prevents murine bronchopulmonary dysplasia induced by perinatal inflammation and hyperoxia. *Proc Natl Acad Sci U S A*, 110, 14384-9.

- NOLD, M. F., NOLD-PETRY, C. A., ZEPP, J. A., PALMER, B. E., BUFLER, P. & DINARELLO, C. A. 2010. IL-37 is a fundamental inhibitor of innate immunity. *Nat Immunol*, 11, 1014-22.
- NYGAARD, I., BARBER, M. D., BURGIO, K. L., KENTON, K., MEIKLE, S., SCHAFFER, J., SPINO, C., WHITEHEAD, W. E., WU, J. & BRODY, D. J. 2008. Prevalence of symptomatic pelvic floor disorders in US women. *Jama*, 300, 1311-6.
- NYGAARD, I. E., MCCREERY, R., BRUBAKER, L., CONNOLLY, A., CUNDIFF, G., WEBER, A. M. & ZYCZYNSKI, H. 2004. Abdominal sacrocolpopexy: a comprehensive review. *Obstet Gynecol*, 104, 805-23.
- OHGUSHI, H., KOTOBUKI, N., FUNAOKA, H., MACHIDA, H., HIROSE, M., TANAKA, Y. & TAKAKURA, Y. 2005. Tissue engineered ceramic artificial joint--ex vivo osteogenic differentiation of patient mesenchymal cells on total ankle joints for treatment of osteoarthritis. *Biomaterials*, 26, 4654-61.
- OLSEN, A. L., SMITH, V., BERGSTROM, J., COLLING, J. & CLARK, A. L. 1997. Epidemiology of surgically managed pelvic organ prolapse and urinary incontinence. *Obstet. Gynecol.*, 89, 501-506.
- OTTO, L. N., SLAYDEN, O. D., CLARK, A. L. & BRENNER, R. M. 2002. The rhesus macaque as an animal model for pelvic organ prolapse. *Am J Obstet Gynecol*, 186, 416-21.
- PALADINI, D., DI SPIEZIO SARDO, A., MANDATO, V. D., GUERRA, G., BIFULCO, G., MAURIELLO, S. & NAPPI, C. 2007. Association of cutis laxa and genital prolapse: a case report. *Int Urogynecol J Pelvic Floor Dysfunct*, 18, 1367-70.

- PASCUAL, G., RODRIGUEZ, M., GOMEZ-GIL, V., GARCIA-HONDUVILLA, N., BUJAN, J. & BELLON, J. M. 2008. Early tissue incorporation and collagen deposition in lightweight polypropylene meshes: bioassay in an experimental model of ventral hernia. *Surgery*, 144, 427-35.
- PATEL, A. N., PARK, E., KUZMAN, M., BENETTI, F., SILVA, F. J. & ALLICKSON, J. G. 2008. Multipotent menstrual blood stromal stem cells: isolation, characterization, and differentiation. *Cell Transplant*, 17, 303-11.
- PEPPAS, G., GKEGKES, I. D., MAKRIS, M. C. & FALAGAS, M. E. 2010. Biological mesh in hernia repair, abdominal wall defects, and reconstruction and treatment of pelvic organ prolapse: a review of the clinical evidence. *Am Surg*, 76, 1290-9.
- PERON, J. P., JAZEDJE, T., BRANDAO, W. N., PERIN, P. M., MALUF, M., EVANGELISTA, L. P., HALPERN, S., NISENBAUM, M. G., CZERESNIA, C. E., ZATZ, M., CAMARA, N. O. & RIZZO, L. V. 2012. Human endometrial-derived mesenchymal stem cells suppress inflammation in the central nervous system of EAE mice. *Stem Cell Rev*, 8, 940-52.
- PERSU, C., CHAPPLE, C. R., CAUNI, V., GUTUE, S. & GEAVLETE, P. 2011. Pelvic Organ Prolapse Quantification System (POP-Q) - a new era in pelvic prolapse staging. *J Med Life*, 4, 75-81.
- PITTENGER, M. F., MACKAY, A. M., BECK, S. C., JAISWAL, R. K., DOUGLAS, R., MOSCA, J. D., MOORMAN, M. A., SIMONETTI, D. W., CRAIG, S. & MARSHAK, D. R. 1999. Multilineage potential of adult human mesenchymal stem cells. *Science*, 284, 143-7.

- PROCKOP, D. J. 2013. Concise review: two negative feedback loops place mesenchymal stem/stromal cells at the center of early regulators of inflammation. *Stem Cells*, 31, 2042-6.
- PROCKOP, D. J. & OH, J. Y. 2012. Medical therapies with adult stem/progenitor cells (MSCs): a backward journey from dramatic results in vivo to the cellular and molecular explanations. *J Cell Biochem*, 113, 1460-9.
- QUALLS, J. E., KAPLAN, A. M., VAN ROOIJEN, N. & COHEN, D. A. 2006. Suppression of experimental colitis by intestinal mononuclear phagocytes. *J Leukoc Biol*, 80, 802-15.
- RIDGEWAY, B., CHEN, C. C. & PARAISO, M. F. 2008. The use of synthetic mesh in pelvic reconstructive surgery. *Clin Obstet Gynecol*, 51, 136-52.
- ROMAN, S., MANGERA, A., OSMAN, N. I., BULLOCK, A. J., CHAPPLE, C. R. & MACNEIL, S. 2014. Developing a tissue engineered repair material for treatment of stress urinary incontinence and pelvic organ prolapse-which cell source? *Neurourol Urodyn*, 33, 531-7.
- RORTVEIT, G., SUBAK, L. L., THOM, D. H., CREASMAN, J. M., VITTINGHOFF, E., VAN DEN EEDEN, S. K. & BROWN, J. S. 2010. Urinary incontinence, fecal incontinence and pelvic organ prolapse in a population-based, racially diverse cohort: prevalence and risk factors. *Female Pelvic Med Reconstr Surg*, 16, 278-83.
- RUDNICKI, M., LAURIKAINEN, E., POGOSEAN, R., KINNE, I., JAKOBSSON, U. & TELEMANN, P. 2016. A 3-year follow-up after anterior colporrhaphy compared with

- collagen-coated transvaginal mesh for anterior vaginal wall prolapse: a randomised controlled trial. *Bjog*, 123, 136-42.
- SACCHETTI, B., FUNARI, A., MICHIEZI, S., DI CESARE, S., PIERSANTI, S., SAGGIO, I., TAGLIAFICO, E., FERRARI, S., ROBEY, P. G., RIMINUCCI, M. & BIANCO, P. 2007. Self-renewing osteoprogenitors in bone marrow sinusoids can organize a hematopoietic microenvironment. *Cell*, 131, 324-36.
- SCHIMPF, M. O., ABED, H., SANSES, T., WHITE, A. B., LOWENSTEIN, L., WARD, R. M., SUNG, V. W., BALK, E. M. & MURPHY, M. 2016. Graft and Mesh Use in Transvaginal Prolapse Repair: A Systematic Review. *Obstet Gynecol*, 128, 81-91.
- SCHINDELIN, J., ARGANDA-CARRERAS, I., FRISE, E., KAYNIG, V., LONGAIR, M., PIETZSCH, T., PREIBISCH, S., RUEDEN, C., SAALFELD, S., SCHMID, B., TINEVEZ, J. Y., WHITE, D. J., HARTENSTEIN, V., ELICEIRI, K., TOMANCAK, P. & CARDONA, A. 2012. Fiji: an open-source platform for biological-image analysis. *Nat Methods*, 9, 676-82.
- SCHWAB, K. E., CHAN, R. W. S. & GARGETT, C. E. 2005. Putative stem cell activity of human endometrial epithelial and stromal cells during the menstrual cycle. *Fertility and Sterility*, 84, 1124-1130.
- SCHWAB, K. E. & GARGETT, C. E. 2007. Co-expression of two perivascular cell markers isolates mesenchymal stem-like cells from human endometrium. *Hum Reprod*, 22, 2903-11.
- SCHWERTNER-TIEPELMANN, N., THAKAR, R., SULTAN, A. H. & TUNN, R. 2012. Obstetric levator ani muscle injuries: current status. *Ultrasound Obstet Gynecol*, 39, 372-83.

- SHAFIEE, A. & ATALA, A. 2016. Tissue Engineering: Toward a New Era of Medicine. *Annu Rev Med*.
- SHAFIEE, A. & ATALA, A. 2017. Tissue Engineering: Toward a New Era of Medicine. *Annu Rev Med*, 68, 29-40.
- SHULTZ, L. D., ISHIKAWA, F. & GREINER, D. L. 2007. Humanized mice in translational biomedical research. *Nat Rev Immunol*, 7, 118-30.
- SINGER, N. G. & CAPLAN, A. I. 2011. Mesenchymal stem cells: mechanisms of inflammation. *Annu Rev Pathol*, 6, 457-78.
- SMART, N. J., BRYAN, N. & HUNT, J. A. 2012. A scientific evidence for the efficacy of biologic implants for soft tissue reconstruction. *Colorectal Dis*, 14 Suppl 3, 1-6.
- SMITH, F. J., HOLMAN, C. D., MOORIN, R. E. & TSOKOS, N. 2010a. Lifetime risk of undergoing surgery for pelvic organ prolapse. *Obstet Gynecol*, 116, 1096-100.
- SMITH, F. J., HOLMAN, C. D. J., MOORIN, R. E. & TSOKOS, N. 2010b. Lifetime Risk of Undergoing Surgery for Pelvic Organ Prolapse. *Obstetrics & Gynecology*, 116, 1096-1100.
- SNOOKS, S. J., SETCHELL, M., SWASH, M. & HENRY, M. M. 1984. Injury to innervation of pelvic floor sphincter musculature in childbirth. *Lancet*, 2, 546-50.
- SOCIETY, T. R. 2017. *Obstract: interpreting the abstraction of tissue regeneration and re-engineering of female pelvic floor disorders in clinical practice* [Online]. Available: <https://royalsociety.org/science-events-and-lectures/2017/10/pelvic-floor/> [Accessed].

- SODERBERG, M. W., FALCONER, C., BYSTROM, B., MALMSTROM, A. & EKMAN, G. 2004. Young women with genital prolapse have a low collagen concentration. *Acta Obstet Gynecol Scand*, 83, 1193-8.
- SOKOL, A. I., IGLESIA, C. B., KUDISH, B. I., GUTMAN, R. E., SHVEIKY, D., BERCIK, R. & SOKOL, E. R. 2012. One-year objective and functional outcomes of a randomized clinical trial of vaginal mesh for prolapse. *American Journal of Obstetrics and Gynecology*, 206, 86.e1-86.e9.
- SOLCHAGA, L. A., YOO, J. U., LUNDBERG, M., DENNIS, J. E., HUIBREGTSE, B. A., GOLDBERG, V. M. & CAPLAN, A. I. 2000. Hyaluronan-based polymers in the treatment of osteochondral defects. *J Orthop Res*, 18, 773-80.
- SOTIROPOULOU, P. A., PEREZ, S. A., GRITZAPIS, A. D., BAXEVANIS, C. N. & PAPAMICHAIL, M. 2006. Interactions between human mesenchymal stem cells and natural killer cells. *Stem Cells*, 24, 74-85.
- SPAGGIARI, G. M., CAPOBIANCO, A., BECCHETTI, S., MINGARI, M. C. & MORETTA, L. 2006. Mesenchymal stem cell-natural killer cell interactions: evidence that activated NK cells are capable of killing MSCs, whereas MSCs can inhibit IL-2-induced NK-cell proliferation. *Blood*, 107, 1484-90.
- SPENCER, T. E., HAYASHI, K., HU, J. & CARPENTER, K. D. 2005. Comparative developmental biology of the mammalian uterus. *Curr Top Dev Biol*, 68, 85-122.
- SRIDHARAN, R., CAMERON, A. R., KELLY, D. J., KEARNEY, C. J. & O'BRIEN, F. J. 2015a. Biomaterial based modulation of macrophage polarization: a review and suggested design principles. *Materials Today*, 18, 313.

- SRIDHARAN, R., CAMERON, A. R., KELLY, D. J., KEARNEY, C. J. & O'BRIEN, F. J. 2015b. Biomaterial based modulation of macrophage polarization: a review and suggested design principles. *Materials Today*, 18, 313-325.
- STANFORD, E. J., MATTOX, T. F. & PUGH, C. J. 2011. Outcomes and complications of transvaginal and abdominal custom-shaped light-weight polypropylene mesh used in repair of pelvic organ prolapse. *J Minim Invasive Gynecol*, 18, 64-7.
- SU, K., EDWARDS, S. L., TAN, K. S., WHITE, J. F., KANDEL, S., RAMSHAW, J. A., GARGETT, C. E. & WERKMEISTER, J. A. 2014. Induction of endometrial mesenchymal stem cells into tissue-forming cells suitable for fascial repair. *Acta Biomater*, 10, 5012-20.
- SULTAN, A. H., KAMM, M. A. & HUDSON, C. N. 1994. Pudendal nerve damage during labour: prospective study before and after childbirth. *Br J Obstet Gynaecol*, 101, 22-8.
- SUNDERKOTTER, C., NIKOLIC, T., DILLON, M. J., VAN ROOIJEN, N., STEHLING, M., DREVETS, D. A. & LEENEN, P. J. 2004. Subpopulations of mouse blood monocytes differ in maturation stage and inflammatory response. *J Immunol*, 172, 4410-7.
- TANG, L., JENNINGS, T. A. & EATON, J. W. 1998. Mast cells mediate acute inflammatory responses to implanted biomaterials. *Proc Natl Acad Sci U S A*, 95, 8841-6.
- TIJDINK, M. M., VIERHOUT, M. E., HEESAKKERS, J. P. & WITHAGEN, M. I. 2011. Surgical management of mesh-related complications after prior pelvic floor reconstructive surgery with mesh. *Int Urogynecol J*, 22, 1395-404.

- ULRICH, D., EDWARDS, S. & SU, K. 2014a. Human endometrial mesenchymal stem cells modulate the tissue response and mechanical behavior of polyamide mesh implants for pelvic organ prolapse repair. *Tissue Eng Part A*, 20, 785-798.
- ULRICH, D., EDWARDS, S., SU, K., TAN, K. S., WHITE, J., RAMSHAW, J., LO, C., ROSAMILIA, A., WERKMEISTER, J. & GARGETT, C. E. 2014b. Human Endometrial Mesenchymal Stem Cells Modulate the Tissue Response and Mechanical Behavior of Polyamide Mesh Implants for Pelvic Organ Prolapse Repair. *Tissue Eng. Part A*, 20, 785-798.
- ULRICH, D., EDWARDS, S. L., LETOUZEY, V., SU, K., WHITE, J. F., ROSAMILIA, A., GARGETT, C. E. & WERKMEISTER, J. A. 2014c. Regional variation in tissue composition and biomechanical properties of postmenopausal ovine and human vagina. *PLoS One*, 9, e104972.
- ULRICH, D., EDWARDS, S. L., WHITE, J. F., SUPIT, T., RAMSHAW, J. A., LO, C., ROSAMILIA, A., WERKMEISTER, J. A. & GARGETT, C. E. 2012. A preclinical evaluation of alternative synthetic biomaterials for fascial defect repair using a rat abdominal hernia model. *PLoS One*, 7, e50044.
- ULRICH, D., MURALITHARAN, R. & GARGETT, C. E. 2013a. Toward the use of endometrial and menstrual blood mesenchymal stem cells for cell-based therapies. *Expert Opinion on Biological Therapy*, 13, 1387-1400.
- ULRICH, D., MURALITHARAN, R. & GARGETT, C. E. 2013b. Toward the use of endometrial and menstrual blood mesenchymal stem cells for cell-based therapies. *Expert Opin Biol Ther*, 13, 1387-400.

- ULRICH, D., TAN, K. S., DEANE, J., SCHWAB, K., CHEONG, A., ROSAMILIA, A. & GARGETT, C. E. 2014d. Mesenchymal stem/stromal cells in post-menopausal endometrium. *Hum Reprod*, 29, 1895-905.
- UNDERWOOD, R. A., USUI, M. L., ZHAO, G., HAUCH, K. D., TAKENO, M. M., RATNER, B. D., MARSHALL, A. J., SHI, X., OLERUD, J. E. & FLECKMAN, P. 2011. Quantifying the effect of pore size and surface treatment on epidermal incorporation into percutaneously implanted sphere-templated porous biomaterials in mice. *J Biomed Mater Res A*, 98, 499-508.
- URBANKOVA, I., VDOVIAKOVA, K., RYNKEVIC, R., SINDHWANI, N., DEPREST, D., FEOLA, A., HERIJGERS, P., KROFTA, L. & DEPREST, J. 2017. Comparative Anatomy of the Ovine and Female Pelvis. *Gynecol Obstet Invest*.
- VACANTI, J. P. & LANGER, R. 1999. Tissue engineering: the design and fabrication of living replacement devices for surgical reconstruction and transplantation. *Lancet*, 354 Suppl 1, Si32-4.
- VALENTIN, J. E., STEWART-AKERS, A. M., GILBERT, T. W. & BADYLAK, S. F. 2009. Macrophage participation in the degradation and remodeling of extracellular matrix scaffolds. *Tissue Eng Part A*, 15, 1687-94.
- VILALTA, M., DEGANO, I. R., BAGO, J., GOULD, D., SANTOS, M., GARCIA-ARRANZ, M., AYATS, R., FUSTER, C., CHERNAJOVSKY, Y., GARCIA-OLMO, D., RUBIO, N. & BLANCO, J. 2008. Biodistribution, long-term survival, and safety of human adipose tissue-derived mesenchymal stem cells transplanted in nude mice by high sensitivity non-invasive bioluminescence imaging. *Stem Cells Dev*, 17, 993-1003.

- WALKER, G. J. & GUNASEKERA, P. 2011. Pelvic organ prolapse and incontinence in developing countries: review of prevalence and risk factors. *Int Urogynecol J*, 22, 127-35.
- WANG, Y., CHEN, X., CAO, W. & SHI, Y. 2014. Plasticity of mesenchymal stem cells in immunomodulation: pathological and therapeutic implications. *Nat Immunol*, 15, 1009-16.
- WEISSER, S. B., BRUGGER, H. K., VOGLMAIER, N. S., MCLARREN, K. W., VAN ROOIJEN, N. & SLY, L. M. 2011. SHIP-deficient, alternatively activated macrophages protect mice during DSS-induced colitis. *J Leukoc Biol*, 90, 483-92.
- WEISSER, S. B., VAN ROOIJEN, N. & SLY, L. M. 2012. Depletion and reconstitution of macrophages in mice. *J Vis Exp*, 4105.
- WINTERS, J. C., FITZGERALD, M. P. & BARBER, M. D. 2006. The use of synthetic mesh in female pelvic reconstructive surgery. *BJU Int*, 98 Suppl 1, 70-6; discussion 77.
- WITHAGEN, M. I., MILANI, A. L., DEN BOON, J., VERVEST, H. A. & VIERHOUT, M. E. 2011. Trocar-guided mesh compared with conventional vaginal repair in recurrent prolapse: a randomized controlled trial. *Obstet Gynecol*, 117, 242-50.
- WOESSNER, J. F. & BREWER, T. H. 1963. FORMATION AND BREAKDOWN OF COLLAGEN AND ELASTIN IN THE HUMAN UTERUS DURING PREGNANCY AND POST-PARTUM INVOLUTION. *Biochem J*, 89, 75-82.
- WOLF, M. T., CARRUTHERS, C. A., DEARTH, C. L., CRAPO, P. M., HUBER, A., BURNSED, O. A., LONDONO, R., JOHNSON, S. A., DALY, K. A., STAHL, E. C., FREUND, J. M., MEDBERRY, C. J., CAREY, L. E., NIEPONICE, A., AMOROSO, N. J. & BADYLAK, S. F. 2014. Polypropylene surgical mesh coated with

- extracellular matrix mitigates the host foreign body response. *J Biomed Mater Res A*, 102, 234-46.
- WU, J. M., HUNDLEY, A. F., FULTON, R. G. & MYERS, E. R. 2009. Forecasting the prevalence of pelvic floor disorders in U.S. Women: 2010 to 2050. *Obstet Gynecol*, 114, 1278-83.
- XIA, Z. D., ZHU, T. B., DU, J. Y., ZHENG, Q. X., WANG, L., LI, S. P., CHANG, C. Y. & FANG, S. Y. 1994. Macrophages in degradation of collagen/hydroxylapatite(CHA), beta-tricalcium phosphate ceramics (TCP) artificial bone graft. An in vivo study. *Chin Med J (Engl)*, 107, 845-9.
- YOUNG, N., ROSAMILIA, A., ARKWRIGHT, J., LEE, J., DAVIES-TUCK, M., MELENDEZ, J., WERKMEISTER, J. & GARGETT, C. E. 2016. Vaginal wall weakness in parous ewes: a potential preclinical model of pelvic organ prolapse. *Int Urogynecol J*.
- YOUNG, N., ROSAMILIA, A., ARKWRIGHT, J., LEE, J., DAVIES-TUCK, M., MELENDEZ, J., WERKMEISTER, J. & GARGETT, C. E. 2017. Vaginal wall weakness in parous ewes: a potential preclinical model of pelvic organ prolapse. *Int Urogynecol J*, 28, 999-1004.
- ZENG, D., LAN, F., HOFFMANN, P. & STROBER, S. 2004. Suppression of graft-versus-host disease by naturally occurring regulatory T cells. *Transplantation*, 77, S9-s11.
- ZHAO, Y., ZHANG, Z., WANG, J., YIN, P., ZHOU, J., ZHEN, M., CUI, W., XU, G., YANG, D. & LIU, Z. 2012. Abdominal hernia repair with a decellularized dermal scaffold seeded with autologous bone marrow-derived mesenchymal stem cells. *Artif Organs*, 36, 247-55.

Appendix

Identification and Characterization of Human Endometrial Mesenchymal Stem/Stromal Cells and Their Potential for Cellular Therapy

SAEEDH DARZI,^{a,b} JEROME A. WERKMEISTER,^{b,c} JAMES A. DEANE,^{a,b} CAROLINE E. GARGETT^{a,b}

^aThe Ritchie Centre, Hudson Institute of Medical Research, Clayton, Victoria, Australia; ^bDepartment of Obstetrics and Gynaecology, Monash University, Clayton, Victoria, Australia; ^cCommonwealth Scientific and Industrial Research Organisation, Clayton, Victoria, Australia

SUMMARY

Human endometrium is a highly regenerative tissue, undergoing more than 400 cycles of proliferation, differentiation, and shedding during a woman's reproductive life. Adult stem cells, including mesenchymal stem/stromal cells (MSCs), are likely responsible for the immense cellular turnover in human endometrium. The unique properties of MSCs, including high proliferative ability, self-renewal, differentiation to mesodermal lineages, secretion of angiogenic factors, and many other growth-promoting factors make them useful candidates for cellular therapy and tissue engineering. In this review, we summarize the identification and characterization of newly discovered MSCs from the human endometrium: their properties, the surface markers used for their prospective isolation, their perivascular location in the endometrium, and their potential application in cellular therapies. *STEM CELLS TRANSLATIONAL MEDICINE* 2016;5:1127–1132

SIGNIFICANCE

The endometrium, or the lining of uterus, has recently been identified as a new and accessible source of mesenchymal stem cells, which can be obtained without anesthesia. Endometrial mesenchymal stem cells have comparable properties to bone marrow and adipose tissue mesenchymal stem cells. Endometrial mesenchymal stem cells are purified with known and novel perivascular surface markers and are currently under investigation for their potential use in cellular therapy for several clinical conditions with significant burden of disease.

INTRODUCTION

Mesenchymal stem/stromal cells (MSCs) are attractive candidates for cellular therapies. Initial enthusiasm centered on the capacity of MSCs to differentiate into mesodermal lineages and generate skeletal tissues [1]. It is now recognized that MSCs act in a paracrine manner, secreting multiple factors that stimulate angiogenesis, reduce fibrosis, and promote endogenous cell proliferation to effect tissue repair [2]. The immunomodulatory and anti-inflammatory properties of MSCs are also appealing [3, 4] and have been exploited for the treatment of graft-versus-host disease [4, 5] and to reduce graft failure in haploidentical transplants [3]; however, MSCs appear less effective in humans than in rodent preclinical studies [6].

The ability of systemically administered MSCs to home to injured tissues to exert their paracrine actions is another attractive feature [7]. By exerting immunomodulatory effects, MSCs have been used for bone and cartilage regeneration in osteoporotic fracture and arthritis, and also for repair of cardiac tissue after myocardial infarction [3], seemingly acting in a paracrine manner rather than directly differentiating into specialized cells to regenerate new tissue [8]. Despite these promising findings on the utility of

MSCs as a cell-based therapy, more scientific studies are required to better characterize the MSC populations used (Table 1) [9].

Limitations on the clinical use of MSCs include their rarity in tissues necessitating in vitro expansion [10], donor age affecting their proliferative capacity [11], and invasive methods required for harvesting bone-marrow aspirates. Apart from bone marrow, MSCs for therapeutic use are commonly sourced from adipose and placental tissues using a variety of markers (Table 1).

Adipose tissue has recently emerged as an attractive source of MSCs for cell-based therapies, readily available in modern society and frequently harvested by relatively invasive liposuction procedures. Adipose-derived stem cells (ASCs) (Table 1) are relatively abundant in the stromal vascular fraction of fat tissue and are often used without culturing [12].

Human placenta also offers an easily accessible source of MSCs as it is medical waste tissue. Maternal MSCs are generally derived from the placental tissue [13], whereas fetal MSCs are obtained from the umbilical cord, amniotic membrane, and amniotic fluid.

Another source of MSCs is the endometrium, a highly remodeling tissue. Human endometrium is the mucosal lining of the uterus, which undergoes more than 400 cycles of regeneration, differentiation, and shedding during a woman's reproductive life [14]. Each

Correspondence: Caroline E. Gargett, Ph.D., The Ritchie Centre, Hudson Institute of Medical Research, 27–31 Wright Street, Clayton, Victoria 3168, Australia. Telephone: 61 3 85 72 2795; E-Mail: caroline.gargett@hudson.org.au Received August 7, 2015; accepted for publication March 23, 2016; published Online First on May 31, 2016. ©AlphaMed Press 1066-5099/2016/\$20.00/0; http://dx.doi.org/10.5966/sctm.2015-0190

Table 1. Comparison of phenotypic markers of endometrial, bone marrow, and adipose tissue MSCs isolated as CFU-F, by plastic adherence or by SUSD2 or CD34 cell sorting

MSC type	Markers (% positive cells)												References
	CD29	CD31	CD34	CD44	CD45	CD73	CD90	CD105	CD140b	CD146	STRO1	HLA-DR	
Clonogenic eMSCs	>95	—	0	85	0	85	92	16	68.5	19	0	—	[19]
BM plastic-adherent MSCs	>95	—	0	—	0	≥ 90	≥ 90	≥ 90	>95	15–20	3.8	0	[33, 45, 46]
Adipose tissue plastic-adherent MSCs	>95	—	0	64	0	25	55	5	—	21	0	1	[47, 48]
CD146 ⁺ CD140b ⁺ eMSCs cultured in DMEM/EGF/FGF2 SFM	95.1	—	0	86	0.8	79	—	92	69	37	—	—	[43]
SUSD2 ⁺ eMSCs, freshly isolated	11.6	5.3	—	77	4.7	99	71	99	85	28	60	—	[26]
SUSD2 ⁺ eMSCs cultured in serum medium	93	2.3	0.5	93	—	99.9	98	99.5	50	1–2	0.9	0	[49], unpublished
SUSD2 ⁺ bone marrow MSCs, freshly isolated	—	26	5	70	90	—	0	20	—	4	—	22	[50]
SUSD2 ⁺ bone marrow MSCs cultured in serum medium	—	5.33	1.4	83	1.6	—	81	64	—	95	—	1.7	[50]
CD34 ⁺ ASCs, freshly isolated	—	38	78	81	57	—	39	28	—	41	—	10	[50]
CD34 ⁺ ASCs cultured in serum medium	—	6.7	17	98	5.8	—	56	79	—	13	—	4.9	[50]

SUSD2 can be used for isolating endometrial and bone marrow MSCs but does not isolate clonogenic ASCs; however, CD34 does.

Abbreviations: —, no data; ASC, adipose-derived stem cell; BM, bone marrow; CFU-F, colony-forming unit fibroblast; DMEM, Dulbecco's modified Eagle's medium; EGF, epidermal growth factor; eMSC, endometrial mesenchymal stem cell; FGF2, fibroblast growth factor 2; HLA-DR, human leukocyte antigen DR; MSC, mesenchymal stem/stromal cell; SFM, serum-free medium.

month, 5–10 mm of new endometrial mucosa grows during the first 4–10 days of the menstrual cycle from the residual basal layer (0.5–1 mm thick) to generate a new functionalis layer into which the embryo subsequently implants (Fig. 1A). Within 48 hours of endometrial shedding, regeneration begins with rapid repair/re-epithelialization of the endometrial surface to cover the exposed basal surface [15]. Fragments of shedding endometrial tissue contribute to this repair and gene profiling has demonstrated that the lysed stroma is enriched in genes involved in extracellular matrix biosynthesis and degradation [16]. As circulating estrogen levels rise during the proliferative stage of the menstrual cycle, epithelial, stromal, and vascular cells rapidly proliferate to generate the glands and supportive stroma of the rapidly growing functionalis layer. Following ovulation, the secretory phase of the cycle commences under the influence of progesterone to block cell division and promote terminal differentiation of the glandular epithelium. Stromal differentiation into decidual cells occurs around blood vessels and beneath the luminal epithelium into which an embryo implants. In the absence of an implanting embryo, the functionalis regresses and is shed as menstruation proceeds; then, a new cycle commences [19]. During the last 10 years, an MSC subpopulation has been identified and characterized in human endometrium and in menstrual blood. Endometrial mesenchymal stem/stromal cells (eMSCs) are easily isolated from endometrial biopsy tissue, which is obtained noninvasively without anesthesia in an office-based procedure. eMSCs are the focus of this perspective.

ENDOMETRIAL MESENCHYMAL STEM CELLS

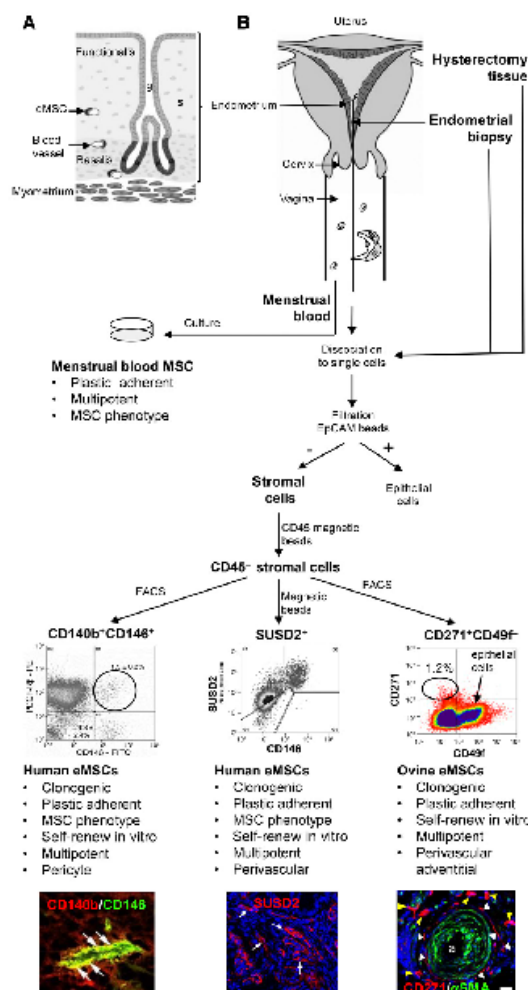
Human eMSCs were first identified in cell cloning studies from single cells dissociated directly from full thickness endometrium obtained from hysterectomy tissue (Fig. 1B). A small

proportion of the stromal colonies were large (1.3%), comprising small, densely packed cells likely originating from stromal stem/progenitor cells or colony-forming unit fibroblast (CFU-F) [17, 18]. Single, large endometrial CFU-F showed high proliferative capability undergoing 30 population doublings before reaching senescence, generating 6.5×10^{11} cells [19]. Single endometrial CFU-F serially propagated at very low cloning densities (5–10 cells/cm²) up to five times, demonstrating self-renewal in vitro [19]. Single endometrial CFU-F also differentiated into the classic mesodermal lineages (adipocyte, osteocyte, myocyte, and chondrocyte) and expressed the typical pattern of MSC surface markers, CD29, CD44, CD73, and CD90 and lacked CD31, CD34, and CD45 (Table 1) [20]. A greater percentage of CFU-F was observed in the proliferative stage of the menstrual cycle when the endometrium is rapidly growing under the influence of rising circulating estrogen levels. CFU-Fs were also detected in inactive, noncycling endometrium from women on oral contraceptives and from postmenopausal women, suggesting that stromal CFU-F may have a role in regenerating atrophic endometrial stroma when circulating estrogen levels are restored. Further evidence for eMSCs comes from label-retaining cells (LRCs) in mouse endometrium, which are perivascular and participate in endometrial regeneration [21].

PROSPECTIVE ISOLATION OF HUMAN eMSCs USING SPECIFIC MARKERS

Colocalization of CD140b and CD146 (pericyte markers) first identified eMSCs and their pericyte location in human endometrium [22]. These markers were also used to identify perivascular MSCs in many fetal and adult tissues [23]. Almost all the endometrial CFU-Fs are found in the CD140b⁺CD146⁺

Figure 1. Schematic showing procedures for eMSC isolation from human endometrium and menstrual blood. (A): eMSC location in human endometrium. eMSCs are perivascular cells in the germinal basalis and in the menstruated functional layers. (B): Human eMSCs are isolated from hysterectomy and endometrial biopsy (office procedure) tissue by enzymes and mechanical dissociation; stromal cells are then sequentially negatively selected from endometrial epithelial cells using EpCAM magnetic beads and leukocytes removed using CD45 magnetic beads, followed by either FACS for CD140b⁺CD146⁺ as shown in the FACS plot or magnetic bead sorting for SUS2⁺. Ovine eMSCs are sorted directly from dissociated endometrium collected from hysterectomy tissue using FACS for CD271⁺CD49f⁺ cells (CD49f removes contaminating epithelial cells) as shown in the FACS plot. The properties of the MSC isolated by each marker/ marker combination are also indicated. Confocal images show CD140b⁺CD146⁺ pericytes (yellow, white arrows) and perivascular SUS2⁺ (red, white arrows) cells in human endometrium. Scale bar = 50 μ m. Adventitial perivascular CD271⁺ (red, white arrowheads) ovine eMSCs located adjacent to α -smooth muscle actin⁺ vascular smooth muscle cells (green) of an arteriole (a) in ovine endometrium (yellow arrowheads are nonvessel associated CD271⁺ cells). Scale bar = 20 μ m. Endometrial stromal cells are directly cultured from menstrual blood as plastic-adherent cells in a similar manner to bone marrow. FACS plots and images reprinted from KE Schwab, CE Gargett, Co-expression of two perivascular cell markers isolates mesenchymal stem-like cells from human endometrium. *Hum Reprod* 2007;22:2903–2911, by permission from Oxford University Press [CD140b, CD146] [22], IngentaConnect (SUS2) [26], and *PLoS One* (CD271) [32]. Abbreviations: eMSC, endometrial mesenchymal stem cell; EpCAM, epithelial cell adhesion molecule; FACS, fluorescence-activated cell sorting; FITC, fluorescein isothiocyanate; g, gland; MSC, mesenchymal stem/stromal cell; PDGF-R β , platelet-derived growth factor receptor β ; PE, phycoerythrin; s, stroma.



fraction, with an 8-fold enrichment over unsorted stromal cells and 17-fold over CD140b⁺CD146⁺ cells [22]. The CD140b⁺CD146⁺ cells, constituting 1.5% of endometrial stromal cells, fulfilled the classic MSC criteria [24, 25].

Given the damaging effect of flow cytometry sorting on eMSC clonogenicity [22], a single marker was sought to enable selection with magnetic beads. Screening with antibodies marking the perivascular region identified the WSCS antibody as a novel single marker for isolating multipotent, self-renewing eMSCs that reconstitute stromal and vascular tissue *in vivo* [26]. WSCS⁺ cells constitute 4.2% of the stromal population, almost 3 times more than the CD140b⁺CD146⁺ population. WSCS cells showed a 6-fold increase in CFU-F activity over unsorted endometrial stromal cells and an 18-fold increase over the WSCS⁺ cells, indicating that most clonogenic cells were in the WSCS⁺ population. The epitope recognized by the WSCS antibody is Sushi-domain-containing-2 (SUSD2) [27].

SUSD2⁺ eMSCs were also identified in estrogen-regenerated and atrophic postmenopausal endometrium as clonogenic, multipotent, and serially clonogenic cells, although their MSC functional activity including clonogenicity, self-renewal, and differentiation ability was lower than premenopausal eMSCs [28]. An RNA sequencing study comparing cultured human endometrial SUSD2⁺ and SUSD2[−] cells identified 12 marker genes reflecting the perivascular location of SUSD2⁺ cells [29]. A single marker of perivascular eMSCs enables their prospective isolation using magnetic bead sorting, an important consideration for their use in cellular therapies.

CD271, the low affinity nerve growth factor receptor, has been used to isolate bone marrow MSCs [30]. CD271⁺ MSCs are clonogenic, express the classic MSC surface markers, and are multipotent [30]. The CD271 antibody cross-reacts with clonogenic bone marrow MSCs in several large animals often used in preclinical studies: ovine, monkey, goat, canine, and porcine species [31]. CD271 isolates MSCs from ovine endometrium when used in combination with CD49f to exclude endometrial epithelial cells (Fig. 1B). Ovine CD271⁺CD49f[−] endometrial stromal cells were more clonogenic, underwent more rounds of serial cloning, and showed greater mesodermal differentiation than CD271[−]CD49f[−] stromal fibroblasts [32].

eMSC In Vivo Identity

eMSC activity is likely regulated by the niche microenvironment. A perivascular niche for eMSCs was first identified in 40% of stromal IRLs found near the endometrial-myometrial junction, many of which expressed α -smooth muscle actin (α -SMA), indicating their perivascular identity [20]. In human endometrium, both CD140b⁺CD146⁺ and SUSD2⁺ cells are perivascular (Fig. 2) in both the functionalis and basalis layers (Fig. 1A). By confocal microscopy, CD140b⁺CD146⁺ coexpressing eMSCs are pericytes (Figs. 1B, 2) [22]. The precise perivascular location of SUSD2⁺ cells is less clear. These are more abundant than CD140b⁺CD146⁺ cells and possibly both pericytes and adventitial cells around larger vessels [26]. An adventitial, but not pericyte perivascular, location was identified for ovine CD271⁺ eMSCs in arterioles and larger venules (Figs. 1B, 2) [32]. Ovine CD271⁺ eMSCs are not in close apposition with vWF⁺ endothelial cells and did not express α -SMA but were adjacent to α -SMA⁺ vascular smooth muscle cells in the vessel media, similar to bone marrow MSCs and adipose-derived MSCs [23]. Whether SUSD2⁺ cells are located in both

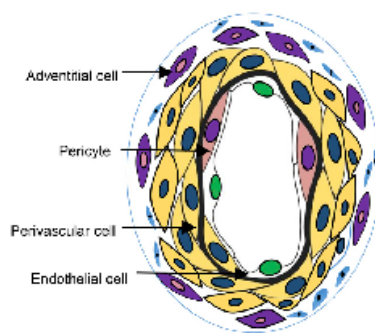


Figure 2. Schematic of a blood vessel profile showing the perivascular location of human, ovine, and mouse endometrial mesenchymal stem/stromal cells. Human CD140b⁺CD146⁺ cells (pink cytoplasm) are pericytes and SUSD2⁺ cells are perivascular cells (yellow cytoplasm). Ovine CD271⁺ cells (violet cytoplasm) are adventitial cells in arterioles and venules. Mouse stromal label-retaining cells are perivascular cells (yellow cytoplasm). Endothelial cells are indicated by white cytoplasm.

pericyte and adventitial perivascular regions remains to be determined.

Menstrual Blood MSCs

The endometrial functionalis layer is shed during menstruation. Given the location of CD140b⁺CD146⁺ and SUSD2⁺ eMSCs in both the functionalis and basalis layers, it is not surprising that eMSCs are found in menstrual blood (Fig. 1B). Viable stromal cells with classic properties of MSCs have been cultured from menstrual blood. Menstrual blood stromal cells are plastic-adherent, multipotent, express the classic pattern of MSC surface markers, and retain a stable karyotype in culture [33].

Menstrual blood represents a source of eMSCs easily collected from waste tissue and cultured similarly to bone marrow aspirates; however, without selective marker enrichment as is achieved for endometrial biopsy-derived eMSCs, they may not be as consistent or as efficacious.

Potential Clinical Application of eMSCs

Cellular therapy is an emerging field in clinical medicine. Many adult stem cells or pluripotent cell derivatives are in clinical trials for treatment of chronic and degenerative disease, the most common being bone marrow MSCs followed by ASCs. Tissue engineering involves the generation of a tissue substitute comprising a scaffold seeded with stem/progenitor cells for restoring or maintaining normal tissue/organ function. Scaffolds provide a three-dimensional environment supporting MSC adhesion and growth, facilitating delivery of cells to target sites to promote the growth of new tissue. eMSCs could be an ideal candidate for seeding biomaterials because they are easily acquired in an office-based biopsy without anesthesia.

EMSCs FOR TREATMENT OF PELVIC ORGAN PROLAPSE

Pelvic organ prolapse (POP) is the herniation of the pelvic organs into the vagina causing urinary and fecal incontinence, and voiding and sexual dysfunction. POP affects 25% of all women and up to 50% of parous postmenopausal women. Nineteen percent of women have a lifetime risk of undergoing an operation for POP [34, 35]. Due to high failure rates of native tissue surgery, synthetic meshes became popular for POP treatment, particularly monofilament, nondegradable polypropylene (PP) meshes with large pore sizes. Significant adverse events resulting from the use of mesh for POP surgery, including exposure, contraction, and pain led the U.S. Food and Drug Administration to post several warnings on the use of vaginal mesh [34, 36]. To address these problems, we developed and evaluated a new polyamide/gelatin composite mesh (PA+G) with improved mechanical and tissue integration properties, compared with commercial PP meshes in a rat abdominal hernia repair model [37]. These PA+G meshes seeded with eMSCs, and implanted into a rat subcutaneous fascial defect model, promoted more neovascularization resulting in a higher density of α -SMA⁺ vessel profiles in the neotissue surrounding mesh filaments compared with unseeded PA+G mesh. There was an initial early leukocyte response mainly involving M1 inflammatory macrophages for both eMSC-seeded and unseeded meshes, which switched to a M2 wound healing phenotype only in eMSC/PA+G implanted tissues. In the long term (90 days), the macrophages at the mesh filament-tissue interface were markedly reduced in the eMSC/PA+G mesh compared with PA+G alone. Crimped, more organized collagen fibers were deposited around cell-seeded mesh suggesting that eMSCs might promote physiological collagen production, which led to improved biomechanical properties with a more compliant, less stiff mesh/tissue complex than PA+G mesh alone [38, 39]. Because the eMSCs persisted for only 2 weeks, new tissue formation was likely due to the paracrine effects of eMSCs. In vitro, PA+G mesh seeded with eMSCs differentiated into smooth muscle-myosin heavy chain-expressing smooth muscle cells and collagen-producing fibroblasts, with concomitant downregulation of α -SMA expression [40]. Fibroblasts and smooth muscle cells are the desired cell types for regenerating the human vaginal wall and synthesizing and organizing the extracellular matrix. Based on this promising result in a xenogenic, small animal pre-clinical model of POP repair surgery, a large animal ovine model is being developed to examine the efficacy and mechanism of action of PA+G mesh seeded with autologous ovine eMSCs [32] on vaginal repair of parous ewes with demonstrated vaginal wall weakness. Although there are many sources of MSCs for cell-based therapies, few studies have been conducted for pelvic organ repair and there are no clinical trials for POP. Evidence suggests that these cells, and in particular eMSCs, may offer an improved therapeutic option for POP in the near future.

REFERENCES

1. Bianco P, Cao X, Frenette PS et al. The meaning, the sense and the significance: Translating the science of mesenchymal stem cells into medicine. *Nat Med* 2013;19:35–42.
2. Bernardo ME, Pagliara D, Locatelli F. Mesenchymal stromal cell therapy: A revolution in regenerative medicine? *Bone Marrow Transplant* 2012;47:164–171.
3. Horwitz EM, Dominici M. How do mesenchymal stromal cells exert their therapeutic benefit? *Cytotherapy* 2008;10:771–774.
4. Le Blanc K, Mougiakalos D. Multipotent mesenchymal stromal cells and the innate immune system. *Nat Rev Immunol* 2012;12:383–396.
5. Tolar J, Villeneuve P, Keating A. Mesenchymal stromal cells for graft-versus-host disease. *Hum Gene Ther* 2011;22:257–262.
6. Luk F, de Witte SF, Brämmer WM et al. Efficacy of immunotherapy with mesenchymal stem cells in man: A systematic review. *Expert Rev Clin Immunol* 2015;11:617–636.
7. Karp JM, Leng Teo GS. Mesenchymal stem cell homing: The devil is in the details. *Cell Stem Cell* 2009;4:206–216.
8. D'Souza N, Rossignol F, Gohelli G et al. Mesenchymal stem/stromal cells as a delivery platform in cell and gene therapies. *BMC Med* 2015;13:186.

MENSTRUAL BLOOD MSCs PROMOTE MYOCARDIAL REPAIR

Menstrual blood MSCs have been used to repair the heart using a tissue engineering approach in a myocardial infarct nude rat model [41]. Cultured enhanced green fluorescent protein-labeled menstrual blood MSCs were harvested as a sheet from temperature sensitive culture plates and grafted onto the infarcted area. The MSCs differentiated into striated, troponin I-expressing cardiac muscle cells. In comparison with bone marrow MSCs, the menstrual blood MSCs reduced the infarcted area more and showed greater improvement in echocardiographic parameters of myocardial function, indicating the potential promise of menstrual blood-derived MSCs for clinical translation.

CONCLUSION

The highly regenerative endometrium provides a new, readily available source of MSCs with capabilities similar to those of bone marrow MSCs. Endometrial tissue is easily harvested from women with minimal pain and morbidity [42]. Specific perivascular markers of eMSCs have been identified and methods developed to prospectively isolate them from endometrial cell suspensions and to expand them under Good Manufacturing Practice guidelines [43]. These developments and the increasing recognition of the uterus as a source of MSCs will ensure their use in autologous and allogeneic cellular therapy, as well as homologous tissue engineering applications for regenerating endometrium in thin endometrial infertility disorders and endometrial scarring (Asherman's syndrome) [44].

ACKNOWLEDGMENTS

This work was supported by National Health and Medical Research Council (NHMRC) of Australia Project Grant 1081944 (C.E.G., J.A.W.), an NHMRC Senior Research Fellowship (1042298) (C.E.G.), a Monash University International Research Postgraduate Scholarship (S.D.), a Monash Graduate Scholarship (S.D.), and the Victorian government's Operational Infrastructure Support Program.

AUTHOR CONTRIBUTIONS

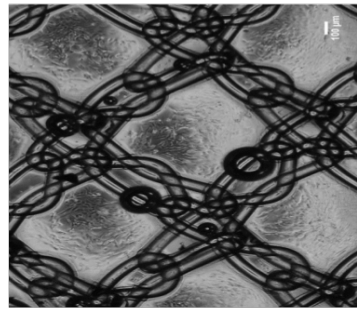
S.D.: collection and assembly of data, manuscript writing, final approval of manuscript; J.A.W. and J.A.D.: manuscript editing, final approval of manuscript; C.E.G.: conception and design, financial support, manuscript writing, manuscript editing, final approval of manuscript.

DISCLOSURE OF POTENTIAL CONFLICTS OF INTEREST

The authors indicated no potential conflicts of interest.

9. Prockop DJ, Prockop SE, Bertoncello I. Are clinical trials with mesenchymal stem/progenitor cells too far ahead of the science? Lessons from experimental hematology. *Stem Cells* 2014;32:3055-3061.
10. Rastegar F, Shenaq D, Huang J et al. Mesenchymal stem cells: Molecular characteristics and clinical applications. *World J Stem Cells* 2010;2:67-80.
11. Bañe O, Fonseca VC, Cooper LL et al. Impact of aging on the regenerative properties of bone marrow, muscle, and adipose-derived mesenchymal stem/stromal cells. *PLoS One* 2014;9:e115963.
12. Mizuno H, Tobita M, Uysal AC. Concise review: Adipose-derived stem cells as a novel tool for future regenerative medicine. *Stem Cells* 2012;30:808-810.
13. Hazelwood CF, Sherrill H, Ryan J et al. High incidence of contaminating maternal cell overgrowth in human placental mesenchymal stem/stromal cell cultures: A systematic review. *Stem Cells Transl Med* 2014;3:1305-1311.
14. Jabbour HN, Kelly RW, Fraser HM et al. Endocrine regulation of menstruation. *Endocr Rev* 2006;27:17-46.
15. Gargett CE, Nguyen HP, Ye L. Endometrial regeneration and endometrial stem/progenitor cells. *Rev Endocr Metab Disord* 2012;13:235-251.
16. Henriot P, Gaide Chavonnay HP, Marbach E. The endocrine and paracrine control of menstruation. *Mol Cell Endocrinol* 2012;358:197-207.
17. Chan RW, Schwab KE, Gargett CE. Clonogenicity of human endometrial epithelial and stromal cells. *Biol Reprod* 2004;70:1739-1750.
18. Schwab KE, Chan RW, Gargett CE. Putative stem cell activity of human endometrial epithelial and stromal cells during the menstrual cycle. *Fertil Steril* 2005;84(suppl 2):1124-1130.
19. Gargett CE, Schwab KE, Zillwood RM et al. Isolation and culture of epithelial progenitors and mesenchymal stem cells from human endometrium. *Biol Reprod* 2009;80:1136-1145.
20. Chan RW, Gargett CE. Identification of label-retaining cells in mouse endometrium. *Stem Cells* 2006;24:1529-1538.
21. Gargett CE, Schwab KE, Deane JA. Endometrial stem/progenitor cells: The first 10 years. *Hum Reprod Update* 2016;22:137-163.
22. Schwab KE, Gargett CE. Co-expression of two perivascular cell markers isolates mesenchymal stem-like cells from human endometrium. *Hum Reprod* 2007;22:2903-2911.
23. Crisan M, Yap S, Castella L et al. A perivascular origin for mesenchymal stem cells in multiple human organs. *Cell Stem Cell* 2008;3:301-313.
24. Dominici M, Le Blanc K, Mueller I et al. Minimal criteria for defining multipotent mesenchymal stromal cells. The International Society for Cellular Therapy position statement. *Cytotherapy* 2006;8:315-317.
25. Spitzer TL, Rojas A, Zelenko Z et al. Perivascular human endometrial mesenchymal stem cells express pathways relevant to self-renewal, lineage specification, and functional phenotype. *Biol Reprod* 2012;86:58.
26. Masuda H, Anwar SS, Bühring HJ et al. A novel marker of human endometrial mesenchymal stem-like cells. *Cell Transplant* 2012;21:2201-2214.
27. Shesubramanian K, Harichandan A, Schumann S et al. Prospective isolation of mesenchymal stem cells from human bone marrow using novel antibodies directed against Sushi domain containing 2. *Stem Cells Dev* 2013;22:1944-1954.
28. Ulrich D, Tan KS, Deane J et al. Mesenchymal stem/stromal cells in postmenopausal endometrium. *Hum Reprod* 2014;29:1895-1905.
29. Murakami K, Lee YH, Lucas ES et al. Decidualization induces a secretome switch in perivascular niche cells of the human endometrium. *Endocrinology* 2014;155:4542-4553.
30. Battula VL, Tremblé S, Bareiss PM et al. Isolation of functionally distinct mesenchymal stem cell subsets using antibodies against CD56, CD271, and mesenchymal stem cell antigen-1. *Haematologica* 2009;94:173-184.
31. Roemmler H, Fris H, Naajkins B et al. Prospective isolation of mesenchymal stem cells from multiple mammalian species using cross-reacting anti-human monoclonal antibodies. *Stem Cells Dev* 2010;19:1911-1921.
32. Letouzey V, Tan KS, Deane JA et al. Isolation and characterization of mesenchymal stem/stromal cells in the ovine endometrium. *PLoS One* 2015;10:e0127531.
33. Darzi S, Zamani AH, Jaddi-Tehrani M et al. Osteogenic differentiation of stem cells derived from menstrual blood versus bone marrow in the presence of human platelet releasate. *Tissue Eng Part A* 2012;18:1720-1728.
34. Maher C, Felner B, Baessler K et al. Surgical management of pelvic organ prolapse in women. *Cochrane Database Syst Rev* 2013;4:CD004034.
35. Smith FL, Holman CD, Mootin RE et al. Life time risk of undergoing surgery for pelvic organ prolapse. *Obstet Gynecol* 2010;116:1096-1100.
36. de Teyrac R, Deffieux X, Gervaise A et al. Long-term anatomical and functional assessment of transvaginal cystocele repair using a tension-free polypropylene mesh. *Int Urogynecol J Pelvic Floor Dysfunct* 2006;17:489-498.
37. Ulrich D, Edwards SL, White JF et al. A preclinical evaluation of alternative synthetic biomaterials for fascial defect repair using a rat abdominal hernia model. *PLoS One* 2012;7:e50044.
38. Edwards SL, Ulrich D, White JF et al. Temporal changes in the biomechanical properties of endometrial mesenchymal stem cell seeded scaffolds in a rat model. *Acta Biomater* 2015;13:286-294.
39. Ulrich D, Edwards SL, Su K et al. Human endometrial mesenchymal stem cells modulate the tissue response and mechanical behavior of polyamide mesh implants for pelvic organ prolapse repair. *Tissue Eng Part A* 2014;20:785-798.
40. Su K, Edwards SL, Tan KS et al. Induction of endometrial mesenchymal stem cells into tissue-forming cells suitable for fascial repair. *Acta Biomater* 2014;10:5012-5020.
41. Hida N, Nishiyama N, Miyoshi S et al. Novel cardiac precursor-like cells from human menstrual blood-derived mesenchymal cells. *Stem Cells* 2008;26:1695-1704.
42. Ulrich D, Muralidharan R, Gargett CE. Toward the use of endometrial and menstrual blood mesenchymal stem cells for cell-based therapies. *Expert Opin Biol Ther* 2013;13:1387-1400.
43. Rajaraman G, White J, Tan KS et al. Optimization and scale-up culture of human endometrial multipotent mesenchymal stromal cells: potential for clinical application. *Tissue Eng Part C Methods* 2013;19:80-92.
44. Gargett CE, Ye L. Endometrial reconstruction from stem cells. *Fertil Steril* 2012;98:11-20.
45. Bourin P, Bunnell BA, Castellani L et al. Stromal cells from the adipose tissue-derived stromal vascular fraction and culture expanded adipose tissue-derived stromal/stem cells: A joint statement of the International Federation for Adipose Therapeutics and Science (IFATS) and the International Society for Cellular Therapy (ISCT). *Cytotherapy* 2013;15:641-648.
46. Vogel W, Grünbach F, Masmun CA et al. Heterogeneity among human bone marrow-derived mesenchymal stem cells and neural progenitor cells. *Haematologica* 2003;88:126-133.
47. Giannos S, Franklin DM, Leddy HA et al. Surface protein characterization of human adipose tissue-derived stromal cells. *J Cell Physiol* 2001;189:54-63.
48. Mitchell JB, McIntosh K, Zvonik S et al. Immunophenotype of human adipose-derived cells: temporal changes in stromal-associated and stem cell-associated markers. *Stem Cells* 2006;24:376-385.
49. Gurung S, Werlemester JA, Gargett CE. Inhibition of transforming growth factor- β receptor signaling promotes culture expansion of undifferentiated human endometrial mesenchymal stem/stromal cells. *Sci Rep* 2015;5:15042.
50. Busser H, Najjar M, Ralovic G et al. Isolation and characterization of human mesenchymal stromal cell subpopulations: Comparison of bone marrow and adipose tissue. *Stem Cells Dev* 2015;24:2142-2157.

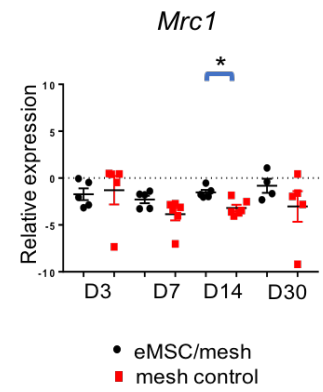
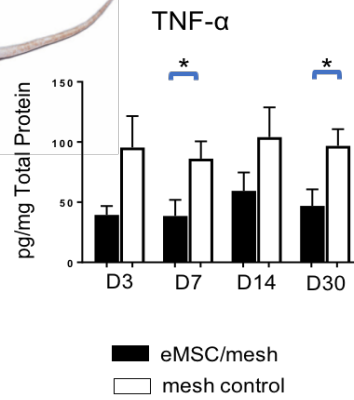
eMSC seeded on PA+G mesh



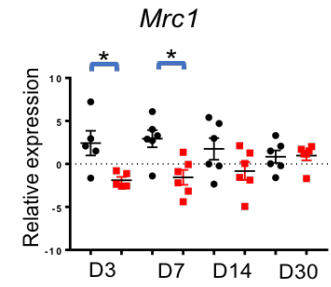
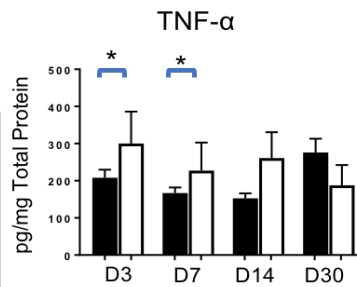
NSG
Immunocompromised



eMSC reduced inflammation and increased M2 macrophage markers at later time points



C57BL6
Immunocompetent



eMSC reduced inflammation and increased M2 macrophage markers at earlier time points